

**Implication of the TREM2/DAP12 Complex
in Microglial-mediated Tissue Homeostasis
under Healthy and Pathological Conditions**

Dissertation

zur

Erlangung des Doktorgrades (Dr. rer. nat.)

der

Mathematisch-Naturwissenschaftlichen Fakultät

der

Rheinischen Friedrich-Wilhelms-Universität Bonn

vorgelegt von

Liviu-Gabriel Bodea

aus

Constanța, Rumänien

Bonn 2014

Angefertigt mit Genehmigung der Mathematisch-Naturwissenschaftlichen Fakultät der
Rheinischen Friedrich-Wilhelms-Universität Bonn

1. Gutachter: Prof. Dr. Harald Neumann

2. Gutachter: Prof. Dr. Waldemar Kolanus

Tag der Promotion: 26 Feb 2014

Erscheinungsjahr: 2014

Contents

Abbreviations	I
Abstract.....	IV
1. Introduction.....	1
1.1 Microglia - the Brain's Immune Cells	1
1.1.1 Origin and Localization of Microglial Cells	2
1.1.2 Microglial Functions and Morphology	3
1.1.2.1 The Beneficial Microglia	3
1.1.2.2 The Harmful Microglia	5
1.2 Microglial Involvement in Neurodegenerative Diseases	7
1.2.1 Nasu-Hakola Disease (NHD)	8
1.2.1.1 The TREM2/DAP12 Signaling Complex	8
1.2.2 Parkinson's Disease (PD)	12
1.2.2.1 Animal Models of PD.....	14
1.2.2.1.1 Lipopolysaccharide (LPS)-triggered Dopaminergic Degeneration	15
1.2.3 Alzheimer's Disease (AD)	17
1.3 Objectives of the Thesis	21
2. Materials and Methods	22
2.1 Mice.....	22
2.1.1 Mice Genotyping.....	22
2.1.2 LPS Treatment Schemes.....	23
2.1.3 Tissue Collection and Storage	24
2.2 Cell Cultures	25
2.2.1 Primary Cell Cultures.....	25
2.2.1.1 Microglia Primary Cell Cultures.....	25
2.2.1.2 Neuronal Primary Cell Cultures.....	25
2.2.2 Cell Lines	25
2.2.2.1 General Cell Lines Handling	26
2.2.3 Microglia-Neurons Cocultures	27
2.2.4 Cellular Functional Assays.....	28
2.2.4.1 Phagocytosis Assay	28
2.2.4.2 Detection of Superoxide Production.....	28
2.2.4.3 Neurites Length Analysis.....	28
2.3 Molecular Biology.....	29
2.3.1 PCR, RT, sqRT-PCR.....	29
2.3.1.1 RNA Isolation and RT.....	29
2.3.1.2 sqRT-PCR	30

2.3.2 Bacterial cloning.....	31
2.3.2.1 Bacterial cultures	31
2.3.2.2 Plasmid isolation	32
2.3.2.3 Plasmid Digestion and Ligation	32
2.3.2.4 Bacterial Transformation and Ligation Confirmation	33
2.3.3 Lentivirus Generation and Transduction of Cells.....	35
2.3.3.1 Fluorescence-Activated Cell Sorting (FACS) Isolation of Transduced Cells.....	36
2.3.4 cDNA Microarray.....	36
2.3.5 RNA Sequencing.....	37
2.4. Immunochemistry	37
2.4.1 Immunohistochemistry (IHC)	37
2.4.2 Immunocytochemistry (ICC)	39
2.4.3 Immunoprecipitation (IP).....	40
2.4.4 Western Blot (WB)	40
2.4.5 Enzyme-Linked Immunosorbent Assay (ELISA).....	41
2.6 Other General Materials	41
2.6.1 Technical Equipment.....	41
2.6.2 Consumables.....	43
2.6.3 Chemicals and Reagents	44
2.6.4 Kits.....	45
2.7 Softwares and Databases.....	46
2.8 Statistical Analysis	46
3. Results.....	47
3.1 TREM2 Deficient Mouse Characterization.....	47
3.1.1 Aged TREM2 Deficient Mice Show Increased Levels of Inflammatory Transcripts	47
3.1.2 Changed Microglial Morphology in Adult TREM2 KO Mice	48
3.1.3 Similar Inflammatory Transcripts in TREM2 KO and WT mice after Systemic LPS Challenges ..	49
3.2 Immune System Involvement in Dopaminergic Degeneration Induced by Systemic LPS Challenges	50
3.2.1 Microglial Activation by Systemic LPS Treatments	50
3.2.2 Proinflammatory Transcripts in Mice Systemically Challenged with LPS	52
3.2.3 Loss of Dopaminergic Neuronal Triggered by Systemic LPS Challenges.....	54
3.2.4 Brain Transcriptome Analysis of Systemic LPS Challenged Mice	55
3.2.5 Phagosome- and Complement-related Pathways Enriched by Systemic LPS Challenges	57
3.2.6 C3 Deficiency Abrogates Dopaminergic Neuronal Loss after Repeated LPS Challenges	61
3.3 DAP12/TYROBP Acts as Causal Regulator in Late Onset AD (LOAD).....	64
3.3.1 Microglial Cluster Enriched in Transcripts of LOAD Brains	64
3.3.2 Features of LOAD Recapitulated by DAP12 Overexpressing Microglial Cells	65

3.3.3 Amyloid- β (A β) Internalization by Functional Dap12 Overexpressing Microglial Cells	68
3.3.4 Neuron Degeneration by Functional Dap12 Overexpressing Microglial Cells	70
3.3.5 Superoxide Release by Functional Dap12 Overexpressing Microglial Cells.....	72
4. Discussions	74
4.1 The Effects of Microglial TREM2 Deficiency.....	74
4.1.1 Involvement of TREM2/DAP12 Complex in Nasu-Hakola Disease.....	75
4.1.2 TREM2 Deficient Mouse Characterization	76
4.1.2.1 Age-related Changes in the mRNA of TREM2 Deficient Mice.....	76
4.1.2.2 Altered Microglial Morphology in TREM2 KO Mice	77
4.2 Mechanisms of Neurodegeneration Triggered by Systemic LPS Application	81
4.2.1 Contribution of Systemic Inflammation to Neurodegeneration.....	81
4.2.2 Complement Involvement in Dopaminergic Neurodegeneration	83
4.2.2.1 Microglial Activation and Dopaminergic Degeneration Triggered by Systemic LPS Application in Mice	83
4.2.2.2 Enriched Immune-related Transcripts in Mice Systemically Treated with LPS.....	84
4.2.1.3 The Contribution of Complement Component 3 in LPS-induced Dopaminergic Degeneration	85
4.3 DAP12/TYROBP Involvement in LOAD	86
4.3.1 The Genetic Background of LOAD.....	86
4.3.2 Mechanisms of DAP12 Mediated Neurotoxicity in LOAD.....	87
4.3.2.1 DAP12 Revealed as Key Regulator by Transcriptome Analysis of LOAD.....	87
4.3.2.2 DAP12 Modified Microglial Cells Recapitulate Features of LOAD	88
4.3.2.3 DAP12-mediated Mechanism of A β -triggered Neurotoxicity.....	88
4.4 Summary.....	90
Appendix	93
Specific genes enriched by the repeated (4x) LPS challenges of mice	93
Common genes enriched by the repeated (4x) and single (1x) LPS challenge of mice	94
Specific genes enriched by the single (1x) LPS challenge of mice	94
References.....	95
Acknowledgements.....	107
Curriculum Vitae.....	108
Declaration.....	110

Abbreviations

3D	tridimensional	DHE	dihydroethidium
6-OHDA	6-hydroxydopamine	DNA	deoxyribonucleic acid
Ab	antibody	dNTPs	deoxyribonucleotides
AD	Alzheimer's disease	dsRNA	double stranded ribonucleic acid
ADAM	a disintegrin- and metalloprotein-family enzyme	DTT	dithiothreitol
<i>Aif1</i>	allograft inflammatory factor 1 gene	E	embryonic (day)
ANOVA	analysis of variance	EAE	experimental autoimmune encephalomyelitis
AP-1	activation protein-1	EDTA	Ethylenediaminetetraacetic acid
APH1	anterior pharynx-defective 1	EF1 α	Elongation factor 1 alpha
APOE	apolipoprotein E	eGFP	enhanced green fluorescence protein
APP	Amyloid precursor protein	ELISA	Enzyme-linked immunoabsorbent assay
ATP	adenosine triphosphate	EOAD	early onset Alzheimer's disease, FAD
A β	amyloid β	ERK	extracellular signal-regulated kinases
BACE1	β -site APP-cleaving enzyme 1	ESdM	Embryonic stem cell derived microglia
BBB	blood brain barrier	FACS	Fluorescence-activated cell sorting
BDNF	brain-derived neurotrophic factor	FAD	familial Alzheimer's disease, EOAD
BL6	C57BL/6J mouse line	FADD	FAS-associated protein with death domain
BMDMs	bone marrow derived monocytes/macrophages	FASL	Fas-ligand
C1q	complement component 1q	FC	fold change
C3	complement component 3	<i>Fcer1g</i>	common γ -chain gene
CAM5	intracellular adhesion molecule 5	FCS	Fetal Calf Serum
cDNA	complementary DNA	FDR	false discovery rate
CNS	central nervous system	Gapdh	glyceraldehyde-3-phosphate dehydrogenase
CO ₂	carbon dioxide	gbw	gram body weight
COX2	cyclooxygenase 2	GFP	green fluorescent protein
CR3	complement component 3 receptor	GMCSF	granulocyte-macrophage colony stimulating factor
Crry	complement receptor 1-related protein	gp91	cytochrome b-245, β polypeptide
<i>Ctss</i>	Cathepsin S	GWAS	genome wide association studies
CX3CL1	CX3C Chemokine Ligand 1, fractalkine	HA	hemagglutinin
CX3CR1	fractalkine receptor	HBSS	Hank's balanced salt solution
CXCR3	CXC chemokine receptor 3	HPLC	High performance liquid chromatography
Cy3	cyanine 3 dye	Hsp60	heat shock protein 60
<i>Cyba</i>	cytochrome b-245, α polypeptide	I	isoleucine
<i>Cybb</i>	cytochrome b-245, β polypeptide	i.p.	intraperitoneal
DA	dopamine/dopaminergic	Iba1	Ionized calcium-binding adapter molecule
DAMPs	damage-associated molecular pattern molecules	ICC	immunocytochemistry
DAP12	DNAX-activating protein of molecular mass 12 kDa	IFN γ	interferon γ
DB	data base	IHC	immunohistochemistry
DCs	dendritic cells	IKK α/β	Inhibitor of nuclear factor kappa-B kinase subunit α/β
DE	Germany	IL 1 β	interleukin 1 β
DEG	differentially expressed genes	IL10	Interleukin 10

IL10R	Interleukin 10 receptor
IL6	interleukin 6
iNOS	inducible nitric oxide synthase
IP	immunoprecipitation
IPA	Ingenuity pathway analysis
IRAK4	Interleukin 1 receptor-associated kinase 4
IRES	internal ribosome entry site
IRF3	Interferon regulatory factor
Irf8	interferon regulatory factor 8
IT	Italy
ITAM	immunoreceptor tyrosine-based activatory motif
<i>Itgam</i>	integrin $\alpha_M\beta_2$, subunit of CR3 gene
ITIM	immunoreceptor tyrosine-based inhibitory motif
JP	Japan
KEGG	Kyoto Encyclopedia of Genes and Genomes
KO	Knock-out
L	leucine
LAT	linker for activation of T cells
LB	Luria Broth media
LFA1	lymphocyte function associated antigen 1
LOAD	late onset Alzheimer's disease, SAD
LPS	lipopolysaccharides
LRP1	low density lipoprotein-related protein 1
<i>LRRK2</i>	leucine-rich repeat kinase 2 gene
MAC1	macrophage antigen 1, integrin $\alpha_M\beta_2$, ITGAM
MAPK	mitogen activated protein kinase
MARCO	macrophage receptor with collagenous structure
Mcp1	monocyte chemotactic protein 1
MCSF	macrophage colony-stimulating factor
MD2	myeloid differentiation factor 2
MEF	mouse embryonic fibroblast
MES	2-(N-morpholino)ethanesulfonic acid
MHC	major histocompatibility
MPTP	1-methyl-4-phenyl-1,2,3,6-tetrahydropyridine
mRNA	messenger ribonucleic acid
MS	multiple sclerosis
MyD88	myeloid differentiation primary response protein 88
N ₂	nitrogen
NADPH	nicotinamide adenine dinucleotide phosphate
NeuN	Neuronal nuclei
NFkB	nuclear factor kappa-light-chain-enhancer of activated B cells
NFT	neurofibrillary tangles

NHD	Nasu-Hakola disease
NKs	natural killer cells
NMDA	N-methyl-D-aspartate
NO	nitric oxide
NOS	nitric oxide synthase
NTAL	non-T cell activation linker
NURR1	Nuclear receptor related protein 1
O ₂ ⁻	superoxide
P	postnatal (day)
p22phox	cytochrome b-245, α polypeptide
P2X7	P2X purinoceptor 7
PAMPs	pathogen-associated molecular patterns
<i>PARKs</i>	parkinson genes
PBMCs	peripheral blood mononuclear cells
PBS	phosphate buffered saline
PBST	phosphate buffered saline + tween
PCR	polymerase chain reaction
PD	Parkinson's disease
PEN2	presenilin enhancer 2
PFA	paraformaldehyde
PGE2	prostaglandin E2
PI3K	phosphoinositol 3-kinase
PLC γ	phospholipase C γ
PLOSL	polycystic lipomembranous osteodysplasia with sclerosing encephalopathy, NHD
PPAR γ	Peroxisome proliferator-activated receptor γ
PRRs	Pattern recognizing receptors
PS	presenilin
PTP	phosphotyrosine phosphatases
RAGE	receptor for advanced glycation endproducts
RIPA	Radioimmunoprecipitation assay buffer
ROS	reactive oxygen species
RT	reverse transcription
Runx1	Runt related transcription factor 1
S	serine
SAD	sporadic Alzheimer's disease, LOAD
SDS	Sodium dodecyl sulfate
SEM	standard error measurement
SHP1	SH2 domain containing phosphatase 1
Siglec	sialic acid-binding immunoglobulin-like lectin
SIRP α	signal regulatory protein α
SIRP β 1	signal regulatory protein β 1
SN	substantia nigra
<i>SNCA</i>	α -synuclein gene
<i>SNpc</i>	substantia nigra <i>pars compacta</i>
<i>SNpr</i>	substantia nigra <i>pars reticulata</i>
sqRT-PCR	Semiquantitative real-time polymerase chain reaction

SR-A	scavenger receptor A
SR-B1	Scavenger receptor B class I
Syk	spleen tyrosine kinase
tau	protein τ
TGF β	transforming growth factor β
TGF β R	transforming growth factor β receptor
TH	tyrosine hydroxylase
TIRAP	Toll-interleukin 1 receptor domain containing adaptor protein
TLRs	toll-like receptors
TLT1	trem-like transcript 1
TNF α	tumor necrosis factor α
TRAF6	TNF receptor associated factor 6
TRAM	TRIF-related adaptor molecule
TREM2	triggering receptor expressed on myeloid cells 2
TRIF	TIR-domain-containing adapter-inducing interferon β
TYROBP	TYRO protein tyrosine kinase-binding protein, DAP12
UK	United Kingdom
USA	United States of America
V	valine
v/v	volume per volume
VLDL	very-low-density-lipoprotein receptor
vs.	versus
WB	Western blott
WT	wild type
Y	tyrosine
ZAP-70	ζ -chain-associated protein kinase of 70 kDa

Abstract

Microglial activation was previously associated with neurodegenerative diseases such as Parkinson's disease (PD) or Alzheimer's disease (AD). The prototype of primary microglia neurodegenerative disorder is represented by the Nasu-Hakola disease (NHD), which is caused by loss of function mutations in the microglial triggering receptor expressed in myeloid cells 2 (TREM2) or its associated adaptor molecule DNAX-activating protein of molecular mass 12 kDa (DAP12). Recently, mutations in *TREM2* were associated with late onset AD (LOAD). The mechanisms of TREM2/DAP12-mediated neurodegeneration are still not fully understood.

Within this thesis, *in vitro* and/or *in vivo* models of NHD, PD and LOAD were investigated with an emphasis on the mechanisms of microglia-mediated neurodegeneration.

As model for NHD, TREM2 knock-out (KO) animals were found to develop an activated-like microglial phenotype when compared with appropriate wild type (WT) controls. However, only the old TREM2 KO animals present altered microglial-related gene expressions. Systemic lipopolysaccharide (LPS) stimulation of mice accentuated the differences in TREM2 KO microglial phenotype, but without inducing significant differences between microglia-related proinflammatory transcripts in TREM2 KO compared with control mice. LPS challenges were previously associated with dopaminergic loss, a neuropathological trait of PD. To investigate the mechanism of LPS-triggered dopaminergic degeneration, WT mice were challenged with LPS and transcriptome analysis of whole brains was performed. The analysis revealed enrichment in microglial phagosome and complement-related genes. To prove the complement involvement in neuronal loss, C3 KO animals were challenged with LPS. Dopaminergic neuronal loss was found to be ameliorated in C3 KO mice. LOAD investigation using genome wide association studies revealed specific enrichment of the immune-related module, with *DAP12* acting as causal regulator. Modified microglia cell lines overexpressing functional or non-functional DAP12 were generated and were able to recapitulate expression patterns specific to LOAD brains. Furthermore, microglial cells were able to take up amyloid and release neurotoxic superoxide only when expressing functional DAP12.

The present thesis proposes microglial-related mechanisms in which different immune-related pathways are converging, contributing to the neurodegenerative processes.

1. Introduction

Evolutionary pressure drove living organisms into gradually developing more sophisticated defense mechanisms against potential dangerous foreign entities, culminating with the formation of complex immune system. In vertebrates, the immune system encompasses a highly intricate and dynamic network of cells, tissues and organs capable to recognize and appropriately respond to a broad variety of dangerous or non-self structures. However, in certain conditions, these mechanisms can turn against own structures, as in the case of neurodegenerative diseases.

1.1 Microglia - the Brain's Immune Cells

The resident innate immune cells exclusive to central nervous system (CNS) are represented by microglia. Even though many microglial properties were known from anatomy and pathology studies of the late 19th century, the concept of microglial cell was first introduced by Pió del Rió-Hortega in 1932 (Barron, 1995; Kettenmann and Hanisch, 2011). After this period, the study of microglia entered a decline until the 1960s when many debates and questions related with the brain immunity reemerged.

Most of del Rió-Hortega's observations on microglial cells remain valid until today. Indeed microglial cells have a mesodermal origin, entering the future brain during early development, when they present amoeboid morphology. After reaching their final anatomical destination, they display a branched cellular phenotype, presenting little variation and occupying defined non-overlapping territory. Upon a pathological event, microglia can 'transform', becoming again amoeboid. However, some of the intimate mechanisms of microglial physiology remained elusive to the scientific community.

Additional to the microglial population, the CNS presents macrophage populations associated with blood vessels (the perivascular macrophages, sometimes named also 'perivascular microglia'), circumventricular organs, choroid plexus and meninges. However, these cells can be

distinguished from microglial cells based on their morphological differences and localization (Ransohoff and Perry, 2009).

1.1.1 Origin and Localization of Microglial Cells

Even though the origin of microglia has been long debated, the present commonly accepted hypothesis supports a first wave of migration starting from the yolk sack and reaching the embryo between embryonic day (E)7-7.5 and E8 in mice, then populating the future CNS around E10 (Alliot et al., 1999; Ginhoux et al., 2010; Kierdorf et al., 2013). The second wave of sporadic microglial migration occurs at postnatal (P) stages, when circulating bone marrow derived monocytes enter the brain, in mice between P0-P15 (Chan et al., 2007; Soulet and Rivest, 2008). However, the exact identity of these monocytes is still unclear. After this stage, the blood brain barrier (BBB) becomes highly restrictive and the exchange of cells between blood and brain is mostly stopped (Galea et al., 2007).

In the adult organism, microglial cells are found throughout the whole CNS, encompassing 5-20% of the adult brain cells, with higher densities in the grey matter (Lawson et al., 1990). More precisely, an increased number of microglia can be found in the hippocampus, olfactory telencephalon and basal ganglia, an average microglial cells density can be found in the cerebral cortex, thalamus and hypothalamus, and a lower density in fiber tracts, cerebellum and most of the brainstem (Lawson et al., 1990).

The microglial turnover was assessed initially in irradiation chimera studies (in which transplanted bone marrow replaces the constitutive irradiated monocytic cell population with newly derived monocyte population) or experimental autoimmune encephalomyelitis mice (EAE, the model for human multiple sclerosis, MS, which affects CNS and is characterized by an increase of immune cells at the lesion site). These studies led to the belief that brain immune cells are replenished with populations coming from the periphery (Hickey and Kimura, 1988; Lassmann et al., 1993). However, the BBB integrity was altered in all these studies, a phenomenon which does not occur in the physiological normal brain. Further studies showed that indeed green fluorescence protein (GFP) labeled monocytes can enter the brain, but only after a 'preconditioning' step (as in the case of irradiation (Mildner et al., 2007). Another paper reported in EAE mice different behavior and physiology between resident microglia and infiltrating monocytes (Ajami et al., 2011). Moreover, based on specific markers expression and activation responses, different microglial subpopulation were recently described, suggesting that there could be different and more specialized functional subtypes of microglia inside the brain (Chen et al., 2010; Scheffel et al., 2012).

1.1.2 Microglial Functions and Morphology

Due to the presence of the BBB that blocks the transit of other specialized immune cells inside CNS, the brain is considered to be an immunoprivileged organ (Galea et al., 2007). Microglial ability to integrate the signals received from the surrounding parenchyma is accomplished via different intracellular signaling cascades that conclude in generating a prompt and accurate response. Most importantly, this process is achieved in the absence of mediation from other more specialized immune cell types, as in the case of peripheral immunity.

Microglial cells were described as being both beneficial and detrimental, with a thin line between the two states. This can be explained due to the microglial cells ability to integrate a huge variety of signals or even modulate responses elicited via a single type of stimulation. For example, microglial cells are able to detect glutamate neurotransmitter release due to glutamate receptors present on the cell surface, leading to either neuroprotective or neurotoxic outcome (Kaushal and Schlichter, 2008; Taylor et al., 2003).

The morphological differences seen in microglia were for a long time attributed to a simple linear model of microglial progression from the beneficial 'resting' state to the amoeboid activated state. However, many studies were able to show that microglia present various intermediary and interchangeable morphological and functional states, proving the inaccuracy of the linear model (Perry et al., 2007; Ransohoff and Perry, 2009; Sierra et al., 2013; Wake et al., 2013).

1.1.2.1 The Beneficial Microglia

In the physiological healthy brain, the microglia can be found in a ramified phenotype, historically labeled as 'resting' or 'quiescent' (Kettenmann and Hanisch, 2011; Perry et al., 2010; Ransohoff and Engelhardt, 2012). However, microglial cells in this state are not dormant and their processes are not immobile, but continuously scanning the brain parenchyma, as demonstrated by two-photon microscopy studies (Davalos et al., 2005; Nimmerjahn et al., 2005). Interestingly, the area covered by microglia and its processes is highly individualized, with no overlapping territories (Jinno et al., 2007).

Microglial role was evidenced in mice since CNS development, when deficits of the complement components C1q and C3 led to dysfunctions in synaptic pruning of the optic nerve (Schafer et al., 2012; Stevens et al., 2007). The intimate interaction of microglia with synapses was demonstrated also in other studies (Tremblay et al., 2010; Wake et al., 2009). Microglial

implication in synaptic regulation was also described in a study investigating delayed postnatal maturation of hippocampal circuits after impairment of microglial signaling via the fractalkine receptor (Paolicelli et al., 2011). The development of cerebellum is characterized by a reduction in Purkinje cells via apoptosis in which microglial phagocytosis contributes to the elimination of the resulted apoptotic material (Marín-Teva et al., 2004). Interestingly, microglial molecules that are traditionally linked to proinflammatory functions seem to be involved also in normal brain development, as demonstrated in tumor necrosis factor α (Tnf α) deficient mice that present visual cortex functional impairments (Kaneko et al., 2008).

Microglial involvement in neurogenesis and neuronal survival was also documented in several studies. Neurogenesis in hippocampal slice cultures was observed only in the presence of microglial cells (Sierra et al., 2010). However another study showed *in vivo* that neurogenesis can be increased by inhibition of microglial proinflammatory activation (Monje et al., 2003). Microglia can release molecules with beneficial functions for the neuronal parenchyma. For example brain-derived neurotrophic factor (BDNF) was suggested to be produced by microglia to stimulate wound axonal sprouting (Batchelor, 2002) or to modulate the neuronal activity (Coull et al., 2005). Glycine released by microglia plays a role in neuron-microglia communications by activating the N-methyl-D-aspartate (NMDA) receptors of neurons (Hayashi et al., 2006). Pascual and colleagues observed an indirect action of microglia on neurons via astrocytic mediation, in which microglial adenosine triphosphate (ATP) is released, leading to subsequent glutamate discharge by astrocytes and thus contributing to neuronal activity (Pascual et al., 2012). In animals models of traumatic injury and stroke, microglia release IL10 or Tgf β , which also present neuroprotective effects (Hanisch and Kettenmann, 2007; Streit, 2002).

It is considered that microglia are kept in an immune-suppressed state due to the presence of the so called 'off signals' mediated by a variety of ligand-receptor interaction. These off signals are generated for example by members of the immunoglobulin superfamily like neuronal cluster of differentiation 200 (CD200) recognized by the microglial CD200 receptor (CD200R), CD47-CD172a (signal regulatory protein α , SIRP α) or CD22-CD45 (Biber et al., 2007; Galea et al., 2007; Perry et al., 2010; Ransohoff and Cardona, 2010). Other off signals are represented by neuronal fractalkine (CX3C Chemokine Ligand 1, CX3CL1) recognized by the microglial fractalkine receptor (CX3CR1), neuronal intracellular adhesion molecule 5 (ICAM5) recognized by microglial receptor lymphocyte function associated antigen 1 (LFA1 or $\alpha_1\beta_2$ -integrin, formed of CD11a and CD18), interleukin 10 (IL10) and its microglial receptor IL10R, transforming growth factor β (TGF β) and its microglial receptor TGF β R, and also neurotransmitters (Biber et al., 2007; Galea et al., 2007; Perry et al., 2010; Ransohoff and Cardona, 2010). Importantly for further discussions, many of the immune-suppressing receptors present on microglia signal via immunoreceptor tyrosine-based inhibitory motifs (ITIMs) and thus changes in the availability of these signals lead to microglial activation.

Another important function of microglia is phagocytosis. The ability of microglial cells to phagocytosis or even to phagoptose (in case of whole cell ingestion) is generated by the recognition of the so called 'eat-me' signals on the structures to be internalized (Brown and Neher, 2012; Sierra et al., 2013). Microglia can recognize the 'eat-me' signals due to expression of specific receptors and respond accordingly to the stimuli, by either proinflammatory or antiinflammatory mechanisms (Ravichandran and Lorenz, 2007). Phagocytosis in the absence of inflammation is a key aspect of CNS immunity (Neumann et al., 2008). In neurodegenerative diseases, microglia are involved in the removal of potentially dangerous material, such as in taking up amyloid β ($A\beta$) in the case of Alzheimer's disease, AD (Melchior et al., 2010) or myelin debris in MS and EAE models (Bauer et al., 1994).

1.1.2.2 The Harmful Microglia

Alterations of the normal functions of the organism and/or its lower levels of organization can affect also the normal function of CNS. Generally, the detrimental functions of microglia inside CNS were studied more extensively and were more evident compared with the functions of the immunosuppressed microglia.

Subsequent to injury or infection, a systemic response is triggered inside the organism, that leads to metabolic and sickness-behavior changes (Perry et al., 2007). The immune communication between the periphery and CNS was described as being mediated via three different routes: a direct path through the vagal nerve, another through cytokines and other inflammatory molecules carried to sites lacking BBB protection (and thus reaching directly the brain parenchyma), and an indirect path through mediation of the perivascular macrophages that respond to changes in blood composition (Perry et al., 2007). After recognition and integration of these specific stimuli (as well as in the case of direct brain damage), microglia can become activated, changing their morphology progressively from the ramified state to an amoeboidal state (Kreutzberg, 1996). Beside these extrinsic stimuli, microglial phenotype and function are altered by intrinsic stimuli, as for example by runt related transcription factor 1 (Runx1) or interferon regulatory factor 8 (Irf8), which regulate microglial morphological changes (Minten et al., 2012; Zusso et al., 2012).

Following acute brain injury, microglial cells are able to quickly extend their processes to the lesion site (Davalos et al., 2005) and even to move the entire cellular body towards the lesion (Meyer-Luehmann et al., 2008). Moreover, there are evidences pointing out that migration is required for the initiation of other functions, as it was demonstrated in mice lacking the CXC

chemokine receptor 3 (CXCR3), in which microglia do not migrate and as a consequence cannot remove dendrites after brain injury (Rappert et al., 2004).

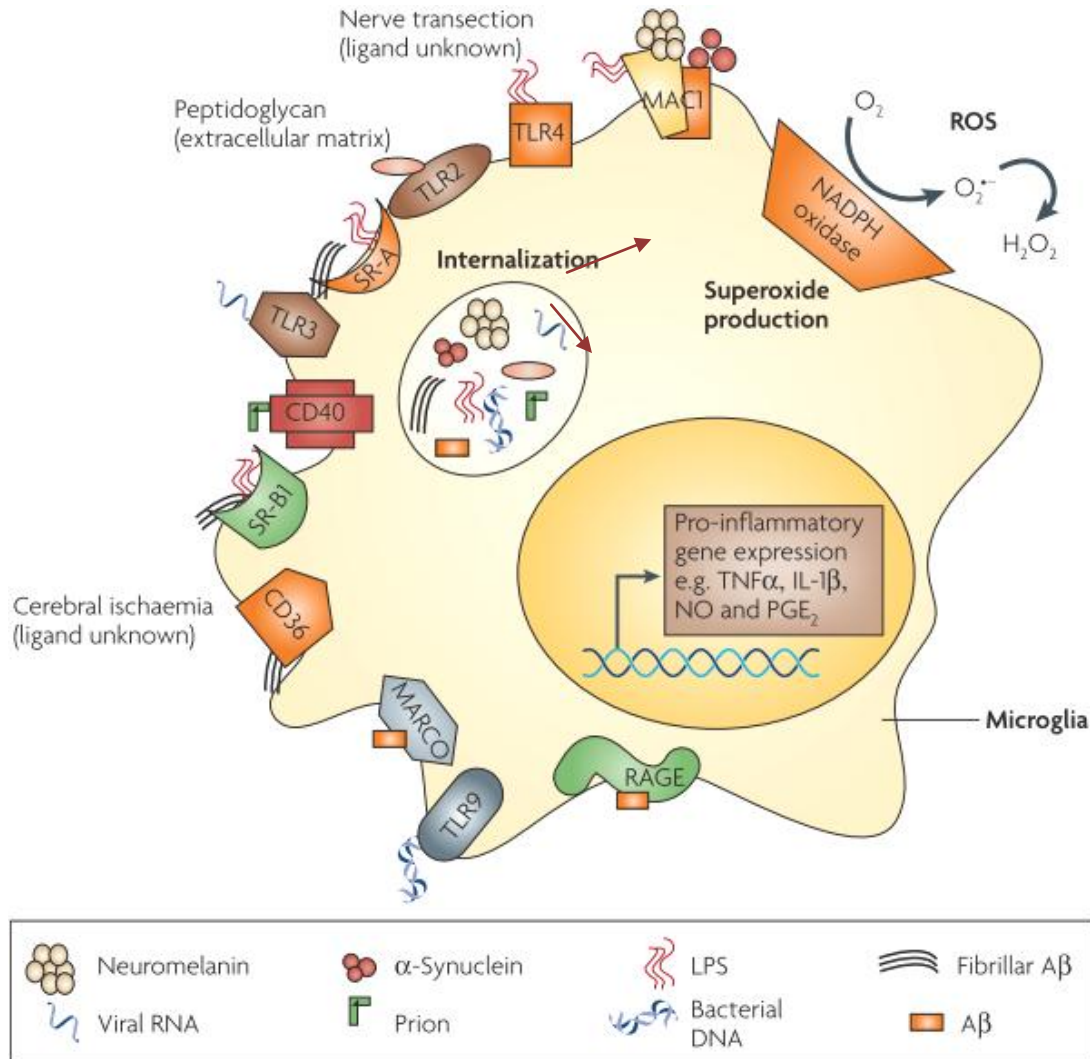


Figure 1.1 – Pattern recognition receptors (PRRs) on the surface of microglia. Microglial cells can identify and internalize extracellular molecules (see box) by recognizing molecular via PRRs or PRR complexes. Subsequently, a specific response is build, consisting in phagocytosis and lysosome-mediated degradation of the internalized structures, release of superoxide (O₂⁻) for killing microbes, or secretion of proinflammatory molecules for intercellular communication (acronyms detailed in the ‘abbreviations’ section; modified from Block et al., 2007).

The damage-associated molecular pattern molecules (DAMPs) found at the site of injury or molecules released by damaged or degenerating cells are recognized by specialized receptors present on microglial surface (Fig. 1.1), like scavenger receptors (Bamberger et al., 2003), toll-like receptors (TLRs; Olson and Miller, 2004) or purinergic receptors (Koizumi et al., 2007). By receptor engagement, microglial cells are able to recognize pathogen-associated molecular patterns (PAMPs) like lipopolysaccharides (LPS) found in the gram negative bacterial wall,

double stranded ribonucleic acids (dsRNA) or other microorganism and viruses related molecules (Kettenmann and Hanisch, 2011; Neumann et al., 2008). Interestingly, in certain pathological conditions, microglia can even be activated by otherwise beneficial self molecules, which are normally not found inside the brain parenchyma, like the serum component fibrinogen (Adams et al., 2007).

Another response to microglial activation is the release of a highly diversified variety of soluble factors, like proinflammatory cytokines including interleukins (IL1 β , IL2, IL6), TGF β 1, macrophage colony-stimulating factor (MCSF), granulocyte-macrophage colony stimulating factor (GMCSF) or TNF α (Cunningham et al., 2005; Kreutzberg, 1996).

Based on the receptors expressed or the response to specific stimuli, there was a tendency to classify microglia by using a system developed in macrophages (Mantovani et al., 2002). Within this system, cells are divided within a classical M1 phenotype (stimulated by LPS plus interferon- γ , IFN γ) or the alternatively activated states M2a (stimulated by IL4/IL13), M2b (IL1) or M2c (TGF β , IL10). However, microglia are significantly different than peripheral macrophages in regard to their activation pattern (Ransohoff and Perry, 2009) and thus this classification terminology is inadequate when referring to microglial cells.

Additionally, microglial response to dangerous signals implies activation of nitric oxide synthase (NOS; Saha and Pahan, 2006) or nicotinamide adenine dinucleotide phosphate oxidase (NADPH oxidase; Block, 2008), which generates either nitric oxide (NO) or superoxide (O $_2^{\cdot-}$). Both NO and O $_2^{\cdot-}$ are toxic to infectious microorganisms, but also for the surrounding brain parenchyma, being correlated with neurodegenerative diseases like PD or AD (Block, 2008; Liu et al., 2002).

1.2 Microglial Involvement in Neurodegenerative Diseases

Microglial involvement in different neurological pathologies was vastly studied (Hanisch and Kettenmann, 2007; Neumann et al., 2008; Perry et al., 2010; Ransohoff and Perry, 2009; Wyss-Coray and Rogers, 2012). Evidence of neurological pathology in which microglial activity is not involved is almost non-existent, as it was demonstrated with a variety of tools, ranging from cellular or animal models to positron emission tomography (PET)-evaluations of human patients (Perry et al., 2010). Compared with brain parenchyma acute injuries, neurodegeneration is a process in which microglia are becoming progressively activated, requiring longer periods of time to reach a fully activated state (Perry et al., 2007).

1.2.1 Nasu-Hakola Disease (NHD)

Nasu-Hakola disease (NHD), also known as polycystic lipomembranous osteodysplasia with sclerosing encephalopathy (PLOS), is a rare recessive human disorder characterized by presenile dementia and bone cysts (Bianchin et al., 2010; Kaneko et al., 2010a; Satoh et al., 2011a). In the affected humans, the first symptoms of the disease are reported in the 3rd to 4th decade of life, when patients present frequent bone lesions (Kaneko et al., 2010a). Further on, the disease progresses towards a form of fronto-temporal dementia, leading to death in a couple of years (Bianchin et al., 2010). The main brain areas affected in NHD are the frontotemporal lobes and the basal ganglia, where neuronal loss together with astroglial cells proliferation and hypertrophy was reported (Kaneko et al., 2010a). However, the main characteristic of NHD is microglia activation (Bianchin et al., 2010; Satoh et al., 2011a).

Today it is known that the molecular feature of NHD is loss of function mutations in the gene encoding the triggering receptor expressed in myeloid cells 2 (TREM2; Paloneva et al., 2002) or the gene encoding TREM2 associated adaptor molecule DNAX-activating protein of molecular mass 12 kDa (DAP12, also known as killer-cell activating receptor-associated protein, KARAP, or TYRO protein tyrosine kinase-binding protein, TYROBP; Kuroda et al., 2007; Paloneva et al., 2000). Functional TREM2 and DAP12 were demonstrated to be required for the normal differentiation and function of myeloid lineage cells osteoclasts (Paloneva et al., 2003). In the absence of TREM2, impaired bone resumption and inability of human NDH-derived osteoclasts to form multinucleated cells was reported (Cella et al., 2003), whereas DAP12 KO mice presented osteopetrosis and hypomyelinoses (Kaifu et al., 2003). Inside brain, *Trem2/DAP12* mRNA expression in mice is detected starting with E14 and colocalised with microglia/macrophages markers (Thrash et al., 2009). Mouse primary cell cultures evidenced that the TREM2/DAP12 complex is involved in microglial removal of apoptotic neurons without inflammation (Takahashi et al., 2005). Based on these data, NHD is emerging as the prototype of the primary microglial disorder inside CNS (Bianchin et al., 2010).

1.2.1.1 The TREM2/DAP12 Signaling Complex

The first TREM family members (TREM1 and TREM2) were discovered in 2000, with functions related to the inflammatory response and associated with the already known DAP12 adaptor molecule (Bouchon et al., 2000). Besides TREM1 and TREM2, other molecules within the TREM family were described: TREM3 (functional gene in mice and pseudogene in humans) or trem-like transcripts (TLT1 and TLT2; Allcock et al., 2003). In vertebrates, the TREM members present

conserved evolutionary structures similar in humans, mice, pigs, cows and chickens (Allcock et al., 2003). The general, the structure of TREMs is composed of an extracellular V-type immunoglobulin-like domain, a single transmembrane domain and a cytoplasmic domain (Colonna, 2003).

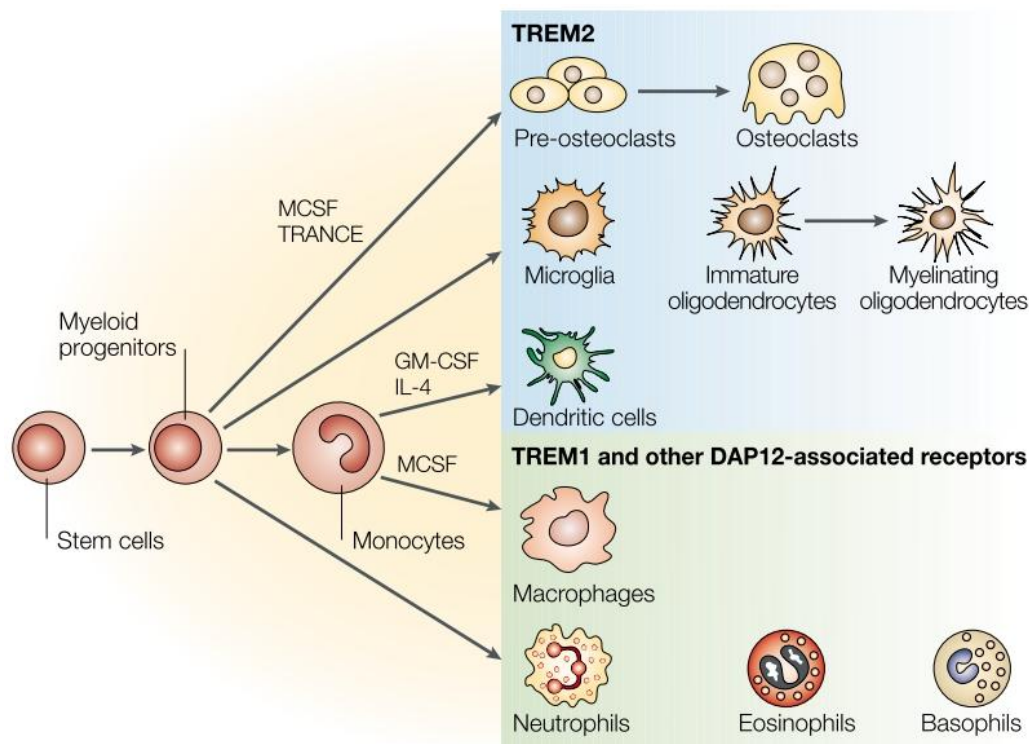


Figure 1.2 – TREM2 and TREM1 expression and regulation in myeloid cells. TREM2 is expressed by monocyte-derived dendritic cells, immature osteoclasts and microglia. TREM1 is expressed in mature neutrophils, monocytes and macrophages (Colonna, 2003).

TREM2 is considered an orphan receptor present on the surface of macrophages, immature dendritic cells, osteoclasts and microglia (Fig. 1.2; Colonna, 2003). The extracellular domain of murine TREM2 seems to be involved in recognizing polyanionic carbohydrate microbial products (Daws et al., 2001; N'Diaye et al., 2009; Quan et al., 2008). However, the specific molecular pattern recognized by TREM2 is not yet clear. The endogenous ligand of TREM2 is yet unknown, even though it was demonstrated that TREM2 is involved *in vitro* in microglial phagocytosis of apoptotic neurons without inflammation (Hsieh et al., 2009; Takahashi et al., 2005). Nevertheless, these findings were not reproduced *in vivo* (Hsieh et al., 2009). The presence of an unidentified ligand on the surface of peritoneal and bone-marrow derived macrophages was observed using TREM2/Fc-chimera fusion proteins (Hamerman et al., 2006). Another study that used both murine and human TREM2 fusion proteins to study their binding to different cell types found that surface-exposed heat shock protein 60 (Hsp60) might act as a possible endogenous ligand for TREM2 (Stefano et al., 2009). However, within the study, mainly

tumoral cell lines were used as targets for TREM2 fusion proteins and thus the extracellular structures might have been already altered compared to the normal extracellular structures.

TREM2, as the majority of the TREM family members, presents a short intracytoplasmic domain that is unable to generate signaling cascades (Fig. 1.3). Thus, TREM2 requires the recruitment of DAP12 for intracellular signaling (Bouchon et al., 2000; Colonna, 2003). TREM2-DAP12 interaction is based on electrostatic bounds between a lysine residue in the transmembrane domain of TREM2 and an aspartatic acid residue in the structure of DAP12 (Bouchon et al., 2000; Colonna, 2003). Based on immunoprecipitation, Takegahara and colleagues were able to show that TREM2 can form a heterocomplex together with PlexinA1, thus connecting PlexinA1 with DAP12 signaling (Takegahara et al., 2006). Interestingly, the PlexinA1 KO animals also present deficits in osteoclast development similar to the ones found in DAP12 KO animals (Takegahara et al., 2006). Interactions between TREM2, DAP12 and other receptors, especially with the similar TREM1, were not yet described.

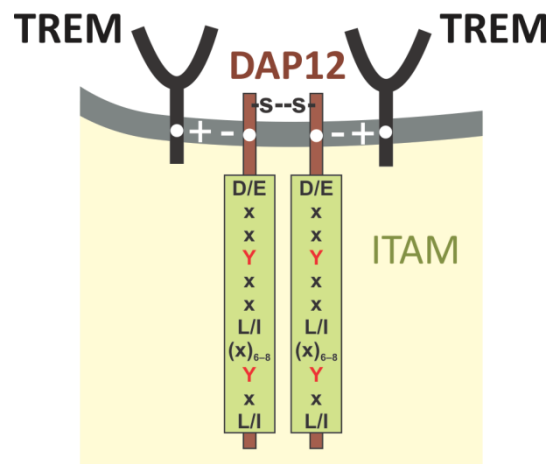


Figure 1.3 – The TREM/DAP12 complex. Transmembrane domain of TREM receptors permits recruitment of DAP12 via charged interactions. DAP12 can form dimers based on an extracellular disulfide bond. Inside the cell, DAP12 presents an immunoreceptor tyrosine-based activating motif (ITAM). The tyrosine residues (red Y) of ITAM can be phosphorylated, releasing intracellular signals following TREM2 activation.

DAP12 is a molecule abundantly expressed by myeloid and natural killer cells (Lanier, 2009). Orthologues of the DAP12 encoding gene (TYROBP) were found throughout all vertebrates (from zebra fish to higher primates; Lanier, 2009; Tomasello and Vivier, 2005). Proteins similar in function could be identified in lower species, as CED1 receptor in *Caenorhabditis elegans* and Draper protein in *Drosophila* (Ziegenfuss et al., 2008). DAP12 presents structural similarities with the common γ -chain (FcR γ , also known as Fc ϵ R1 γ), and CD3 ζ , all having a small extracellular domain containing cysteine residues that can form dimers via an extracellular disulfide bond and an immunoreceptor tyrosine-based activation motif (ITAM) inside the cell (Lanier, 2009). ITAM is a highly conserved sequence consisting of the amino acids D/ExxYxxL/I(x)₆₋₈YxL/I, where 'x' represents any amino acid (Fig1.3; Hamerman et al., 2009; Ivashkiv, 2008).

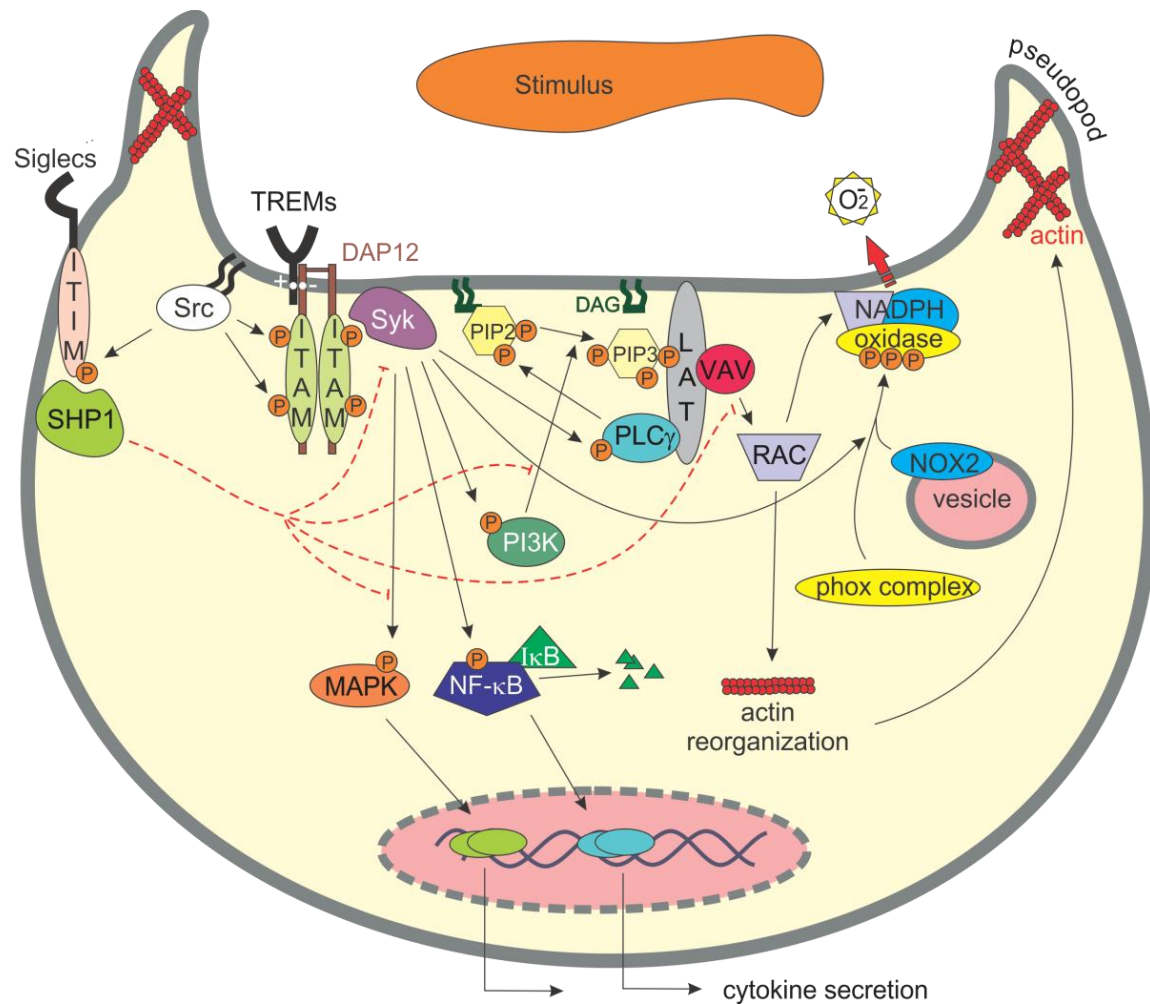


Figure 1.4 – The general TREM/DAP12 signaling pathways. After receptor engagement, signaling inside the cell is generated via the ITAM domain of DAP12 adaptor molecule. The recruited spleen tyrosine kinase (Syk) acts on different substrates, leading to cytokines release via the mitogen activated protein kinase (MAPK) or nuclear factor kB (NFkB) activation, calcium signaling via the phospholipase C γ (PLC γ), actin reorganization via the linker for activation of T cells (LAT) and RAC G-protein, or release of superoxide (O₂^{•-}) via activation of nicotinamide adenine dinucleotide phosphatase-oxidase (NADPH oxidase). The ITAM-related activation is inhibited by signaling via immunoreceptor tyrosine-based inhibitory motifs (ITIM) present in the structure of certain receptors (e.g. sialic acid-binding immunoglobulin-like lectins, Siglecs).

The initial studies on the TREM2/DAP12 pathway by using agonistic TREM2 antibodies revealed increased intracellular calcium and activation of the ERK1/2 (Bouchon et al., 2001). However, no activation of ERK was detected when F(ab)' antibodies were used, indicating that for TREM2-mediated activation at least two receptors must be cross-linked (Bouchon et al., 2001). Further, the signaling cascade initiated by DAP12 after TREM2 engagement by a yet unknown ligand follows the usual DAP12 signaling pathway described in other reports (Lanier, 2009; Tomasello and Vivier, 2005; Turnbull and Colonna, 2007). Thus, it was first proven in natural killer cells (NKs) that the ITAM motif of DAP12 can be phosphorylated, leading to cellular activation via ζ -

chain-associated protein kinase of 70 kDa (ZAP-70) and Syk kinases, a mechanism similar with that of the T- and B-cell antigen receptors via CD3 ζ with which DAP12 presents structural resemblances (Lanier et al., 1998). Other studies contributed to identification of the DAP12 canonical signaling pathway, as reviewed in Turnbull and Colonna (2007): the recruitment of Syk to Dap12 ITAM motif leads to activation of phosphoinositol 3-kinase (PI3K), activation of phospholipase C gamma (PLC γ), together with phosphorylation of scaffolding proteins linker for activation of T cells (LAT) and non-T cell activation linker (NTAL) and ending with activation of protein kinase C (PKC) and ERK, intracellular calcium release and actin polymerisation. This succession of cellular events triggers cellular activation represented by functions like migration, phagocytosis or cytokines release (Turnbull and Colonna, 2007).

Of note, TREM2 engagement, unlike TREM1, does not lead to I κ B α activation with subsequent nuclear transposition of Nf κ B and release of proinflammatory molecules (Bouchon et al., 2001). On the contrary, *in vitro* studies of mouse microglial primary cultures showed that TREM2 present anti-inflammatory functions (Takahashi et al., 2005). Shorthairpin RNA knockdown of TREM2 decreased clearance of apoptotic neurons and induced transcription of *Tnfa* and *Nos2* (Takahashi et al., 2005).

ITAM signaling is under the control of immunoreceptor tyrosine-based inhibitory motif (ITIM)-bearing molecules (Barrow and Trowsdale, 2006; Hamerman et al., 2009). The ITIM sequence is represented by the amino acid sequence S/I/V/LxYxI/V/L, where 'x' represents any amino acid (Ravetch, 2000). ITIM sequences can be found in more than 36 different receptors, among them being sialic acid-binding immunoglobulin-like lectins, Siglecs (Staub et al., 2004). Receptors signaling via ITIM are implicated in supplying the inhibitory 'off signals' to the cell (Fig. 1.4). The inhibitory process is achieved by phosphorylation of the ITIM tyrosine by Src, leading to recruitment of phosphotyrosine phosphatases (PTP), such as SH2 domain containing phosphatase 1 (SHP1) or SH2 domain containing inositol phosphatase 1 (SHIP1), which in turn inhibits ITAM phosphorylation or activation of molecules downstream of ITAM (Peng et al., 2010; Ravetch, 2000).

1.2.2 Parkinson's Disease (PD)

PD is a progressive neurodegenerative disorder characterized by clinical symptoms like bradykinesia, tremor, rigidity and postural instability (Dauer and Przedborski, 2003). PD is only one type of the wider category of Parkinsonian disorders that have different molecular pathologies, but which all present loss of dopaminergic neurons projecting from the substantia nigra *pars compacta* (SNpc) to the putamen (Dickson, 2012). At cellular level, the main

characteristic of PD is the presence of α -synuclein aggregates, the so-called Lewy bodies (inside neuronal bodies) or Lewy neurites (inside dendrites). Different stages of PD were described based on the α -synuclein inclusions (Braak et al., 2003).

Epidemiological studies on PD showed that 95% of the cases are sporadic with late onset, whereas only 5% are familial PD with genetic-determined early onset (Block and Hong, 2005). Familial PD is associated with mutations in several genes like the parkinson genes (*PARKs*), leucine-rich repeat kinase 2 gene (*LRRK2*) or α -synuclein gene (*SNCA*) (Kumar et al., 2012).

Presenting a lower level of glutathione as buffer against the oxidative stress, dopaminergic neurons are a neuronal subpopulation that is more susceptible to the deleterious effects of microglial activation (Loeffler et al., 1994). Moreover, dopamine molecules and tyrosine hydroxylase (TH) involved in dopamine biosynthesis, are promoters of oxidative stress due to their chemical structure (Di Giovanni et al., 2012).

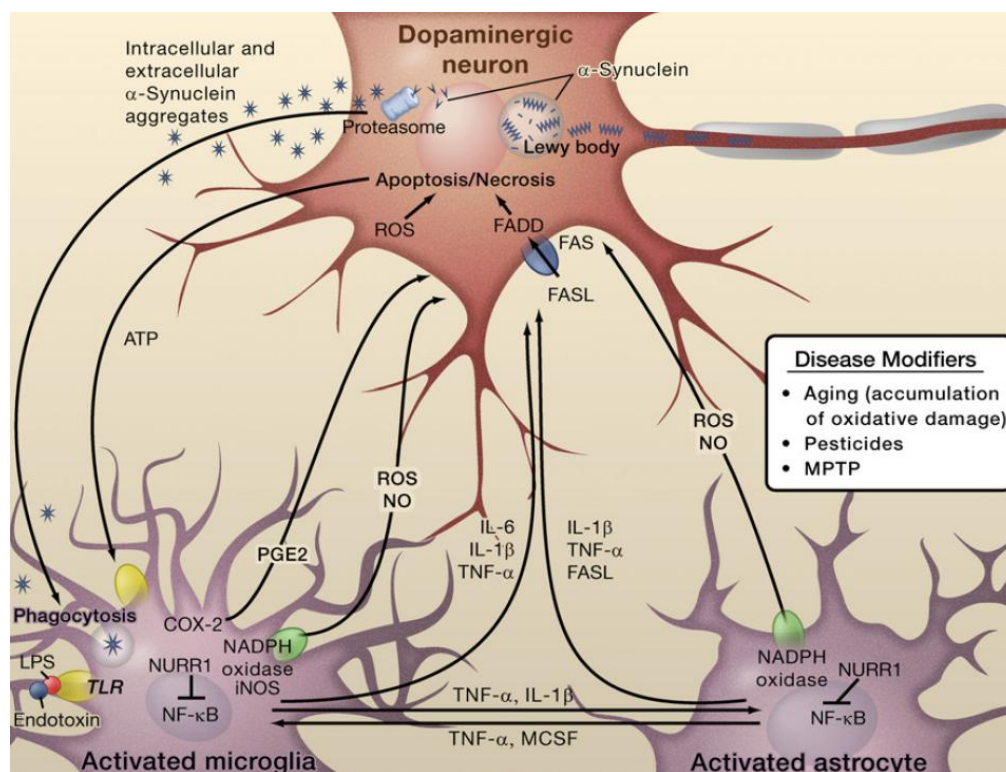


Figure 1.5 – Mechanisms of neurodegeneration in PD. Microglia become activated by detecting extracellular α -synuclein, potentiating the NF κ B pathway and leading to the release of proinflammatory molecules. Together with activation of the NADPH oxidase, inducible nitric oxide synthase (iNOS) and cyclooxygenase 2 (COX2), toxic molecules acting on dopaminergic neurons are released inside the brain parenchyma. These molecules amplify microglial activation and also induce a toxic response from astrocytes, further contributing to the neurodegenerative process (Glass et al., 2010).

The involvement of microglia in the pathology of PD is well documented (Fig1.5; Block and Hong, 2005; Cunningham, 2013; Dauer and Przedborski, 2003; Glass et al., 2010; Hirsch et al.,

2012; Perry, 2012). There is a common scientific consensus that microglia are activated by the α -synuclein aggregates leading to the release of a broad range of proinflammatory molecules. *In vivo* models of PD are characterised by microglial release of IL1 β , IL2, IL6, Tnf α or Tgf β as response to α -synuclein (Glass et al., 2010; Roodveldt et al., 2008). These results confirmed previous studies that mentioned similar cytokine patterns in brains affected by PD (Mogi et al., 1994a, 1994b). In rat and mouse primary cultures microglia contribute to extracellular clearance of α -synuclein via phagocytosis, followed by NADPH oxidase-mediated production of O₂⁻ (Zhang et al., 2005). Indeed, Hunot and colleagues have previously reported increased level of NADPH oxidase and inducible nitric oxide synthase (iNOS) in PD brains (Hunot et al., 1996).

1.2.2.1 Animal Models of PD

Microglial implication in PD was widely studied in different *in vivo* and *in vitro* models. Generally, mouse models were used to reproduce human diseases due to their neuronal physiology and gene-associated homology (Waterston et al., 2002). A broad range of mouse model techniques were used to better characterise the human PD condition, leading to progress in the understanding of some aspects of the disease. However, to this date no generally valid model recapitulates the entire constellation of PD associated symptoms and dysfunctions (Lee et al., 2012; Pickrell et al., 2013). To study the genetic aspect of PD, knock-out (KO), knock-in or conditional transgenic animals were generated for genes implicated in PD. For example, the expression of human α -synuclein in mice was discovered to promote formation of abnormal axons and terminals, age-related impairments in motor coordination and age-related reduction in dopamine content and metabolites (Richfield et al., 2002). A similar phenotype was observed in another study using conditional human α -synuclein mice under a specific neuronal promoter (Nuber et al., 2008). Other PD mouse models have used induction of transgenes via viruses stereotactically injected inside the brain. Thus, injections of expressing viruses into the striatum permitted *in vivo* identification of LKRR2 enzyme inhibitors, thus efficiently protecting the nigrostriatal system against degeneration (Lee et al., 2010).

Toxicological studies proved the specificity of dopaminergic degeneration, also pointing to microglial involvement in the process (Bezard et al., 2013; Dauer and Przedborski, 2003; Miller et al., 2009). Thus, neurotoxins like 6-hydroxydopamine (6-OHDA) or 1-methyl-4-phenyl-1,2,3,6-tetrahydropyridine (MPTP), as well as other toxic compounds (e.g. rotenone, paraquat) were shown to lead to a PD-like phenotype.

1.2.2.1.1 Lipopolysaccharide (LPS)-triggered Dopaminergic Degeneration

Lipopolysaccharides (LPS) were identified as an *in vivo* experimental inducer of dopaminergic neurons degeneration, similar with the one observed in PD (Gao et al., 2002; Qin et al., 2007). LPS is a compound found on the outer membrane of gram-negative bacteria. The general structure of LPS is composed of an O-antigen polysaccharide chain core composed of outer and inner polysaccharides and the so called lipid A, consisting of a diglucosamine to which six fatty acid chains are attached (Erridge et al., 2002).

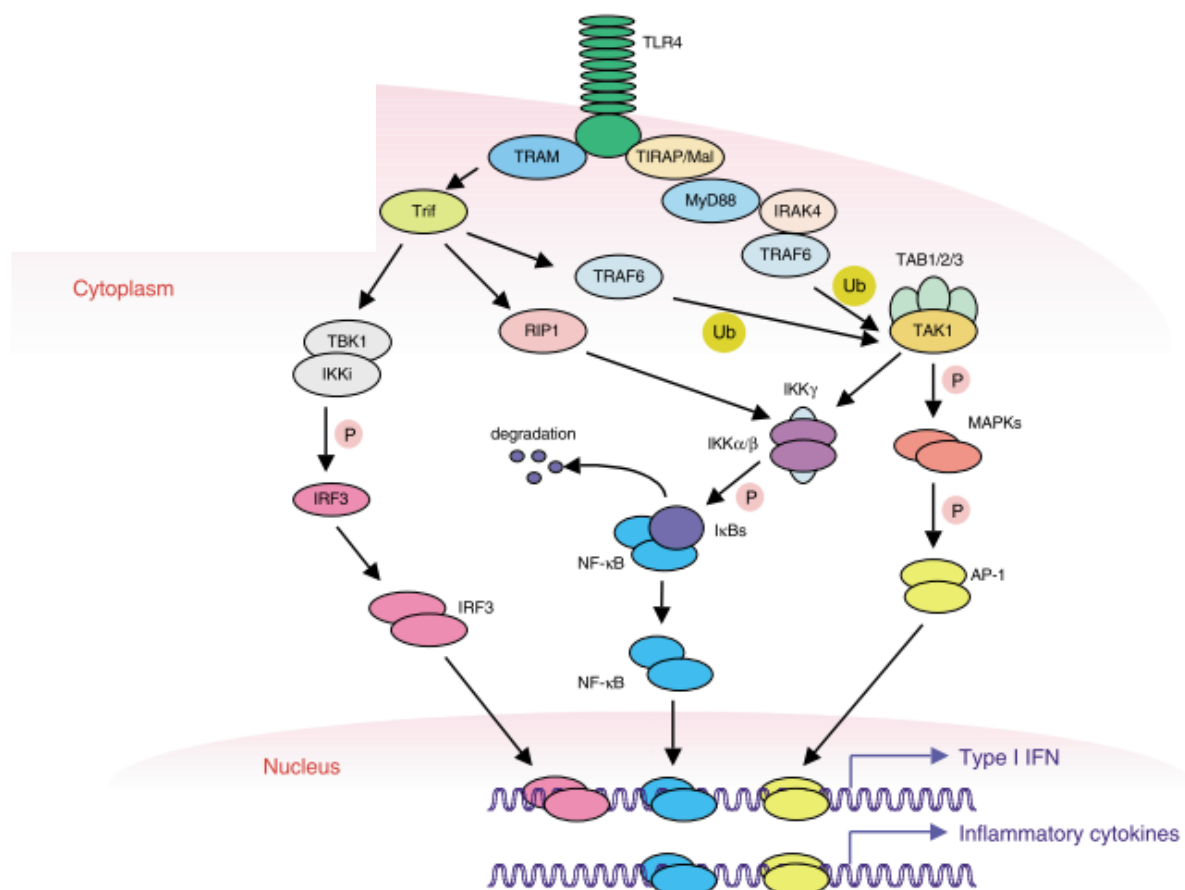


Figure 1.6 – Toll like receptor 4 (TLR4) signaling pathway. Upon ligand (e.g. LPS) engagement, TLR4 activates the myeloid differentiation primary response protein 88 (MyD88)-dependent and the TIR-domain-containing adaptor-inducing interferon- β (Trif)-dependent pathways. MyD88 leads to secretion of proinflammatory cytokines via activation of nuclear factor κ -light-chain-enhancer of activated B cells (NF κ B) nuclear transposition and activation protein-1 (AP-1), whereas Trif-mediated pathway contributes also to the release of proinflammatory cytokine via NF κ B and AP-1 activation, but additionally also to the secretion of type I interferons (IFN; modified after Kawai and Akira, 2006).

LPS driven inflammation was exhaustively studied both *in vitro* and *in vivo*, the signaling pathway released by LPS being well described (Fig. 1.6). LPS is recognized by a complex formed by the toll like receptor 4 (TLR4; CD284) and the myeloid differentiation factor 2 (MD2) in cooperation with CD14 (Miller et al., 2005; Park et al., 2009). After activation, the signaling cascades can follow a myeloid differentiation primary response protein 88 (MyD88)-dependent or MyD88-independent pathway, leading to release of inflammatory cytokines, interferon γ (IFN γ) and IFN-inducible proteins (Kawai and Akira, 2006; O'Neill et al., 2013). LPS leads to activation of immune cells, including microglia (Kettenmann and Hanisch, 2011).

Among the effects of *in vivo* LPS administration were reported circulatory shock, disseminated intravascular coagulation and damages to numerous organs such as CNS, liver, kidney, heart, gastrointestinal tract and lungs, ending with shock and death (Hasegawa et al., 1999)

To study the involvement of LPS in dopaminergic degeneration *in vivo*, different models of LPS application were used, ranging from direct intranigral injection to systemical application of LPS (reviewed in Cunningham, 2013; Dutta et al., 2008). Single injections of LPS directly into the SN of rodents led to increased dopaminergic neurons loss together with decreased levels of dopamine 21 days after the injection (Castaño et al., 1998). Studies on the kinetics of dopaminergic neuron loss showed that microglial cells are promptly activated by intracranial LPS application, increasing their production of inflammatory cytokines (Arai et al., 2004) and ROS (Qin et al., 2004) with loss of dopaminergic neurons detected only a couple of weeks after injection (Fig. 1.7; Liu, 2006; Liu et al., 2000). Similar pattern of microglia activation and dopaminergic degeneration was observed in rats supranigraly infused with LPS over a 2 week period (Gao et al., 2002). Other studies have shown that dopaminergic degeneration reaches an irreversible plateau 8 weeks after LPS application based on LPS concentration, whereas microglial activation gradually subsides (Iravani et al., 2005; Liu, 2006). Injections with LPS into the globus pallidus (part of the basal ganglia involved in movement control) led to loss of SN $_{pc}$ dopaminergic neurons in particular in older animals compared with young ones (Zhang et al., 2005). The model of direct LPS injection inside CNS provided *in vivo* evidence of higher SN $_{pc}$ dopaminergic neuronal sensitivity to the LPS application compared with the SN γ -aminobutyric acid signaling neurons (GABAergic neurons) or even dopaminergic neurons of the ventral tegmental area (Castaño et al., 1998; Gao et al., 2002).

Based on the evidence of communication between the peripheral immunity and the CNS local immunity, systemic inflammation was hypothesized to induce neurodegeneration (Galea et al., 2007; Perry et al., 2010). Indeed, Qin and colleagues showed that one systemic intraperitoneal (i.p.) application of 5 μ g LPS per gram body weight (gbw) leads not only to dopaminergic neuronal loss, but also that the process is progressive (Qin et al., 2007), unlike that of direct

intranigral LPS application. However, the dopaminergic loss was shown to be significant only 7 months after LPS i.p. injection (Qin et al., 2007).

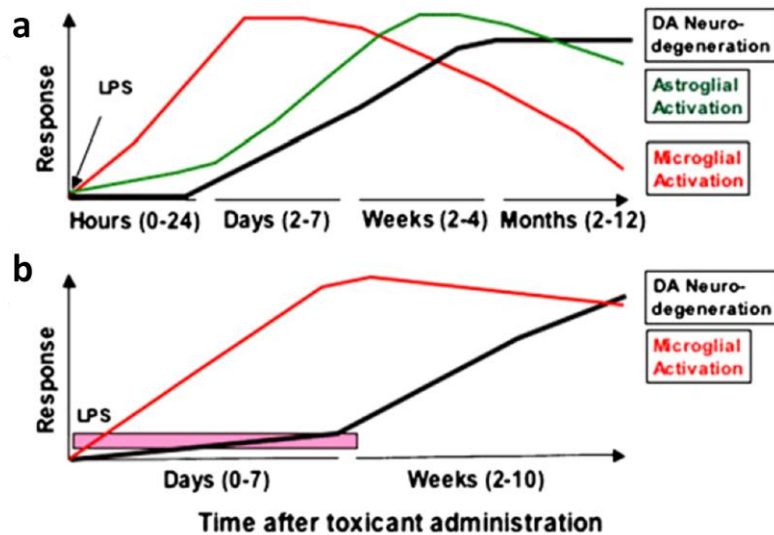


Figure 1.7 – Kinetics of LPS-triggered dopaminergic loss in animal models. **a** – A single intranigral injection of LPS elicits a fast response in microglia (red line) and astrocytes (green line), with dopaminergic loss (black line) reaching a plateau phase in a couple of months after treatment; **b** – Infusing LPS intranigraly for a period of several days decreased the time required to obtain dopaminergic neuronal loss (modified from Liu, 2006).

Dopaminergic degeneration was also explored in relation to LPS exposure in fetal stages. Pups exposed to LPS *in utero* and again a second time after birth, presented specific and significant reduction in the number of SNpc dopaminergic neurons and of striatal dopamine compared with controls (Ling et al., 2006). Moreover, prenatal exposure to LPS increases the susceptibility of dopaminergic degeneration after challenges with other toxins, like Ling and colleagues observed in a rotenone study (Ling et al., 2004).

1.2.3 Alzheimer's Disease (AD)

AD is the most common age-related neurodegenerative disease, characterized by progressive loss of memory and cognitive functions (LaFerla et al., 2007). The first severe neuropathological changes can be observed in the hippocampus, followed by the associated cortical and subcortical structures (Götz and Ittner, 2008). Even though detailed cellular pathology of AD was reported from the 1900s as being represented by extracellular and intracellular depositions inside the brain, the chemical composition of these depositions was not identified until the 1980s. Thus, the extracellular structures (or 'plaques') were described as

being composed of small peptides called amyloid- β ($A\beta$; Glenner and Wong, 1984), whereas the neurofibrillary tangles (NFT) found inside neurons were described as consisting of aggregated and hyperphosphorylated tau protein (Grundke-Iqbal et al., 1986).

$A\beta$ is generated via successive cleavage of the amyloid precursor protein (APP) via successive contribution of specific enzymes, generally termed 'secretases' (Fig. 1.8). The processing of APP can follow either a normal non-amyloidogenic pathway (the non-pathological pathway) or an amyloidogenic pathway (leading to $A\beta$ pathological accumulation; Citron, 2004; LaFerla et al., 2007).

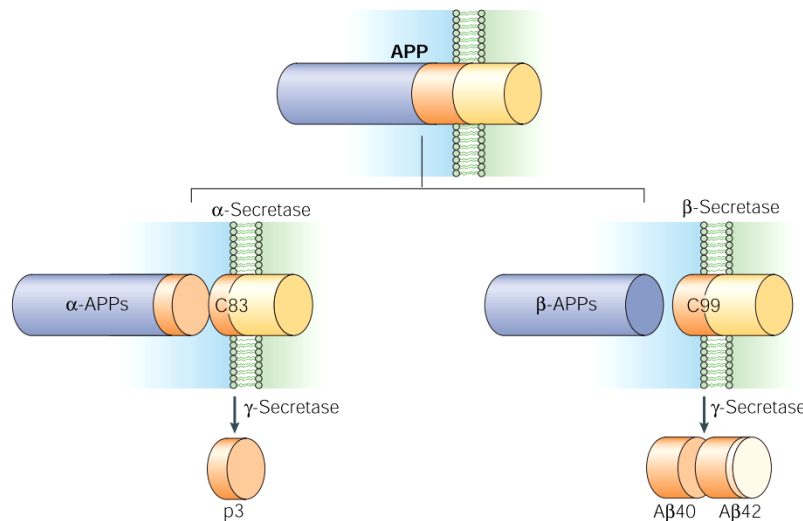


Figure 1.8 – Amyloid precursor protein (APP) processing. **Left** - The non-amyloidogenic pathway is started by the action of α -secretase on APP that releases soluble the α APPs fragment and the C83 membrane fragment. C83 is further processed by γ -secretase, generating the non-toxic p3 fragment; **Right** - The amyloidogenic pathway is initiated by β -secretase cleavage of APP that releases the β APPs fragment and the C99 membrane fragment. C99 can be cleaved via action of γ -secretase, generating $A\beta$ fragments (Citron, 2004).

The non-amyloidogenic pathway requires the initial release of sAPP α N-domain and of C83 C-terminal fragment from APP by the action of α -secretase (a disintegrin- and metalloprotein-family enzyme, ADAM; Allinson et al., 2003). C83 can be subsequently cleaved by γ -secretases releasing the shorter non-toxic fragment p3 (Haass and Hung, 1993). Of note here is that the γ -secretase is a multi-subunit enzyme formed of presenilin (PS), nicastrin, anterior pharynx-defective 1 (APH1) and presenilin enhancer 2 (PEN2; Sisodia and St George-Hyslop, 2002). Mutations in γ -secretase substructures can lead to certain pathological conditions as discussed further.

The pathological amyloidogenic pathway of APP processing leads to release of $A\beta$ fragments of different sizes and with different toxicities via a mechanism that requires an initial cleavage step performed by β -secretase (known also as β -site APP-cleaving enzyme 1, BACE1; Sisodia

and St George-Hyslop, 2002). After β -secretase processing of APP, soluble sAPP β and C99 C-terminal fragments are released. C99 is further processed by γ -secretase which can cleave at different sites and thus releasing A β fragments of different sizes. The A β with 40 amino acid residues (A β 40) is the most abundant product of C99 processing (LaFerla et al., 2007). However, it has been observed that A β 42 is found in great quantity in AD plaques (Braak and Braak, 1991) and that A β 42 is highly toxic for the brain parenchyma (reviewed in Benilova et al., 2012). Moreover, it was proven that A β 42 has a high tendency to aggregate into oligomers or fibrils both *in vitro* (Barrow and Zagorski, 1991) and *in vivo* (McGowan et al., 2005).

Unlike AD plaques that are constituted of A β aggregates, the NFT lesions present aggregates of microtubule-associated protein τ (tau). Under normal physiological conditions, tau presents several phosphorylation sites and is implicated in the stabilization of microtubules inside the axons (Ballatore et al., 2007). However, under pathological conditions, tau was found in a hyperphosphorylated state that contributes to its detachment from microtubules, leading to destabilization of the entire neuronal scaffold system (Götz and Ittner, 2008). Based on postmortem NFT depositions, AD pathology was divided into 6 different stages (Braak and Braak, 1991). There are different theories trying to explain the link between the presence of both A β and tau deposits in the AD diseased brain. However the results are so far inconclusive.

Studies on the etiology of AD have indentified an early onset of the disease (EOAD, also known as familial AD, FAD) or a late onset AD (LOAD, also known as sporadic AD, SAD). EOAD has a higher incidence between 60 and 65 years of age (Bertram and Tanzi, 2008) and accounts for only 1% of the total AD cases (Götz and Ittner, 2008). EOAD was described as being caused by autosomal-dominant mutations in ether the APP encoding gene (*APP*) or in the γ -secretase subunits PS1 (*PSEN1*) or PS2 (*PSEN2*; Bertram and Tanzi, 2008). LOAD on the other hand does not present any autosomal causality, but a high allele diversity across different genes (Bertram and Tanzi, 2008). However, excepting the age of onset (above 65 years), the clinical and histopathological characteristics of LOAD cannot be distinguished from EOAD (Götz and Ittner, 2008). Genome wide association studies (GWAS) have identified several clustering patterns pointing towards immunity (*CLU*, *CR1*, *CD33*, *EPHA1*, *MS4A4A/MS4A6A*), lipid processing (*APOE*, *ABCA7*) or endocytosis (*PICALM*, *BIN1*, *CD2AP*) involvement in LOAD (reviewed in Bettens et al., 2013). Besides the ϵ 4 allele of the apolipoprotein E gene (*APOE*), no other gene has shown high LOAD incidence risk (Bertram et al., 2007; Neumann and Daly, 2013). Recently, *TREM2* gene has been described by two individual groups as having similar odds ratio with that of *APOE* (Guerreiro et al., 2013; Jonsson et al., 2013).

Microglial role in AD is still under debate with studies pointing towards a detrimental role of microglia in AD pathology via activation and release of toxic factors (Fig. 1.9) or with studies providing evidence supporting microglia involvement in the clearance of A β plaques. Initial

studies on the cellular pathology of AD have observed clustering of microglia around the plaques, proposing a direct link between microglial cells and AD pathology (Griffin et al., 1989; Perlmutter et al., 1990). Electron microscopy studies have proven the microglial uptake of A β inside AD brains (D'Andrea et al., 2004). Mouse studies confirmed the A β up-take, providing evidence that microglia migrate towards A β plaques (Bolmont et al., 2008; Meyer-Luehmann et al., 2008) and internalize A β at least partially via a macropinocytosis mechanism (Mandrekar et al., 2009). However, other several *in vitro* studies showed that in a proinflammatory environment, microglia are unable to take up or degrade the internalized A β (Koenigsknecht-Talboo and Landreth, 2005; Zelcer et al., 2007), leading to the idea of long-term use of non-steroidal anti-inflammatory drugs for the treatment of AD (Mandrekar and Landreth, 2010). Many receptors were postulated to be involved in A β recognition and uptake, like TLRs and the co-adaptor molecule CD14 (Liu et al., 2005), a multi-component structure formed of CD36, integrin α 6 β 1, integrin-associated CD47 and scavenger receptor A (Bamberger et al., 2003), or complement components (Koenigsknecht and Landreth, 2004). Subsequent to microglial A β internalization, A β is trafficked towards distinct acidified lysosomes (Bolmont et al., 2008; Majumdar et al., 2007; Mandrekar et al., 2009). Interestingly, inability of lysosomal proteolysis, in which PS1 seems to play an important role, was correlated with AD (Lee et al., 2010).

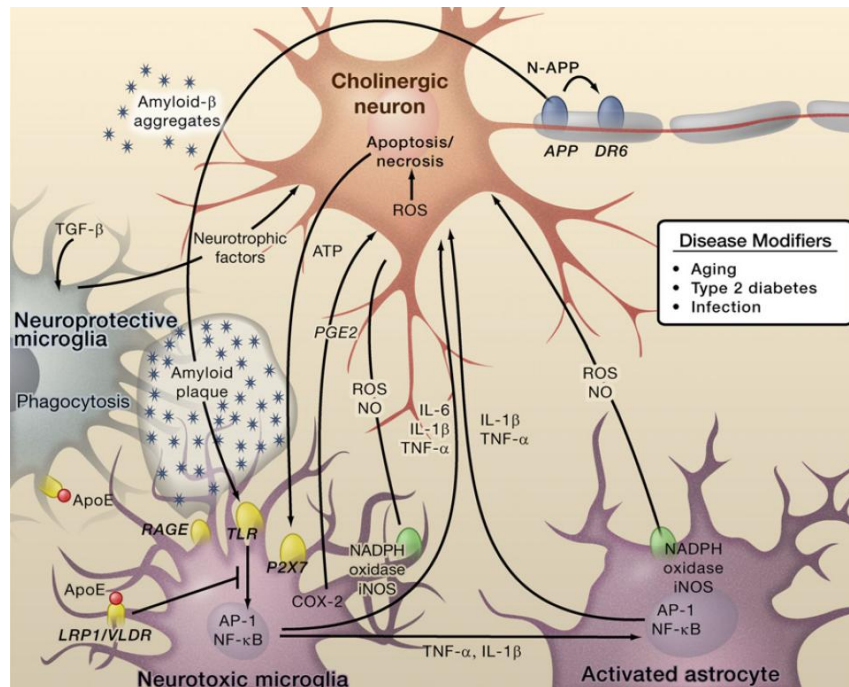


Figure 1.9 – Mechanisms of A β -mediated neurodegeneration in AD. Microglia can recognize A β plaques by a yet not fully known mechanism that leads to activation of the NF κ B pathway and releasing proinflammatory molecules. These molecules can contribute to activation of microglia and astrocytes, resulting in release of toxic molecules. Microglia can present also protective effects by contributing to A β clearance (Glass et al., 2010).

1.3 Objectives of the Thesis

Microglial cells were previously described as presenting both neuroprotective and neurotoxic functions both *in vitro* and *in vivo*. However, the intimate mechanisms involved in the development of microglial-mediated neuropathological conditions are not fully understood.

The present thesis proposes to address these blank spots of microglial physiology.

The first aim of the thesis was to explore the impact of triggering receptor expressed on myeloid cells 2 (TREM2) deficiency in a mouse model of Nasu-Hakola disease, which represents the prototype of primary microglial disorder inside CNS (Bianchin et al., 2010). Previously, TREM2 was described as being involved in microglial phagocytosis of apoptotic neurons and immunosuppression, its absence leading to increased levels of proinflammatory cytokines (Takahashi et al., 2005). In view of this knowledge, it was hypothesised that the absence of TREM2 in microglia should determine an enhanced proinflammatory milieu inside parenchyma, with detrimental consequences for the brain and the organism.

The second aim of the thesis was to investigate the involvement of microglia in bacterial toxin lipopolysaccharide (LPS)-triggered dopaminergic degeneration. Studies on both *in vitro* and *in vivo* models of parkinsonism have reported sensitivity of dopaminergic neurons to LPS, in correlation with microglial activity (Cunningham, 2013; Dutta et al., 2008). Within the present thesis, two LPS treatment paradigms of mice were compared via systems biology methods to identify potential genes involved in the process of microglial-mediated dopaminergic neurodegeneration and to validate them in an *in vivo* model.

The third aim of the thesis was to examine the implications of the TREM2 adaptor molecule DNAX-activating protein of molecular mass 12 kDa (DAP12) in late onset Alzheimer's disease based on a genome-wide association study that identified DAP12 as key regulator of the disease (Zhang et al., 2013). Microglial cells overexpressing functional and non-functional DAP12 were assessed in regard with their amyloid- β internalization capacity and other DAP12-associated cellular functions.

2. Materials and Methods

2.1 Mice

For *in vivo* experiments, different lines of mice were used (Table 2.1). C57BL/6J (referred hereafter as BL6 mice) and B6;129S4-C3^{tm1Crr}/J (referred as C3 KO mice in text) were purchased from Charles River (Sulzfeld, Germany). The C3 KO mice were generated by targeted deletion of nucleotides 1850-2214 within the mouse C3 coding region (AA 620-741, pro-C3 numbering). The B6.129P2-TREM2^{tm1cln} mice (referred hereafter as TREM2 KO mice) were kindly provided by Prof. Dr. Marco Colonna (Department of Pathology and Immunology, Washington University School of Medicine, USA). They were generated by deleting a portion of the mouse TREM2 receptor trans-membrane and cytoplasmic domains (encoded by exons 3 and 4) and backcrossed on C57BL/6J background (Turnbull et al., 2006).

The mice were housed and bred in the institute's animal facility, in a controlled specific pathogen free (SPF) environment, with 12 hours light/night cycles and water and food *ad libitum*. The mice were subsequently intercrossed at least once every 8-10 generations with new BL6 mice to prevent genetic drift, in accordance with the Banbury Conference recommendations (Silva et al., 1997). All experiments were conducted in accordance with local animal ethics procedures.

Table 2.1 Mouse lines

Mouse line	Full Name	Provider	Registered Office/Contact
BL6	C56BL/6J	Charles River	Sulzfeld, DE
C3 KO	B6;129S4-C3 ^{tm1Crr} /J	Charles River	Sulzfeld, DE
TREM2 KO	B6.129P2-TREM2 ^{tm1cln}	Prof.Dr.Marco Colonna	Washington University, USA

2.1.1 Mice Genotyping

Mice were genotyped from tissue of collected ear markings preserved at -80°C until used. For genotyping, tissue samples, primers (Table 2.2) and REExtract-N-AmpTM Tissue Polymerase Chain Reaction (PCR) Kit [for producers and/or details of products, see the 2.6 subchapter]

were used following genotype-specific programs (Table 2.3). The genotyping PCR products were loaded in a 1.5-2% agarose gel, run under 100-130 V and visualized by using a ChemiDoc Gel Imaging System.

Table 2.2 Genotyping primers

Mouse line	Forward Primer (5'→3')	Reverse Primer (5'→3')	Expected length
TREM2 KO	I.CCAGCAGTGGCCTAAATGGA II.CTTATGTGGAAGAGCTCATCG GG	TCTGACCACAGGTGTTCCCG	WT: 337 base pairs (bp) KO: 256 bp hetero: both bands
C3 KO	ATCTTGAGTGCACCAAGCC	I.GGTTGCAGCAGTCTATGAA GG II.GCCAGAGGCCACTTGTGTA G	WT: 350bp KO: 500bp hetero: both bands

Table 2.3 Genotyping programs

TREM2 KO mice			C3 KO mice		
Temperature	Time	Cycles	Temperature	Time	Cycles
94°C	180 s		94°C	180 s	
94°C	45 s	30x	94°C	20 s	12x
58°C	45 s		64°C	30 s	
72°C	45 s		72°C	35 s	
72°C	300 s		94°C	20 s	25x
4°C	∞		58°C	30 s	
			72°C	35 s	
			72°C	120 s	
			10°C	∞	

2.1.2 LPS Treatment Schemes

To induce systemic inflammation in mice, three months old male animals were intraperitoneally (i.p.) injected with lipopolysaccharide (LPS) or with 100 µL phosphate buffer saline (PBS) vehicle as control. For single treatment, animals were injected once with 4 µg LPS per gram body weight (gbw) or vehicle and sacrificed in the 5th or 19th day since the start of the treatment (Fig. 2.1). For repeated treatment, four injections in consecutive days, with 1 µg LPS/gbw or vehicle were performed and the mice were analysed in the 5th or 19th day since the start of the treatment (Fig. 2.1).

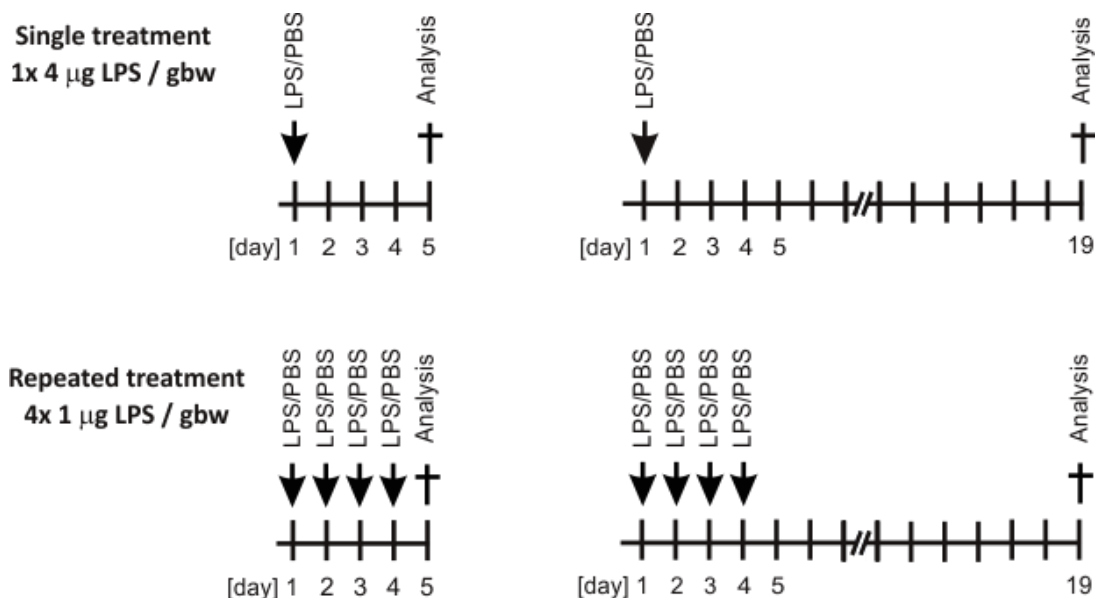


Figure 2.1 – Experimental schemes of single and repeated LPS treatments of mice analysed on the experimental day 5 or 19. Mice were intraperitoneally (i.p.) injected either once with 4 µg lipopolysaccharides (LPS) per gram body weight (gbw, single treatment, top), or with 1 µg/gbw on four consecutive days (repeated treatment, bottom) before analysis.

2.1.3 Tissue Collection and Storage

For brain and/or plasma collection, mice were first deeply anesthetized i.p. with 0.8-1 mL avertin (1.25% v/v; Table 2.4).

Table 2.4 Avertin (2,2,2-tribromoethanol) solution protocol

Step	Mouse line	Quantity	Provider	Registered Office
1. Mix preparation				
	Avertin	50 g	Sigma-Aldrich	München, DE
	t-amyl alcohol (2-methyl-2-butanol)	31 mL	Sigma-Aldrich	München, DE
2. Incubate overnight with shaking, in dark, at room temperature				
3. Filter (0.22 µm) & store at 4°C				
4. Working concentration 1.25% (v/v) in PBS				

Plasma was collected from aortic blood preserved on heparin and centrifuged 1500xg to remove the blood cells. Aliquotes were stored at -20°C until used.

For RNA extraction, mice were intracardially perfused with 20-30 mL PBS, the brains were collected and processed as mention in subchapter 2.3.1.1.

For immunohistochemistry, mice were intracardially perfused with 20-30 mL PBS, followed by 20-30 mL 4% paraformaldehyde (PFA). The PFA-fixed brains were collected, stored at 4°C for another 24h in 4% PFA before immersing in 30% glucose (with 0.1% sodium azide) and storing at 4°C. After 24-48h in the glucose solution, the brains were placed in cryomolds, covered in TissueTek® medium, frozen and processed as mentioned in subchapter 2.1.3.1.

2.2 Cell Cultures

2.2.1 Primary Cell Cultures

2.2.1.1 Microglia Primary Cell Cultures

Primary microglia cells (Table 2.5) were isolated from newborn mice (Yiner Wang and Neumann, 2010). In this regard, P3 brains from BL6 or TREM2 KO mice were isolated, cleaned of meninges and dissociated before plating into cell culture flasks precoated with poly-L-lysine. The cells were kept in primary microglia medium (Table 2.5), in a 37°C incubator, under 5% CO₂ and 95% humidity. The cell culture medium was changed weekly and after 3-4 weeks, the primary microglia were detached by vigorous shaking, counted and used in further experiments.

2.2.1.2 Neuronal Primary Cell Cultures

Hippocampi of E14 BL6 mice were isolated, mechanically dissociated and seeded in poly-L-lysine coated chamber slides at a density of 2.5×10^5 cells/mL and kept in a 37°C incubator, with 5% CO₂ and 95% humidity (Y Wang and Neumann, 2010). Cells were kept in neuronal media (Table 2.5) for at least 5 days before they were used in experiments.

2.2.2 Cell Lines

Embryonic stem cell derived microglia (ESdM) were generated in the lab based on a 5-steps differentiation protocol (Beutner et al., 2010). These cells have been shown to present great

similarity to primary microglial cell cultures (Beutner et al., 2013, 2010). Human Embryonic Kidney 293FT (HEK293FT) cell line was purchased from Invitrogen.

Table 2.5 Primary cells

Cell	Media	Provider/Origin
Primary microglia	Primary microglia medium	3 days old mice (P3)
Primary neurons	Primary neurons medium	14 days mouse embryos (E14)

Table 2.5 Primary cell culture media

Medium	Component	Quantity	Manufacturer	Reg.office
Primary microglia medium				
	Basal Medium Eagle (BME)	500 mL	Gibco, LifeTechnologies	Darmstadt, DE
	Fetal Calf Serum (FCS)	50 mL	PAN Biotech GmbH	Aidenbach, DE
	L-Glutamine	5 mL	Gibco, LifeTechnologies	Darmstadt, DE
	D-Glucose 45%	5 mL	Sigma-Aldrich	München, DE
	Penicillin/Streptomycin	5 mL	Gibco, LifeTechnologies	Darmstadt, DE
Primary neuronal medium				
	BME	500 mL	Gibco, LifeTechnologies	Darmstadt, DE
	B-27 supplement	10 mL	Gibco, LifeTechnologies	Darmstadt, DE
	D-Glucose 45%	5 mL	Sigma-Aldrich	München, DE
	FCS	50 mL	PAN Biotech GmbH	Aidenbach, DE

2.2.2.1 General Cell Lines Handling

Cells (Table 2.6) were thawed fast and washed by centrifugation (1500xg, 3 minutes) within appropriate cell culture media (Table 2.7). The pellet was resuspended, plated in new media and kept in an incubator with 5% CO₂, 95% humidity and 37°C. When reaching cca. 80% confluency, cells were detached either mechanically (scraping) or chemically (Trypsin/EDTA 0.25%, 3-5 minutes), centrifuged (1500xg, 3 minutes) and plated in a new culture dish.

For long time storage, after detaching and centrifugation, cells were resuspended in 1 mL appropriate freezing media (Table 2.7) and placed in cyrotubes. After ≥ 24 h of storage in an isopropanol containing tank at -80°C for slowly freezing, the cells were moved to liquid N₂ for long time storage.

Table 2.6 Cell types

Cell	Full name	Media	Provider/Origin	Registered Office
ESdM	Embryonic Stem cells derived Microglia	N2 medium	(Beutner et al., 2010)	
HEK 293FT	Human Embryonic Kidney 293FT	MEF medium	Invitrogen, Life Technologies	Darmstadt, DE

Table 2.7 Cell culture media

Medium	Component	Quantity	Manufacturer	Registered office
N2 medium				
	Dulbecco's Modified Eagle Media (DMEM) + Factor 12 (1:1) + L-glutamine, + 15 mM HEPES	500 mL	Gibco, LifeTechnologies	Darmstadt, DE
	N2 supplement	5 mL	Gibco, LifeTechnologies	Darmstadt, DE
	L-Glutamine	1.2 mL	Gibco, LifeTechnologies	Darmstadt, DE
	D-Glucose 45%	1.7 mL	Sigma-Aldrich	München, DE
	Penicillin/Streptomycin	5 mL	Gibco, LifeTechnologies	Darmstadt, DE
MEF Medium				
	(DMEM + L-glutamine, - sodium pyruvate, + 4.5 g/L D-glucose	500 mL	Gibco, LifeTechnologies	Darmstadt, DE
	L-Glutamine	5 mL	Gibco, LifeTechnologies	Darmstadt, DE
	Sodium Pyruvate 100 mM	5 mL	Gibco, LifeTechnologies	Darmstadt, DE
	Non-essential amino-acids 10 mM	5 mL	Gibco, LifeTechnologies	Darmstadt, DE
	FCS	50 mL	PAN Biotech GmbH	Aidenbach, DE
	Penicillin/Streptomycin	5 mL	Gibco, LifeTechnologies	Darmstadt, DE
Cell culture freezing medium				
	Appropriate cell culture media	40%		
	Dimethyl sulfoxide (DMSO) 99%	10%	Sigma-Aldrich	München, DE
	Fetal calf serum (FCS)	50%	Sigma-Aldrich	München, DE

2.2.3 Microglia-Neurons Cocultures

For obtaining microglia-neurons cultures, ESdM cells were detached from dish, counted and resuspended in primary neuronal culture (Table 2.5). Half volume of medium from the primary neurons was removed and new ESdM-containing medium was added (5:1 microglia:neurons). The ESdM cells were left to adhere for at least 3 h before experiments.

2.2.4 Cellular Functional Assays

2.2.4.1 Phagocytosis Assay

For obtaining fibrillar amyloid- β (A β), synthetic human A β peptide amino acid 1-42 (1 mg/mL) was incubated in PBS for at least 3 days at 37°C to obtain fibrillar A β . Microglia (ESdM) cells were treated with 10 μ g/mL biotinylated A β or 500 μ g/mL biotinylated albumin for 1 h at 37°C. Cells were fixed and the up-taken biotinylated material was immunostained with streptavidin-Cy3 (2 μ g/mL; see subchapter 2.4.3 for a detailed staining protocol). Percentage of cells having phagocytosed A β or albumin was analysed in 5-10 randomly selected areas per condition by confocal microscopy, 3D reconstruction and ImageJ software.

2.2.4.2 Detection of Superoxide Production

Cells were seeded at a density of 40,000 cells per well in chamber slides and were stimulated for 30 minutes with 10 μ g/mL fibrillary A β , 500 μ g/mL zymosan A, 500 μ g/mL albumin or PBS control. To detect superoxide production culture medium was replaced by Krebs-HEPES-buffer (Table 2.8) and then incubated with 30 μ M DHE for 15 minutes or 30 minutes for the A β group, at 37°C. Cells were washed three times with Krebs-HEPES-buffer, fixed with 4 % PFA and mounted on cover slides with Mowiol 4-88. A number of 6 images per experimental group (30-60 cells per experimental group) were scanned using an Olympus IX81 inverted confocal microscope and quantified using the ImageJ software.

Table 2.8 Krebs-HEPES Buffer

Component	Concentration	Manufacturer	Registered Office
HEPES*	8.3 mM	Carl Roth GmbH	Karlsruhe, DE
NaCl	130.0 mM	Sigma-Aldrich	München, DE
KCl	5.6 mM	Sigma-Aldrich	München, DE
CaCl ₂	2.0 mM	Sigma-Aldrich	München, DE
MgCl ₂	0.24 mM	Sigma-Aldrich	München, DE
Glucose	11.0 mM	Carl Roth GmbH	Karlsruhe, DE

* 4-(2-hydroxyethyl)-1-piperazineethanesulfonic acid

2.2.4.3 Neurites Length Analysis

For analysis of neurite length, preincubated fibrillar biotinylated A β (10 μ g/mL) was added to the primary neuron culture or ESdM-neuron co-culture for 24 hours, after which the cells were

fixed and immunostained (see 2.4.3). Neurons were visualized using anti- β III-tubulin (1 $\mu\text{g}/\text{mL}$) and Cy3-conjugated secondary antibody (2 $\mu\text{g}/\text{mL}$; see subchapter 2.4.3 for a detailed staining protocol). For the detection of A β , Cy5-streptavidin (2 $\mu\text{g}/\text{mL}$) was used. Images (5-10 randomly selected areas in each experimental group) were collected via laser scanning confocal microscope. The mean length of β III-tubulin positive neurites was quantified using the ImageJ software and NeuronJ plugin.

2.3 Molecular Biology

2.3.1 PCR, RT, sqRT-PCR

2.3.1.1 RNA Isolation and RT

Cells or brain tissue (for brain collection see subchapter 2.1.3) were homogenized in 0.5-1 mL QIAzol using a TissueLyser homogenizer. Subsequently, RNA was isolated either using the RNeasy[®] Lipid Tissue Kit, RNeasy[®] Mini Kit after manufacturer's specifications or a modified phenol-chloroform based method (Table 2.9).

Table 2.9 RNA isolation (modified phenol-chloroform method)

Step	Quantity	Sonditions	Time
Adding QIAzol to tissue/cells	1 mL		
Lysis via TissueLyser (50Hz)		Room temperature	3 min
Incubation with chloroform	+ 200 μL	Room temperature	3 min
Centrifugation		13,000xg, 4°C	15 min
Collection of the aqueous phase			
Incubation with isopropanol	1:1 (vol)	-20°C	Overnight
Centrifugation		13,000xg, 4°C	15 min
Collection of the sediment			
Mixing with 70% ethanol	+ 300 μL		
Centrifugation		13,000xg, 4°C	15 min
Collection of the sediment, drying and resuspension in 50 μL RNase free water			

The RNA content was measured using a Nanodrop spectrophotometer. RT of 50 μg total RNA was performed using SuperScript III reverse transcriptase and hexameric random primers (Table 2.10).

Table 2.10 Reverse Transcription

Prepare RT Mix (I)	Component	Amount	Manufacturer	Registered office
	RNA	11 μ L (50 μ g)		
	Hexanucleotids (mM)	1 μ L	Roche	Grenzach-Wyhlen, DE
	dNTPs (mM each)	1 μ L	Paqlab	Erlangen, DE
➤ Start RT Program	Temperature	Time		
	65°C	5 min		
	4°C	1 min		
	4°C	pause		
Add RT Mix (II)	Component	Amount	Manufacturer	Registered office
	Forwards Strand Buffer 5x	4 μ L	Invitrogen, LifeTechnologies GmbH	Darmstadt, DE
	DTT (0.1 M)	2 μ L	Invitrogen, LifeTechnologies GmbH	Darmstadt, DE
	SuperScript III	1 μ L	Invitrogen, LifeTechnologies GmbH	Darmstadt, DE
➤ Continue RT Program	Temperature	Time		
	25°C	5 min		
	55°C	1h		
	70°C	15 min		
	4°C	∞		

2.3.1.2 sqRT-PCR

For evaluating transcriptional levels, sqRT-PCR was performed using 1 μ L cDNA diluted 1:10, SYBR GreenER qPCRSuperMix Universal, and 400 nM mouse primers (Table 2.11) into a final reaction volume of 25 μ L.

Table 2.11 sqRT-PCR Primers

Gene	Accession No.	Forward Primer (5'→3')	Reverse Primer (5'→3')
<i>C1q</i>	NM_011795.2	CTGCAAGAACGGCCAGGTGC	AGCCACGGATGAAAAGGGGTG
<i>C3</i>	NM_009778.2	TAGTGCTACTGCTGCTGTTGGC	GCTGGAATCTTGATGGAGACGCTT
<i>C4</i>	NM_009780.2	TGGAGGACAAGGACGGCTA	GGCCCTAACCTGAGCTGA
<i>Cyba</i>	NM_007806.3	CCTCCACTTCCTGTTGTCGG	TCACTCGGCTTCTTTCGGAC
<i>Cybb</i>	NM_007807.4	GGGAACTGGGCTGTGAATGA	CAGTGCTGACCCAAGGAGTT
<i>Tyrobp</i>	NM_011662.2	ATGGGGGCTCTGGAGCCCT	TCATCTGTAATATTGCCTCTGTGT

Gene	Accession No.	Forward Primer (5'→3')	Reverse Primer (5'→3')
<i>Fcer1g</i>	NM_010185.4	CTGTCTACACGGGCCTGAAC	AAAGAATGCAGCCAAGCACG
<i>Aif1</i>	NM_019467.2	GAAGCGAATGCTGGAGAAAC	AAGATGGCAGATCTCTTGCC
<i>Il1b</i>	NM_008361.3	CTTCCTTGTGCAAGTGTCTG	CAGGTCATTCTCATCACTGTC
<i>Nos2</i>	NM_010927.3	AAGCCCCGCTACTACTCCAT	GCTTCAGGTTCTGATCCAA
<i>Itgam</i>	NM_001082960.1	CATCAAGGGCAGCCAGATTG	GAGGCAAGGGACACACTGAC
<i>Tnfa</i>	NM_013693.2	TGATCCGCGACGTGGAA	ACCGCCTGGAGTTCTGGAA
<i>Gapdh</i>	NM_008084.2	AACTTTGGCATTGTGGAAGG	GGATGCAGGGATGATGTTCT

For amplifications (Table 2.12), a Mastercycler eppgradient S[®] was used and the results were evaluated with the manufacturer's software. Amplification specificity was confirmed by melting curve analysis and the quantification was carried out using the $\Delta\Delta C_t$ method.

Table 2.12 sqRT-PCR Program

Step	Temperature	Time	Cycles
1. Initial denaturation	95°C	10 min	
2. Denaturation	95°C	15 s	40x
3. Annealing	60°C	30s	
4. Elongation	72°C	30s	
5. Inactivation	95°C	10 min	
6. Melting curve	60°C – 95°C	20 min	
7. Final	95°C	15 s	
8. Store	4°C	∞	

2.3.2 Bacterial cloning

2.3.2.1 Bacterial cultures

For starting new bacteria cultures (Table 2.13), inoculums or aliquots were taken from -80°C long storage cryovials into 3-5 mL LB medium (for small scale culture) or 200-250 mL LB medium (for large scale cultures) containing appropriate selection antibiotic, placed in 37°C shaking incubators (200-250 rpm) and grown until required bacterial density was reached (usually overnight or 16 h).

For long term storage, bacteria containing LB media was mixed with glycerol in a 1:1 ratio (v/v), placed in cryotubes and stored at -80°C.

Table 2.13 Bactria strains

Competent bacteria strain	Selection	Manufacturer	Registered Office
Top10	Ampicillin	Invitrogen, LifeTechnolgies GmbH	Darmstadt, DE

2.3.2.2 Plasmid isolation

Bacterial plasmids were isolated from bacterial small cultures (3-5 mL) grown for 8h or overnight, using the QIAprep Spin Miniprep Kit or from big bacterial cultures (200-250 mL) using the PureLink® HiPure Plasmid Filter Maxiprep Kit. DNA concentration was measured using a Nanodrop spectrophotometer.

2.3.2.3 Plasmid Digestion and Ligation

The pSeq Tag Hygro B plasmids containing the full length or truncated *Tyrobp* were kindly provided by the group of Prof.Dr. Jochen Walter (Department of Neurology, University of Bonn, Germany).

Plasmids (1 mg) were digested using *EcoRI* and *BamHI* restriction enzymes in appropriate buffer for 1.5 h, at 37°C (Table 2.14). The resulted bands were visualized by gel electrophoresis (1% agarose), using GelStar® Nucleic Stain on a Dark Reader Transilluminator, in the presence of 100bp ladder. The correct bands were excised and purified via QIAquick Gel Extraction Kit, followed by MiniElute PCR Purification Kit for improved purity.

Table 2.14 Digestion and Ligation Mixes

Mix type	Component	Quantity	Manufacturer	Registered office
Digestion Mix				
	H ₂ O	Up to 20 µL		
	Buffer A	2 µL	Roche	Grenzach-Wyhlen, DE
	DNA	1 mg		
	EcoRI	1 µL (10 U)	Roche	Grenzach-Wyhlen, DE
	BamHI	1 µL (10 U)	Roche	Grenzach-Wyhlen, DE
Ligation Mix				
	DNA fragments	Max 100 ng		
	H ₂ O	Up to 20 µL		
	Buffer 5x	4 µL	Roche	Grenzach-Wyhlen, DE
	T4 ligase	1 µL (5U)	Roche	Grenzach-Wyhlen, DE

Ligation of the purified DNA fragments into modified pLenti plasmids (kindly provided by the group of Prof. Brüstle, Institute of Reconstructive Neurobiology, University of Bonn, Germany) was performed using T4 ligase, overnight at 16°C (Table 2.14). The cloning strategy can be seen in Fig. 2.2.

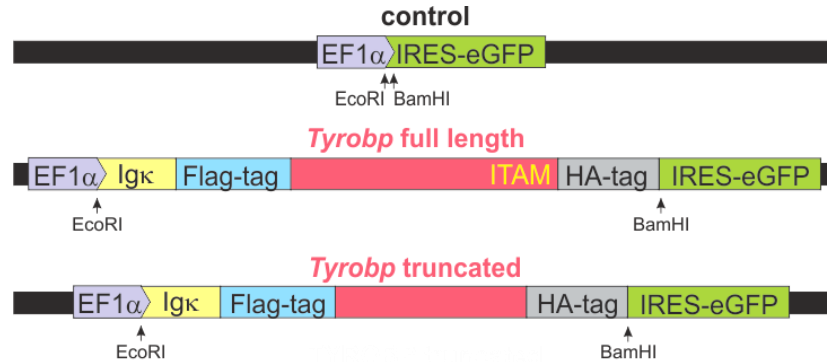


Figure 2.2 – Cloning strategy for obtaining the full length or truncated Dap12/*Tyrobp* overexpressing plasmids. The full length or truncated *Tyrobp* gene sequences were integrated between the EcoRI and BamHI restriction sites of the pLenti expression plasmid. *Tyrobp* had the leading sequences replaced with the Ig κ -leading sequence followed by Flag-tag sequence. A HA-tag sequence was introduced after the *Tyrobp* sequence. The resulting plasmid expresses *Tyrobp* under an Elongation Factor 1 α (EF1 α) promoter and the transduced cells will present GFP signal.

2.3.2.4 Bacterial Transformation and Ligation Confirmation

Competent bacteria were transformed using 10 μ L of the ligation mix (see 2.3.2.3), via the heat-shock method (Table 2.15), then plated on agar containing proper selecting antibiotic (ampicillin 100 μ g/mL) and incubated overnight at 37°C.

Table 2.15 Bacteria Transformation

Step	Quantity	Temperature	Time
1. Bacteria thawing	100 μ L aliquot	on ice	20 min
2. Incubation ligation mix with bacteria	+ 10 μ L	on ice	30 min
3. Heat shock		42°C (water bath)	45 s
4. Bacterial wall restabilisation		on ice	> 1 min
5. Liquid preculturing	+ 900 μ L	37°C (shaker 300rpm)	1 h
6. Bacteria harvesting – centrifugation 7000xg, 3 min			
7. Plating on agar			

Inoculums of resulted colonies were grown in small culture volumes and verified by restriction enzyme digestion and/or sequencing of the isolated plasmids. The general structure of the resulted plasmids can be seen in Fig 2.3 and Table 2.16.

Table 2.16 Cloned Plasmids

Name	Backbone	Bacterial Selection Marker
pLenti GFP	pLenti	Ampicilline
pLenti TYROBP full length	pLenti GFP	Ampicilline
pLenti TYROBP truncated	pLenti GFP	Ampicilline

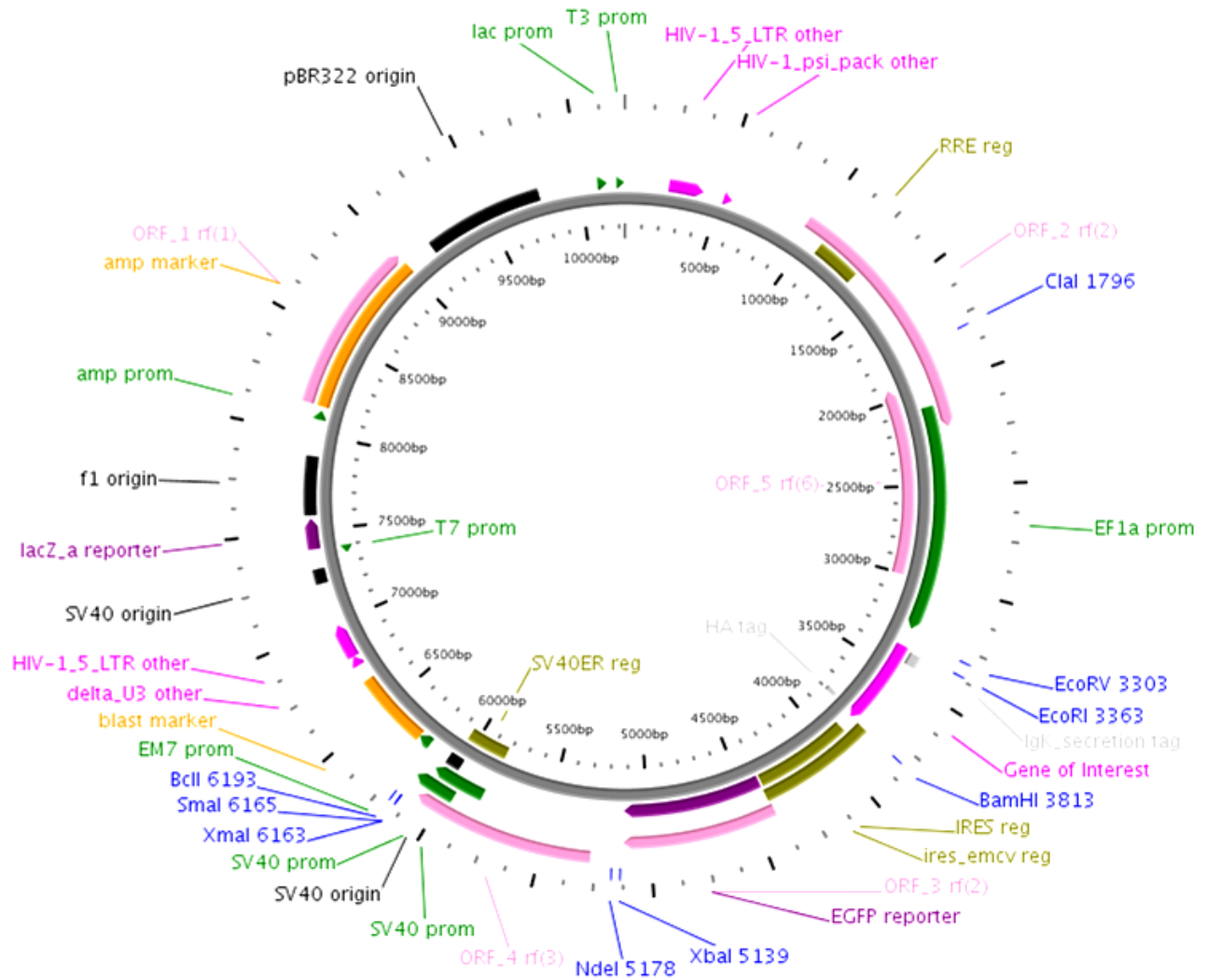


Figure 2.3 – General plasmid map of the vectors resulted after ligation of the inserts into the backbone plasmid. The ‘Gene of interest’ has been inserted between the EcoRI and BamHI restriction sites. The plasmid contains an ampicilline resistance gene for bacterial selection and an IRES-eGFP reporter sequence and blasticidine resistance gene for eukaryotic cell selection (scheme generated by PlasMapper 2.0).

2.3.3 Lentivirus Generation and Transduction of Cells

For the overexpression of mutant proteins, lentiviral particles were generated. In this regard, the lentiviral plasmid containing the fragments of interest were mixed together with packaging plasmids from the ViraPower™ Lentiviral Packaging Mix (Table 2.17) and added on HEK293FT cells pre-seeded on poly-L-lysine, in 15cm² dishes (6.5 x10⁶ cells/dish seeded in MEF media 24h before starting the virus generation protocol), as presented in Table 2.17.

Table 2.17 Packaging Vectors

Name	Backbone	Selection Marker	Manufacturer	Registered Office
pLP1	pLP	Ampicilline	Invitrogen, LifeTechnologies GmbH	Darmstadt, DE
pLP2	pLP	Ampicilline	Invitrogen, LifeTechnologies GmbH	Darmstadt, DE
pLP3	pLP/VSVG	Ampicilline	Invitrogen, LifeTechnologies GmbH	Darmstadt, DE

The virus was harvested 48h after the beginning of the production, filtered, aliquoted and stored frozen or used directly on ESdM cells for transduction. For this, ESdM cells were seeded in 6 well plates and transduced when they were cca. 60% confluent. After 48h, the medium was changed to fresh N2 medium. All the security level 2 (S2) experiments were conducted in accordance with local S2 material handling procedures.

Table 2.18 Lentivirus generation (quantities per 15 cm² dish)

Step	Component	Amount
1. Plasmid Mix	Plasmid of interest	25 µg
	pLP1 (pMDL gag/pol RRE)	25 µg
	pLP2 (pRSV-Rev)	12.5 µg
	pLP3	15 µg
	H ₂ O	Up to 1.125 mL
	CaCl ₂ (mM)	125 µL
	HBSS 2x	1.25 mL
2. Incubation 20 min, room temperature		
3. Adding drop-wise on new MEF media		
4. Refresh medium after 24h		

2.3.3.1 Fluorescence-Activated Cell Sorting (FACS) Isolation of Transduced Cells

The positively transduced cells were selected via fluorescence-activated cell sorting (FACS) based on their GFP expression signal. For this, cells were detached from the dishes, washed and kept in PBS until sorting. After sorting, the cells were collected in N2 media, centrifuged again and plated for expansion. The successfully transduced cells were considered new cell lines and handled accordingly (for details see 2.2.2). The obtained cells are presented in Table 2.19.

Table 2.19 Transduced Cell Lines

Name	Vector inserted	Original cell line	Selection Marker
ESdM DAP12 Full Length	pLenti TYROBP Full	ESdM	eGFP signal
ESdM DAP12 Truncated	pLenti TYROBP Truncated	ESdM	eGFP signal
ESdM GFP	pLenti GFP	ESdM	eGFP signal

2.3.4 cDNA Microarray

To determine changes in gene expression in mice following LPS treatments, microarray analysis of total brain RNA was performed. For this, three months old BL6 mice were i.p. treated with LPS (single or repeated) and analyzed on day 5 (Fig. 2.1). Lysis of whole brain was performed by mechanical homogenization using a TissueLyzer, in the presence of QIAzol reagent. Extraction of RNA was done accordingly to the QIAzol manufacturer recommendations, with -20°C incubation overnight for small RNA precipitation.

Total RNA integrity and purity verification as well as further arrays were performed by Dr. Sinkkonen (Luxembourg Centre for Systems Biomedicine (LCSB), University of Luxembourg, Luxembourg). The RNA was reverse-transcribed into double-stranded complementary DNA (cDNA). Further, cDNA was processed and hybridized onto Affymetrix GeneChip® Mouse Gene 1.0 ST Arrays according to the Ambion® WT Expression kit for Affymetrix® GeneChip® Whole Transcript Expression Array Protocol and GeneChip® Whole Transcript Terminal Labeling and Hybridization User Manual for use with the Ambion® Whole Transcript Expression kit. Microarrays were scanned and imported into Partek® Genomics Suite™ 6.4 for preprocessing, quality control and detection of differentially expressed genes (DEG). Appropriate statistic methods were used. For Ingenuity pathway analysis (IPA) lists of significantly DE mRNAs between (single or repeated) LPS treatment versus (single or repeated) PBS treatment were uploaded in the IPA tool (Ingenuity® Systems).

2.3.5 RNA Sequencing

For genome-wide gene expression assessment in full length *Tyrobp* over-expressing ESdM cells, truncated *Tyrobp* over-expressing ESdM cells and GFP expressing control ESdM cells, the total RNA was extracted via mechanical homogenization using a TissueLyzer, in the presence of QIAzol reagent. Extraction of RNA was done accordingly to the QIAzol manufacturer recommendations, with -20°C incubation overnight for small RNA precipitation.

Further array analysis was performed by Dr. Chris Gaiteri (Sage Bionetworks, Seattle, USA). Total RNA was used for the preparation of the sequence library using RNA TruSeq Kit. After rRNA depletion, the remaining RNA was converted into double stranded cDNA and adenine base was added at the 3' ends of polished cDNA. Illumina supplied specific adaptors were ligated to cDNA and size selected to get an average of 200 bp insert size using AmpPure beads. After 15 cycles PCR amplification and AmpPure beads based purification, the final sequence library was obtained. Read mapping was done using the TopHat RNA-seq aligner (Trapnell and Schatz, 2009).

2.4. Immunochimistry

2.4.1 Immunohistochemistry (IHC)

For collecting and PFA-fixing of brains, the protocol mentioned in section 2.1.3 was used. Coronal plane (20 µm extent in the rostral-caudal plane) slicing was performed using a cryostat microtome. Consecutive slices of 20 or 30 µm thickness containing the substantia nigra area were collected on glass slides and stored at -20°C until stained.

An IHC general protocol is given in Table 2.21, for a more detailed list of the antibodies used, see Table 2.22.

Image acquisition was done using an inverted microscope with ApoTome AxioObserver Z1 or an Olympus IX81 inverted confocal microscope. The pictures were visualized and processed with the manufacturer's software.

Table 2.21 IHC protocol

Step	Solution	Components	Time	Temperature
1. Blocking	Blocking solution	10% bovine serum albumin (BSA) 5% normal goat serum (nGS) 0.2% Triton 100x	1 h	Room temperature
2. Primary antibody incubation		1 st antibody in blocking solution	2 h (overnight)	Room temperature (4°)
3. PBS wash				
4. Secondary antibody incubation		2 nd antibody in PBS	2 h	Room temperature
5. PBS washing				
6. Mounting	Mowiol			

Table 2.22 Antibodies (IHC, ICC, IP, WB)

Antibody	Type	Host	Specificity	Working conc.	Manufacturer	Registered office
Tyrosine hydroxylase (TH)	1 st	mouse		1 µg/mL	Sigma-Aldrich	München, DE
Tyrosine hydroxylase (TH)	1 st	rabbit		1 µg/mL	Millipore	Schwalbach, DE
β-III-tubulin	1 st	mouse		1 µg/mL	Sigma-Aldrich	München, DE
Neuronal nuclei (NeuN)	1 st	rabbit		1 µg/mL	Millipore	Schwalbach, DE
Ionized calcium-binding adapter molecule (Iba1)	1 st	rabbit		0.5µg/mL	Waco	
Spleen tyrosine kinase (Syk)	1 st	rabbit		5 µg/mL	Santa Cruz Biotechnology	Heidelberg, DE
Phospho-tyrosine antibody 4G10	1 st	mouse		5 µg/mL	Millipore	Schwalbach, DE
Biotinylated antibody	2 nd	goat	rabbit	2 µg/mL	Dianova	Hamburg, DE
Biotinylated antibody	2 nd	goat	mouse	2 µg/mL	Dianova	Hamburg, DE
Horseradish peroxidase (HRP)-conjugated streptavidin	2 nd			0.1µg/mL	Millipore	Schwalbach, DE
Cy3-conjugated Ab	2 nd		mouse	2 µg/mL	Dianova	Hamburg, DE
Cy3-conjugated Ab	2 nd		rabbit	2 µg/mL	Dianova	Hamburg, DE
Cy5-conjugated streptavidin	2 nd			2 µg/mL	Dianova	Hamburg, DE
Alexa 488-conjugated	2 nd		rabbit	2 µg/mL	Invitrogen, LifeTechnologies GmbH	Darmstadt, DE

For neuronal quantification, slides were double-stained with antibodies directed against the dopaminergic neuronal marker tyrosine hydroxylase (TH, 1 µg/mL) and with the neuronal nuclei marker (NeuN). TH positive immunostaining was used for the localization of substantia nigra *pars compacta* (SNpc; Baquet et al., 2009). For cell quantification, optical sections of four SNpc matched levels per mouse were used (McCormack et al., 2002). SNpc neurons were distinguished from the ones of ventral tegmental area based on size and orientation (Baquet et al., 2009). The TH positive neurons were only counted when the whole nucleus was contained within the section.

For microglia evaluation, TH immunostaining was used for positioning in the slice, together with an antibody directed against the microglial marker Iba1. Microglial cells were counted in four matched levels containing substantia nigra *pars reticulata* (SNpr) pwe mouse.

2.4.2 Immunocytochemistry (ICC)

For cell culture immunostainings, cells were briefly washed with PBS and stained as mentioned in Table 2.23. For antibodies concentrations and product details, see Table 2.24. The stained material was stored at -20°C.

Table 2.23 ICC Protocol

Step	Solution	Components	Time	Temperature
1. Blocking	Blocking solution	10% BSA 5% nGS 0.2% Triton 100x	30 min	Room temperature
2. Primary antibody incubation		1 st antibody in blocking solution	1 h	Room temperature
3. PBS wash				
4. Secondary antibody incubation		2 nd antibody in PBS	30 min	Room temperature
5. PBS washing				
6. Mounting	Mowiol			

Image acquisition was done using an Olympus Confocal IX81 inverted confocal microscope. The pictures were visualized and processed with the manufacturer's software.

The positive stained cells were counted by using ImageJ software. For neuronal processes quantifications, the length of neurites was traced manually and quantified using the NeuronJ plug-in.

2.4.3 Immunoprecipitation (IP)

For obtaining cell lysates, cells were detached from the dish, washed in PBS and lysed by vortexing and incubation in 100 µL RIPA buffer, in the presence of EDTA, phosphatase and protease inhibitors (Halt™ Protease Inhibitor + EDTA kit), on ice. After 1h, the lysate was centrifuged (13,000xg) at 4°C and the supernatant was used for further determinations.

For antigen precipitation, the lysate supernatant was incubated with magnetic Dynabeads® that were precoated with antibodies according to manufacturer's specifications. The immunoprecipitation of the target antigen was performed as mentioned in Table 2.25.

Table 2.25 Immunoprecipitation Protocol

Step	Solution	Conditions	Manufacturer	Registered office
1. Antigen (lysate) binding to beads	100 µL sample	1h, 4°C, rotation		
	+ Dynabeads®			
2. Magnetic separation of beads		Room temperature	Invitrogen, LifeTechnologies	Darmstadt, DE
3. Wash	200 µL washing buffer	Room temperature	Invitrogen, LifeTechnologies	Darmstadt, DE
4. Elution & Denaturation	20 µL elution buffer	10 min, 70°C	Invitrogen, LifeTechnologies	Darmstadt, DE
	10 µL NuPage® LDS Sample Buffer		Invitrogen, LifeTechnologies	Darmstadt, DE
	1 µL β-mercapto-ethanol		Carl Roth GmbH	Karlsruhe, DE
5. Magnetic beads – antigen separation				

2.4.4 Western Blot (WB)

The antigens isolated by immunoprecipitation (see 2.4.4) were loaded onto 10% NuPAGE® Bis-Tris Gels and run in NuPAGE® MES SDS running buffer, under constant 130V. PageRuler Plus prestained protein ladder was used as marker. The protocol presented in Table 2.25 was used.

Table 2.25 Western Blot Protocol

Step	Solution	Conditions
1. Electrophoresis	NuPAGE® MES SDS	130V
2. Blot	NuPAGE® transfer buffer	380 mA, 1 h, on ice
3. Blocking	PBST (PBS + 0.1% Tween) + 5% blot-grade milk powder	1 h, rotation
4. Primary antibody incubation	PBST + 5% blot-grade milk powder	Overnight, 4°C, rotation
5. PBST washing		3x 15 minutes
6. Secondary biotinylated antibody incubation	PBST	1 h, room temperature, rotation
7. PBST washing		3x 15 minutes
8. Peroxidase labeling	PBST + 5% blot-grade milk powder	1 h, room temperature
9. PBST washing		3x 15 minutes

Detection was performed by using SuperSignal West Pico or SuperSignal West Femto kits and the pictures were visualized and acquired by a ChemiDoc Gel Imaging System.

2.4.5 Enzyme-Linked Immunosorbent Assay (ELISA)

For ELISA, mouse brains and plasma were collected as mentioned in section 2.1.3. After isolation, brains were homogenized in radioimmunoprecipitation assay buffer (RIPA buffer) containing proteases and Halt™ phosphatases inhibitor cocktails. After incubation on ice for 15 minutes, the homogenates were centrifuged (13,000xg) and brain supernatants were collected. Tnf α and Il1 β protein expression levels in the plasma or brain were quantified by using corresponding mouse Quantikine ELISA Kits, according to the manufacturer's instructions.

2.6 Other General Materials

2.6.1 Technical Equipment

Equipment	Article	Manufacturer	Registered Office
Autoclave	Systec D150	Systec GmbH	Wettenberg, DE
Automatic pipettes	1, 10, 100, 1000 μ L	Eppendorf AG	Hamburg, DE
Centrifuge	Megafuge 1.0R	Heraeus Holding GmbH	Buckinghamshare, UK
Centrifuge	MCF 2360	LMS	Tokyo, JP

Equipment (continued)	Article	Manufacturer	Registered Office
Electrophoresis	Power Supply EPS 301	Amersham Biosciences	Buckinghamshare, UK
Electrophoresis	40-0911	Paqlab Biotechnologies	Erlangen, DE
FACS Sorter	BD FACSDiva	BD Biosciences	Franklin Lakes, USA
Flow Cytometer	BD FACSCalibur	BD Biosciences	Franklin Lakes, USA
Freezer (-20°C)	Premium	Liebherr	Biberach, DE
Freezer (-20°C)	Profiline GG5260	Liebherr	Biberach, DE
Freezer (-80°C)	Herafreeze	Heraeus Holding GmbH	Buckinghamshare, UK
Fridge (4°C)	Medline LKUv 1612	Liebherr	Biberach, DE
Gel Imaging System	ChemiDoc	Bio-rad	Munich, DE
Homogenizer	TissueLyserLT	Qiagen	Hilden, DE
Incubator	Hera cell 150	Heraeus Holding GmbH	Buckinghamshare, UK
Incubator Shaker	innova 4300	New Brunswick Scientific	Nürtingen, DE
Incubator Shaker	Innova 44	New Brunswick Scientific	Nürtingen, DE
Laminar flow hood	Hera safe	Kendo Laboratory Products GmbH	Langenselbold, DE
Microscope	Confocal Olympus IX81	Olympus	Hamburg, DE
Microscope	Axoskop 2 plus	Carl Zeiss AG	Oberkochen, DE
Microscope	Axiovert 40 CFL	Carl Zeiss AG	Oberkochen, DE
Microscope	ApoTome AxioObserver Z1	Carl Zeiss AG	Oberkochen, DE
Microtome	Cryostat HM 560 M Cryo-star	Thermo Fisher Scientific	Waltham, USA
Microwave Oven	Severin 800	SEVERIN Elektrogeräte	Sundern, DE
N2 Tank	MVE 611	German-cryo	Jüchen, DE
Peristaltic Pump	Pump drive PD 5001	Heidolph	Schwabach, DE
pH-meter	CG840	Schott	Mainz, DE
Pipetteboy	Cell Mate II	Thermo Fisher Scientific Inc.	Waltham, USA
Scale	Acculab	Sartorius	Göttingen, DE
Shaker	KS-15 control	Edmund Buhler GmbH	Hechingen, DE
Spectrophotometer	NanoDrop 1000	ThermoScientific	Waltham, USA
Thermocycler	T3	Biometra	Göttingen, DE
Thermocycler	Mastercycler egradient S	Eppendorf	Hamburg, DE
Thermoshaker	Thermomixer compact	Eppendorf AG	Hamburg, DE
Transilluminator	DarkReader DR89X	Clare Chemical Research	Dolores, USA
Tube rotor	VWR Tube Rotor	VWR	Langenfeld, DE
Ultracentrifuge	Sorvall Discovery 90 SE	HITACHI	Cambridge, UK
Ultracentrifuge	Sorvall RC 6+	ThermoScientific	Waltham, USA
Ultracentrifuge	Sorvall 5B Plus	Thermoscientific	Waltham, USA

Equipment (continued)	Article	Manufacturer	Registered Office
Vacuum controller	VacuuHandControl	Vacuubrand	Wertheim, DE
Vacuum pump	Vacuu-lan® network for lab	Vacuubrand	Wertheim, DE
Vortex	2X ²	Velp Scientifica	Usmate, IT
Waterbath	WB/OB7-45	Memmert GmbH & CoKG	Schwabach, DE

2.6.2 Consumables

Product	Specifications	Manufacturer	Registered Office
Cell culture pipette	5, 10, 25 mL	Sarstedt	Nümbrecht, DE
Cell scraper	17 mm	Sarstedt	Nümbrecht, DE
Cell strainer	40 µm	BD Biosciences	Heidelberg, DE
Chamber slides	Lab-Tek™ 4 chambers	Nalge Nunc	Wiesbaden, DE
Cryomolds	10 mm x 10 mm x 5mm	Sakura Finetek	Staufen, DE
Culture dish	35, 100, 150 mm	Sarstedt	Nümbrecht, DE
Culture dish	6-wells-plate	Greiner Bio One	Frickenhausen, DE
Culture flask	75 cm ²	Sarstedt	Nümbrecht, DE
Erlenmeyer flask	250 mL	Schott-Duran	Maintz, DE
Filter	0.22 µm	Sarstedt	Nümbrecht, DE
Filter	0.45 µm	Corning Inc.	Kaiserslautern, DE
Filter	0.45 µm; steriflip	Millipore	Schwalbach, DE
Filter	Bottle top 500mL	Millipore	Schwalbach, DE
Glass bottle	100, 500, 1000 mL	Schott-Duran	Maintz, DE
Gloves	Micro-touch ®	Ansell	München, DE
IHC Glass cover slips	24x60 mm	Engelbrecht	Edermunde, DE
IHC Glass slides	Superfrost Plus	ThermoScientific	Rockford, USA
Labels	Tough-Spots ® 3/8''	DiversifiedBiotech	Dedham, USA
Needels perfusion	Venofix ® 23G	Braun	Melsungen, DE
Needles injection	26 G	BD Biosciences	Heidelberg, DE
Neubauer counting-chamber	0.100 mm	Paul Marienfeld GmbH & Co. KG	Lauda-Königshofen, DE
Parafilm ®	M	Sigma-Aldrich	München, DE
Pasteur pipettes	glass	Brand	Wertheim, DE
Pasteur pipettes	plastic	Ratiolab	Dreieich, DE
Pipette tips	10, 100, 200 µL	Starlab GmbH	Hamburg, DE
QPCR Optical Adhesive Film	QPCR Seal	Paqlab Biotechnologies	Erlangen, DE
QPCR Plate	Semi-Skirted 96 wells	Paqlab Biotechnologies	Erlangen, DE
Scalpel	Feather disposable scalpel No.10	Thermo Fisher Scientific	Waltham, USA

Product (continued)	Specifications	Manufacturer	Registered Office
Syringe	1, 50 mL	BD Biosciences	Heidelberg, DE
Tubes	0.2 mL; 8-strip	Biozym Scientific GmbH	Hessich-Oldendorf, DE
Tubes	0.5, 1.5, 2 mL	Biozym Scientific GmbH	Hessich-Oldendorf, DE
Tubes	1.8 mL cryotubes	Nalge Nunc	Wiesbaden, DE
Tubes	5 mL (flow cytometry)	Sarstedt	Nümbrecht, DE
Tubes	15, 30 mL	Sarstedt	Nümbrecht, DE
Tubes	13 mL (for bacteria)	BD Biosciences	Heidelberg, DE

2.6.3 Chemicals and Reagents

Product	Manufacturer	Registered Office
Avertin	Sigma-Aldrich	München, DE
4',6-diamidino-2-phenylindole (DAPI)	Sigma-Aldrich	München, DE
Agarose	Biozym Scientific GmbH	Hessich-Oldendorf, DE
Amyloid- β 1-42 (A β)	Bachem	Weil am Rhein, DE
Bovine serum albumin (BSA)	Sigma-Aldrich	München, DE
Desoxynucleotide triphosphates (dNTPs) 10mM	Paqlab Biotechnologies	Erlangen, DE
Dithiothreiton DTT 10mM	Invitrogen, LifeTechnolgies GmbH	Darmstadt, DE
DNA ladder 100bp or 1kb	Roche	Grenzach-Wyhlen, DE
Ethanol 99%	Carl Roth GmbH	Karlsruhe, DE
Ethidium bromide	Carl Roth GmbH	Karlsruhe, DE
Ethylendiamintetraacetic acid (EDTA)	Carl Roth GmbH	Karlsruhe, DE
Fluorescent beads – Fluoresbrite Polychromatic Red Microspheres 1.0 μ m	Polysciences, Inc.	Eppelheim, DE
GelStar® Nucleic Stain	Lonza Cologne GmbH	Cologne, DE
Glycerol 99%	Sigma-Aldrich	München, DE
Heparine	Ratiopharm	Ulm, DE
Hexanucleotide mix 10x	Roche	Grenzach-Wyhlen, DE
Iso-propanol 99%	Sigma-Aldrich	München, DE
Lipopolysaccharides (LPS) 1 mg/mL	Enzo Life Sciences GmbH	Lörrach, DE
Media Opti-MEM	Gibco, LifeTechnolgies GmbH	Darmstadt, DE
Methanol	Carl Roth GmbH	Karlsruhe, DE
Milk powder	Carl Roth GmbH	Karlsruhe, DE
Mounting reagent Mowiol 4-88	Sigma-Aldrich	München, DE
Normal goat serum	Sigma-Aldrich	München, DE
NuPage® LDS Sample Buffer	Invitrogen, LifeTechnolgies	Darmstadt, DE

Product (continued)	Manufacturer	Registered Office
NuPAGE® Bis-Tris Gels 10%	Invitrogen, LifeTechnolgies GmbH	Darmstadt, DE
NuPAGE® MES SDS	Invitrogen, LifeTechnolgies	Darmstadt, DE
NuPAGE® transfer buffer	Invitrogen, LifeTechnolgies GmbH	Darmstadt, DE
PageRuler Plus	Thermo Fisher Scientific	Waltham, USA
Paraformaldehyde (PFA)	Merk & Co., Inc.	Darmstadt, DE
Phosphate buffer saline (PBS)	Gibco, LifeTechnolgies GmbH	Darmstadt, DE
Poly-L-lysine	Sigma-Aldrich	München, DE
QIAzol®	Qiagen	Hilden, DE
RIPA (RadiolImmunoPrecipitation Assay) buffer	Sigma-Aldrich	München, DE
Sodium azide	Sigma-Aldrich	München, DE
Tissue-Tek® Embedding Reagent	Sakura Finetek	Staufen, DE
Tris	Carl Roth GmbH	Karlsruhe, DE
TritonX100	Sigma-Aldrich	München, DE
Trypan blue 0.4%	Gibco, LifeTechnolgies GmbH	Darmstadt, DE
Trypsin 0.25%	Gibco, LifeTechnolgies GmbH	Darmstadt, DE
Tween	Sigma-Aldrich	München, DE
β-mercaptoethanol 99%	Carl Roth GmbH	Karlsruhe, DE

2.6.4 Kits

Product	Manufacturer	Registered Office
Dynabeads® Protein A or G	Invitrogen, LifeTechnolgies GmbH	Darmstadt, DE
Halt™ Protease Inhibitor Cocktail	Thermo Fisher Scientific	Waltham, USA
MinElute PCR Purification Kit	Qiagen	Hilden, DE
PureLink® HiPure Plasmid Filter Maxiprep Kit	Invitrogen, LifeTechnolgies GmbH	Darmstadt, DE
QIAprep Spin MiniPrep Kit	Qiagen	Hilden, DE
QIAquick Gel Extraction Kit	Qiagen	Hilden, DE
Quantikine® Mouse TNFα Immunoassay	R&D Systems Inc.	
Quantikine® Mouse IL1β Immunoassay	R&D Systems Inc.	
REExtract-N-Amp™ Tissue PCR Kit	Sigma-Aldrich	München, DE
Rneasy® Lipid Tissue Kit	Qiagen	Hilden, DE
Rneasy® Mini Kit	Qiagen	Hilden, DE
SuperSignal West Femto	Thermo Fisher Scientific	Waltham, USA
SuperSignal West Pico	Thermo Fisher Scientific	Waltham, USA

2.7 Softwares and Databases

Name	Manufacturer	Registered Office
GraphPrism	GraphPad Software, Inc.	San Diego, USA
ImageJ	National Institute of Health	Mayland, USA
IPA	Ingenuity [®] Systems	Redwood, USA
KEGG Pathways Database	http://www.genome.jp/kegg/pathway.html	
PlasMapper 2.0	http://wishart.biology.ualberta.ca/PlasMapper/index.html	

2.8 Statistical Analysis

Data presented as mean \pm SEM (standard error measurements) of at least three independent experiments. Data analyzed by students t-test or one-way ANOVA followed by Bonferroni *post-hoc* test comparing all columns using GraphPrism computer software (GraphPad Software, USA). Results are considered significant if * $p < 0.05$, ** $p < 0.01$, *** $p < 0.001$.

3. Results

3.1 TREM2 Deficient Mouse Characterization

3.1.1 Aged TREM2 Deficient Mice Show Increased Levels of Inflammatory Transcripts

It was reported previously that the absence of TREM2 *in vitro* (Takahashi et al., 2005) and *in vivo* (Piccio et al., 2007; Takahashi et al., 2007), as well as in Nasu-Hakola disease (Bianchin et al., 2010; Kaneko et al., 2010b; Satoh et al., 2011b) leads to different microglial cytokine release. Thus, in the present study, the cytokine profile of the TREM2 KO mouse model was investigated in whole mouse brain by sqRT-PCR (Fig. 3.1).

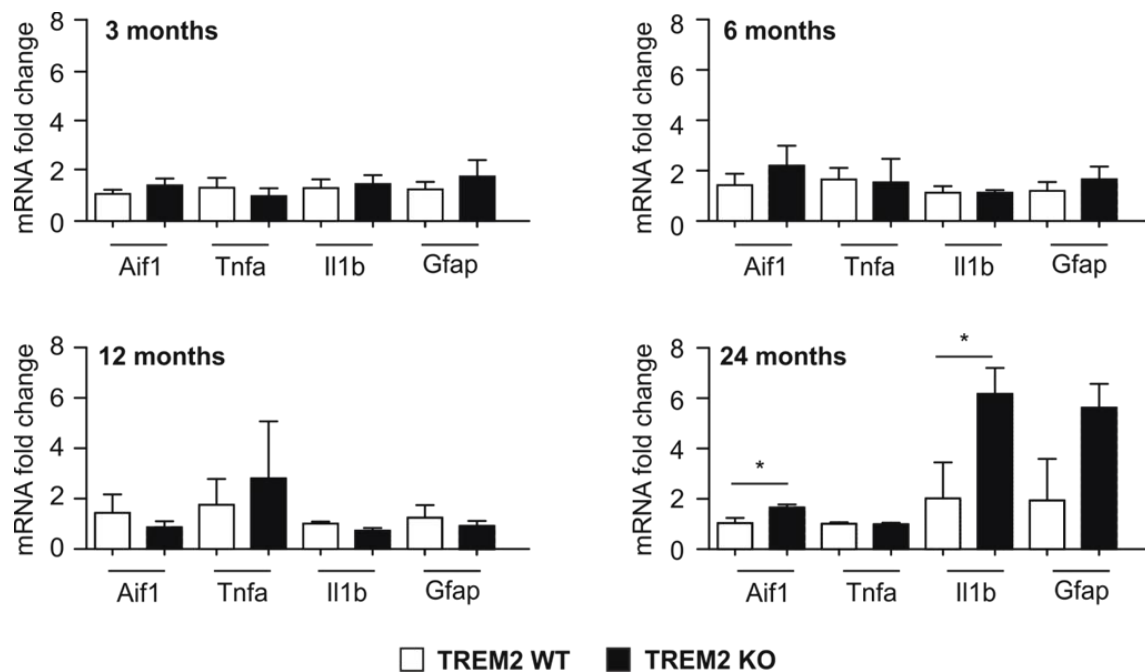


Figure 3.1 – Increase of microglia- and astrocytes-related mRNA levels in aged TREM2 knock-out (KO) mice. Transcripts of microglial *Allograft inflammatory factor 1* (*Aif1*), *Tumor necrosis factor alpha* (*Tnfa*), *Interleukin 1 beta* (*Il1b*) or astroglia specific marker *Glial fibrillary acidic protein* (*Gfap*) were measured in TREM2 KO or wild type (WT) control mice of 3, 6, 12 or 24 months of age. Differences in the transcript levels were observed only in 24 months old TREM2 KO mice. $n \geq 3$ animals.

Mice screened at 3, 6 or 12 months presented similar levels of microglia activation markers *Aif1*, *Tnfa*, *Il1b* mRNA levels (Fig. 3.1). At 24 months, TREM2 KO animals presented higher levels of *Aif1* and *Il1b* compared with TREM2 WT controls (Fig. 3.1). Due to the presence of astrogliosis in brains affected by Nasu-Hakola disease (Satoh et al., 2011b), astroglia specific marker *Gfap* mRNA was also assayed in TREM2 KO mice of different ages. At 24 months, TREM2 KO animals

presented higher levels of *Gfap* compared with TREM2 WT controls, but without reaching significance (Fig. 3.1).

3.1.2 Changed Microglial Morphology in Adult TREM2 KO Mice

A feature of microglial cells is their ability to respond to stimuli by changing their cellular shape and processes (Ransohoff and Perry, 2009). To investigate possible dysfunctions in the response of TREM2 deficient microglia to inflammatory stimulation, additional groups of mice were challenged with LPS or PBS accordingly to a repeated LPS challenge paradigm described by Cardona and colleagues (4 daily doses of 1 μ g LPS per gram body weight, gbw LPS; Cardona et al., 2006; Fig. 2.1). Brain slices of 3 months-old TREM2 KO and WT controls were stained against the microglial marker Iba1 and different morphological parameters were used to measure the microglial changes in TREM2 KO and WT mice (Fig. 3.2).

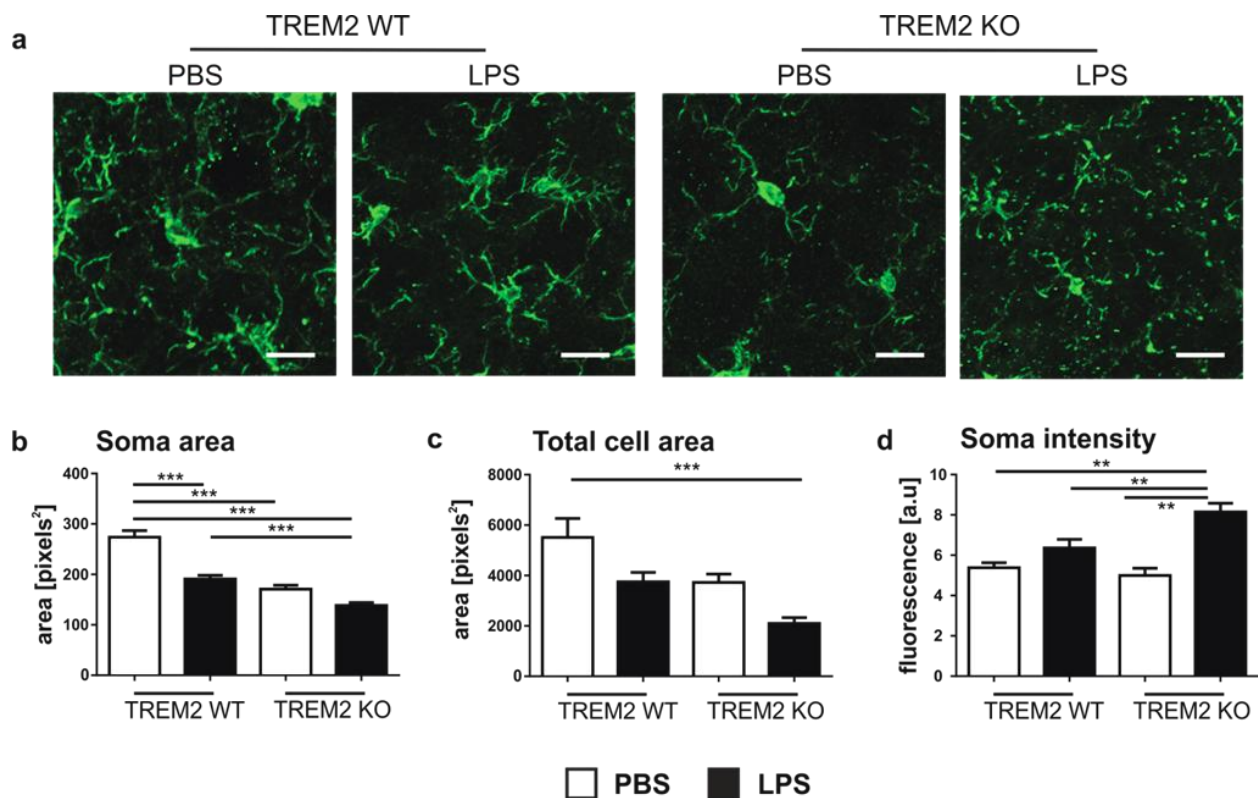


Figure 3.2 – Changed microglial morphology in TREM2 KO animals. **a** – Representative images of microglial marker Iba1 immunostaining showing genotype- and treatment-related morphological differences. Scale bar: 25 μ m; **b** - Total area covered by microglia soma or **(c)** soma plus processes presents decreased area coverage in TREM2 KO mice, further accentuated by LPS treatments; **d** - Iba1 soma intensity measurement presents a significant increase in the TREM2 KO animals treated with LPS compared with the other experimental groups. a.u. – arbitrary units; n=4.

The TREM2 KO animals showed significantly reduced microglial cell bodies area compared with TREM2 WT animals in the absence of LPS treatment (155.9 ± 7.68 pixels² in TREM2 KO mice vs. 262.3 ± 13.59 pixels² in TREM2 WT, $p < 0.001$; Fig. 3.2b). LPS treatment decreased further the microglial soma area in TREM2 KO animals (from 155.9 ± 7.68 pixels² in PBS treated mice to 127.5 ± 4.67 pixels² in TREM2 KO animals treated with LPS, $p < 0.001$; Fig. 3.2b). After LPS treatment, TREM2 WT animals showed decreased microglial soma area compared with PBS treated mice (from 262.3 ± 13.59 pixels² in PBS group to 174.7 ± 5.41 pixels² in LPS treated TREM2 WT mice, $p < 0.001$; Fig. 3.2b).

The total area covered by microglia (soma and processes) presents a similar pattern with the soma area in TREM2 WT and KO animals treated with PBS or LPS (Fig. 3.2b). However, only the TREM2 KO animals treated with LPS were statistically significantly different compared to PBS treated TREM2 WT animals (from 5507 ± 759 pixels² in PBS treated TREM2 WT mice, to 2094 ± 234 pixels² in LPS treated TREM2 KO animals, $p < 0.001$; Fig. 3.2c).

The intensity of the Iba1 staining was measured as additional readout of microglial activation, showing similar levels between TREM2 WT and KO animals when treated with PBS, and significantly higher levels in the TREM2 KO animals after the repeated LPS treatment compared with the WT animals (from 5.02 ± 0.72 fluorescence units in TREM2 WT treated with LPS to 8.37 ± 0.94 fluorescence units in TREM2 KO treated with LPS, $p < 0.01$; Fig. 3.2d).

3.1.3 Similar Inflammatory Transcripts in TREM2 KO and WT mice after Systemic LPS Challenges

To investigate possible changes in gene expression triggered by LPS challenges, the mRNA levels of microglial marker gene *Aif1* and proinflammatory genes *Il1b* or *Tnfa* were investigated in TREM2 KO mice and WT controls. The transcripts showed similar response to LPS application in both TREM2 KO and WT animals (Fig. 3.2).

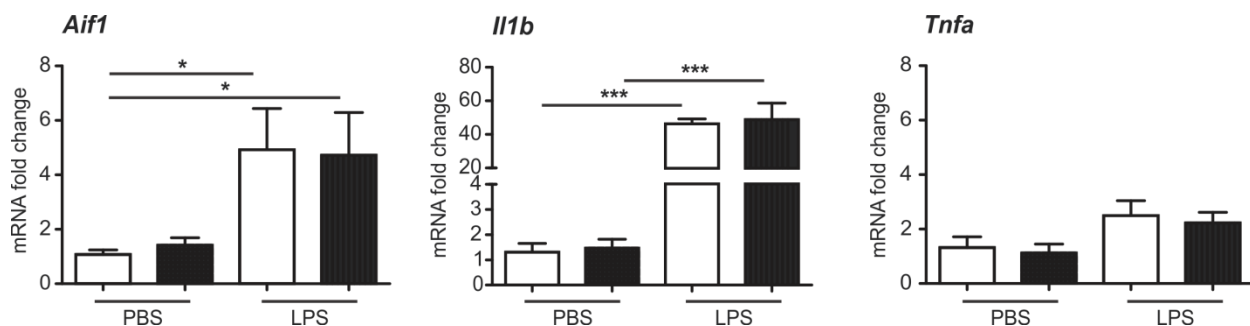


Figure 3.3 – TREM2 deficiency is not affecting the normal proinflammatory response inside CNS. Mice were treated with LPS intraperitoneally. $n \geq 3$.

3.2 Immune System Involvement in Dopaminergic Degeneration Induced by Systemic LPS Challenges

Cardona and colleagues briefly described a fast protocol of neuroinflammation triggered by repeated i.p. LPS challenges of mice (Cardona et al., 2006). To obtain insights on the mechanisms involved in this process, the repeated LPS treatment protocol was in BL6 mice and compared with a single cumulative dose of i.p. LPS (Fig. 2.1).

3.2.1 Microglial Activation by Systemic LPS Treatments

The effect of single or repeated LPS challenge on microglia of BL6 mice was investigated at two different time points: on experimental day 5 and 19 (Fig. 2.1). A sqRT-PCR analysis of the microglial marker *Aif1* mRNA in the whole mouse brain lysate revealed that on day 5 after single LPS treatment, a slight increase in the mRNA level was detectable, whereas after the repeated LPS treatment was registered a significant increase compared with the single LPS treatment (from 1.66 ± 0.28 FC in single LPS treated group to 3.08 ± 0.18 FC in repeated LPS group, $p < 0.01$; Fig. 3.4). Nineteen days after the start of the treatment, the mRNA level of *Aif1* gene has returned to normal control values (Fig. 3.4).

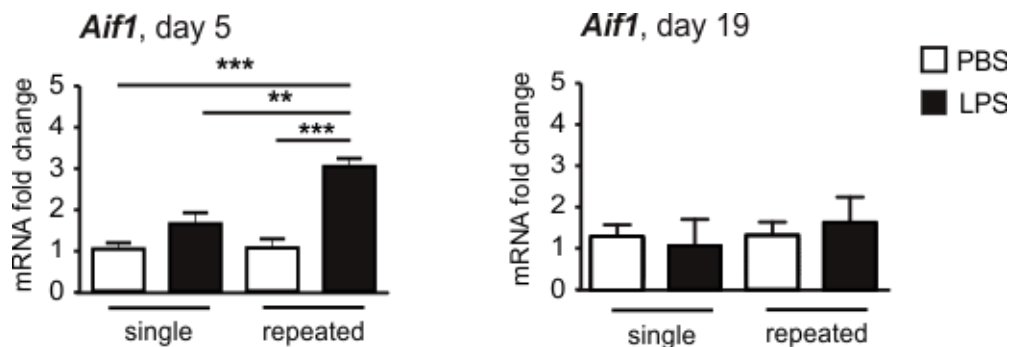


Figure 3.4 – *Aif1* mRNA levels in whole mouse brain are significantly increased on day 5 after repeated LPS treatment (left) and returned to control values on day 19 (right). On day 5 after LPS treatment, sqRT-PCR measurements of *Aif1* mRNA show increased levels that were significant after repeated LPS application. The *Aif1* transcript levels returned to control levels on day 19. $n \geq 3$.

Next, the levels of the *Aif1* expression product, the Ionized calcium-binding adapter molecule 1 (Iba1), were investigated in mice after i.p. application of LPS. In this regard, substantia nigra *pars reticulata* (SN_{pr}), a brain region that presents a relative high amount of microglial cells

compared with other brain regions (Kim et al., 2000; Lawson et al., 1990), was immunohistochemically (IHC) analyzed in mice systemically challenged with LPS accordingly to the single or repeated treatment paradigms (Fig. 3.5a). On day 5, IHC analysis showed an increase of Iba1 immunoreactivity after a single LPS challenge (from 32.53 ± 2.11 cells per section in PBS controls to 145.3 ± 8.35 cells per section in LPS challenged mice, $p < 0.001$; Fig. 3.9b). However, after repeated LPS application, mice showed on day 5 a lesser extent of Iba1 staining after repeated treatments (from 32.53 ± 2.11 cells per section in PBS controls to 77.07 ± 2.24 cells per section in LPS treated mice, $p < 0.001$) (Fig.3.5b). On day 19, the immunoreactivity of Iba1 returned to the initial levels (Fig. 3.5b).

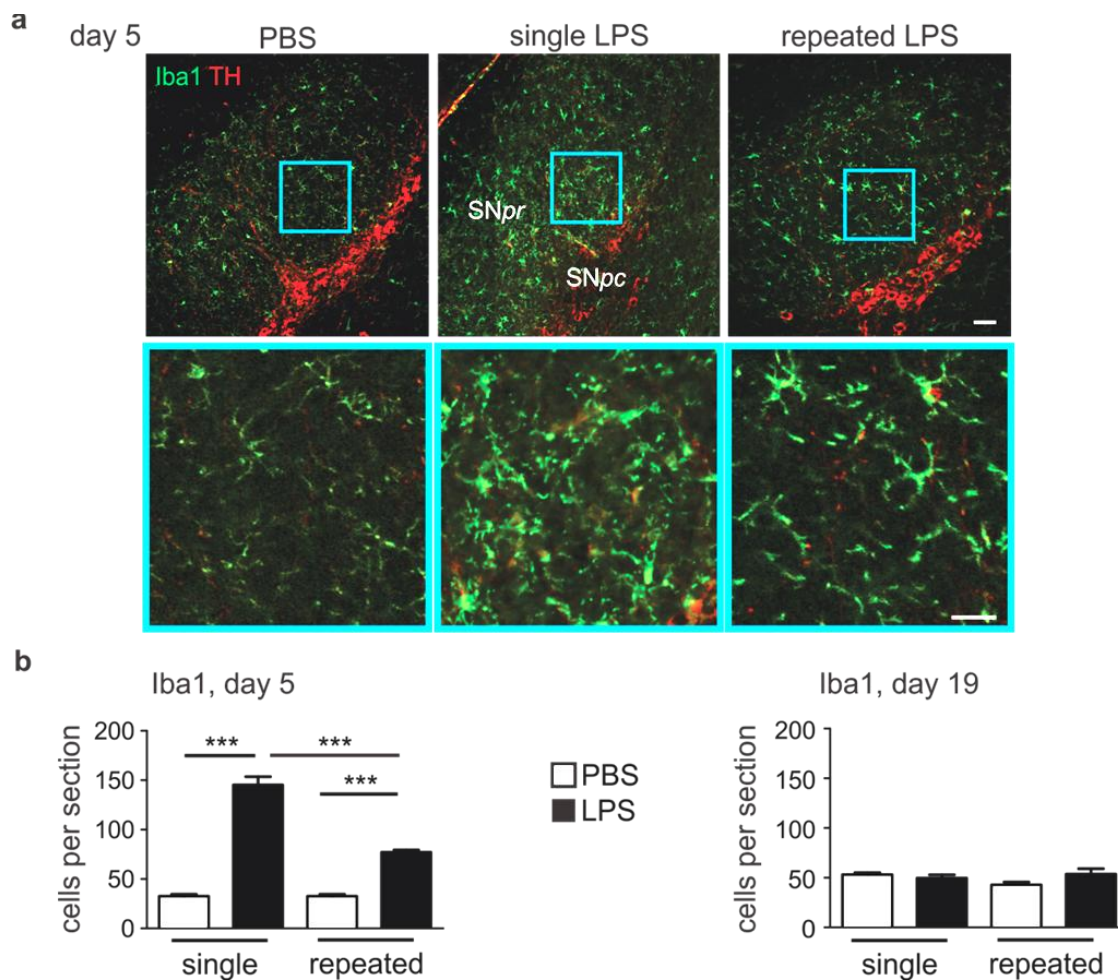


Fig 3.5 - Immunoreactivity of the microglial marker Iba1 is significantly increased on day 5 after LPS treatments and returns to control level on experimental day 19. **a** – Representative images of Iba1 immunostaining (green) in the substantia nigra *pars compacta* (SNpc) and *pars reticulata* (SNpr) presented. Dopaminergic marker tyrosine hydroxylase (TH, red) was used for defining the SNpc and SNpr anatomical areas. Scale bar: 50 μ m, insert: 25 μ m; **b** – Quantification of the Iba1 positive cells on day 5 after treatment (left) presents increased Iba1 immunoreactivity after LPS application, with the single LPS challenge exceeding significantly the levels reached by the repeated LPS treatment. On day 19, Iba1 immunoreactivity returned to control levels. $n \geq 3$ animals.

3.2.2 Proinflammatory Transcripts in Mice Systemically Challenged with LPS

Activated microglia release a broad spectrum of pro- or anti-inflammatory molecules as response to changes in the brain parenchyma (reviewed in Neumann et al., 2008; Ransohoff and Perry, 2009). For this reason, a proinflammatory cytokines profile in whole brain of mice was carried out by sqRT-PCR on day 5 or 19 after systemical application of LPS accordingly to the single or repeated treatment paradigms (Fig. 3.6). For this, *Tnfa*, *Il1b* and *Nos2* mRNA were chosen as markers of microglial activation. When assayed on day 5, mice i.p. challenged once with LPS showed a slight up-regulation of *Tnfa* and *Il1b* brain mRNA levels, but no modulation of *Nos2* mRNA (Fig 3.6). However, the repeated LPS challenge of mice lead to a significant increase of *Tnfa* mRNA compared with PBS treated controls or even single treated mice (from 3.26 ± 1.17 FC after single LPS challenge, to 8.88 ± 2.19 FC after repeated LPS application, $p < 0.05$; Fig. 3.6a). The *Il1b* mRNA level was also significantly increased by the repeated treatment (from 7.27 ± 1.46 FC after single LPS treatment, to 32.47 ± 12.5 FC after the repeated treatment; Fig. 3.6a). In contrast with the single LPS application, the *Nos2* mRNA was induced by the repeated treatment (0.8 ± 0.08 FC after single LPS application, to 3.2 ± 0.4 FC after repeated LPS application, $p < 0.001$; Fig 3.6a).

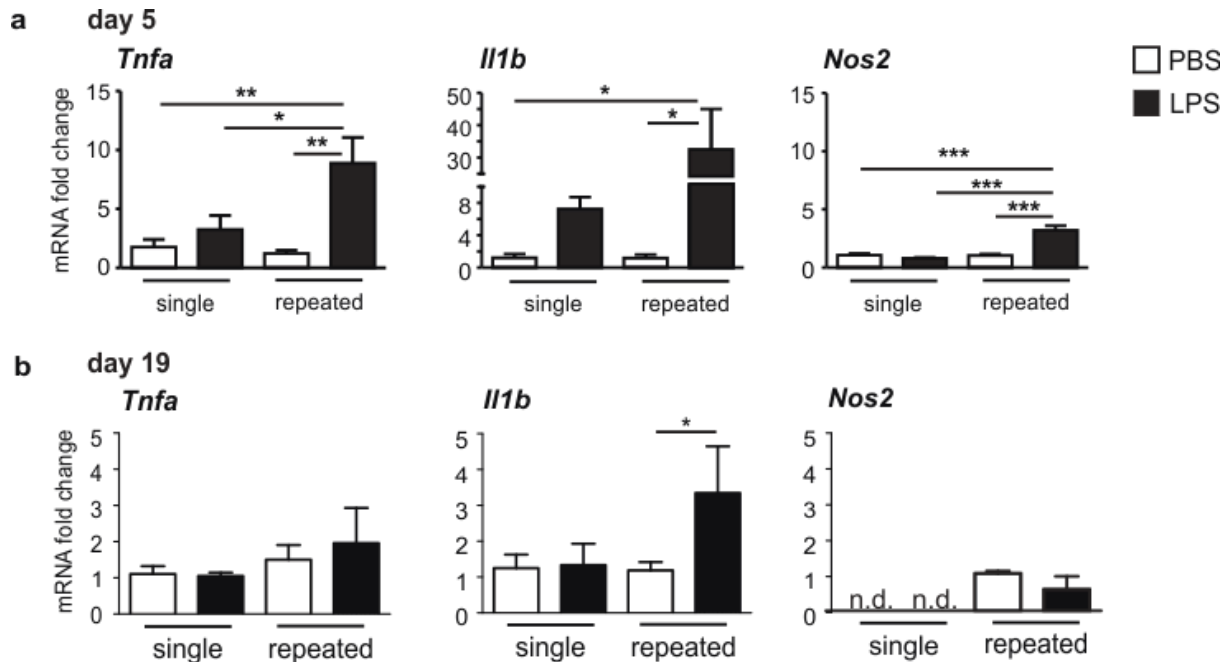


Figure 3.6 – Transcription levels of proinflammatory markers *Tnfa*, *Il1b* and *Nos2* in whole mouse brain were increased on day 5 after repeated LPS treatments, with values returning to control level on day 19. a – On day 5, *Tnfa*, *Il1b* and *Nos2* mRNA levels were increased after LPS treatments, with the highest increase reached after repeated challenges; b – On experimental day 19, the transcripts levels were unchanged after single or repeated LPS challenge compared to the control, with the exception of *Il1b* which maintained an increased mRNA level after repeated LPS challenge. n.d.: not detected. $n \geq 3$.

However, on day 19, only *Ii1b* mRNA level after the repeated LPS treatment showed significant differences (from 1.33 ± 0.6 FC in single LPS treatment to 3.35 ± 1.3 FC after repeated LPS treatment, $p < 0.05$; Fig 3.6b). The levels of *Tnfa* and *Nos2* mRNA in whole mouse brain lysates were similar in single or repeated LPS or PBS challenged animals (Fig. 3.6b).

Since the method of LPS application is based on i.p. injections, the brain response to LPS was next compared with the peripheral response to LPS. In this regard, Enzyme-Linked Immunosorbent Assay (ELISA) was used to assay the protein levels of $Tnf\alpha$ and $Il1\beta$ in brain and blood plasma of mice on day 5 after single or repeated LPS i.p. challenges (Fig. 3.11). Data show that the response to single or repeated peripheral LPS application leads to increase levels of $Tnf\alpha$ and $Il1\beta$ cytokines productoin in the brain after both treatment paradigms. After the repeated LPS treatments, $Tnf\alpha$ and $Il1\beta$ levels are significantly increased compared with the single LPS application: for $Tnf\alpha$ from 3.5 ± 1.4 pg/mL after single LPS application to 44.4 ± 12.1 pg/mL after repeated LPS application ($p < 0.001$) and for $Il1\beta$ from 21.4 ± 4.8 pg/mL (single LPS) to 84.2 ± 12.4 pg/mL (repeated LPS; $p < 0.05$; Fig. 3.7a). In plasma however, both $Tnf\alpha$ and $Il1\beta$ levels are increased after the LPS treatments, but to similar levels (Fig. 3.7b).

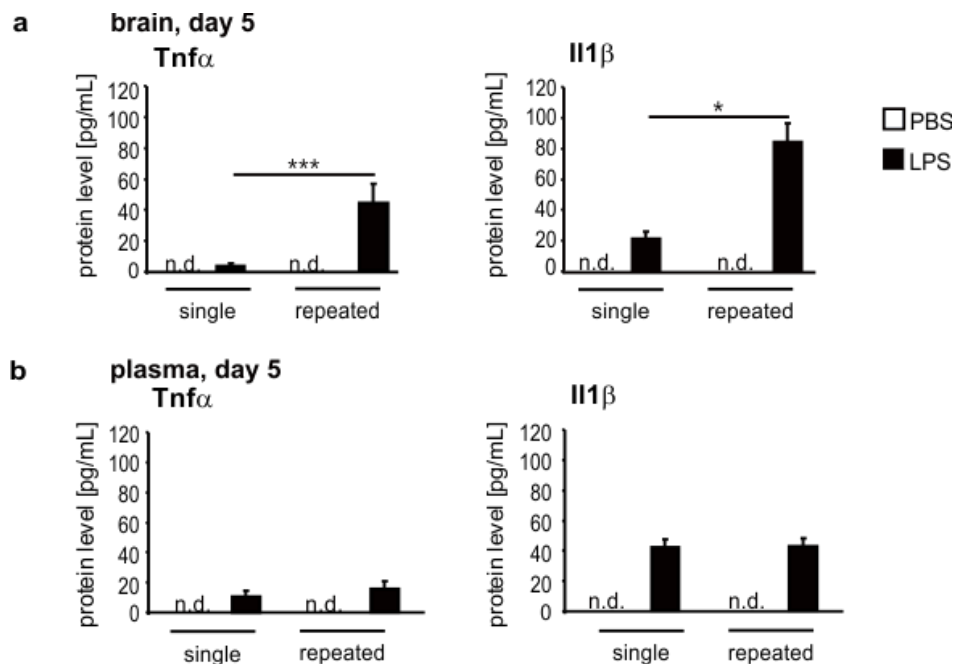


Figure 3.7 – Different proinflammatory cytokines response to LPS stimulation in the brain compared with the periphery when measured on experimental day 5. a - Enzyme-linked immunosorbent assay (ELISA) measurements of cytokines in brain shows pronounced elevation of $Tnf\alpha$ and $Il1\beta$ cytokines after repeated treatment; **b** – Plasma levels of $Tnf\alpha$ and $Il1\beta$ showed similar response to LPS after single or repeated treatment. n.d.: not detected. $n = 3$; data provided by Dr. Yiner Wang.

3.2.3 Loss of Dopaminergic Neuronal Triggered by Systemic LPS Challenges

Dopaminergic neurons were previously demonstrated to be affected by LPS-triggered microglia activation (Arai et al., 2004; Hernández-Romero et al., 2012; Kim et al., 2000). Therefore, the dopaminergic system after single or repeated LPS administration in BL6 mice was explored next.

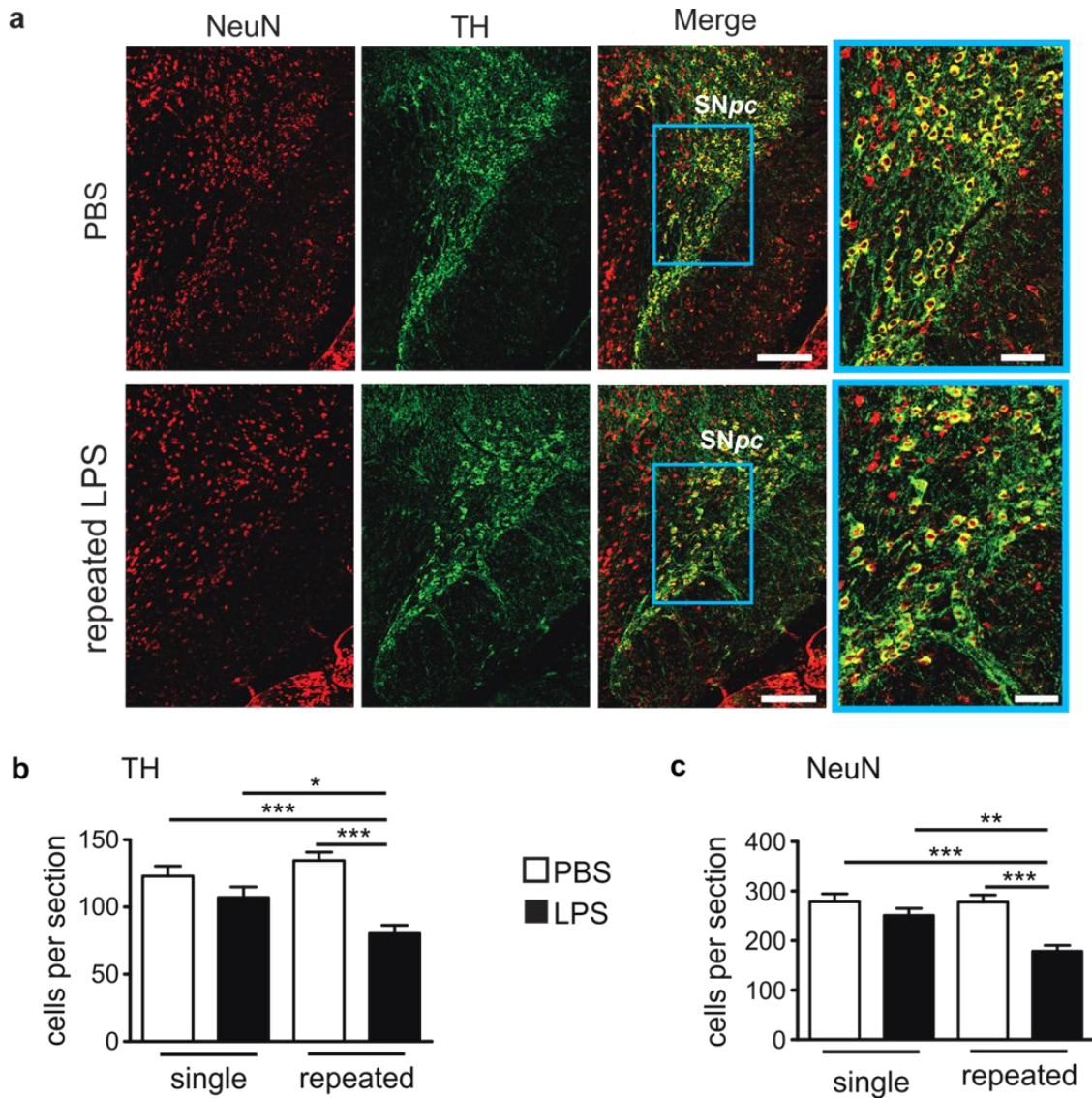


Figure 3.8 – Repeated LPS challenge of mice lead to dopaminergic neuronal loss on day 19. a – Representative images of TH/NeuN immunostaining in the repeated LPS treatment group (bottom) compared with the repeated PBS treatment group (top). Scale bar: 150 μ m, insert: 50 μ m; **b –** Quantification of TH and NeuN positive cells shows induced loss of TH and NeuN positive neurons after systemic repeated LPS application. $n \geq 3$.

SN *pars compacta* (SNpc) region of the brain contains the highest accumulation of dopaminergic perykaria. Serial sections of SNpc were analyzed on day 19 after single or repeated LPS challenges of mice by immunostaining of the dopaminergic specific marker Tyrosine hydroxylase (TH) and Neuronal nuclei marker (NeuN). SNpc serial sections showed a relative reduction of the number of TH positive cell bodies (from an average of 134.6 ± 6.24 cells per section, to 80.28 ± 6.20 cells per section, $p < 0.001$; Fig. 3.8b) and of NeuN positive cells (from 277.9 ± 14.30 cells per section to 178.4 ± 12.25 cells per section, $p < 0.001$; Fig. 3.8c) after repeated LPS application.

3.2.4 Brain Transcriptome Analysis of Systemic LPS Challenged Mice

To identify key players in the dopaminergic degeneration triggered by the LPS treatments, a transcriptome analysis comparing the single LPS challenge and the repeated LPS treatment was performed next.

Whole brain cDNA array of mice challenged with LPS was analysed. A number of 194 genes were found significantly changed after the single LPS treatment and 334 genes after the repeated treatment, compared with appropriate PBS controls (false discovery rate (FDR) < 0.05 ; absolute \log_2 fold change (FC) ≥ 0.5). Volcano plot representation proved that the differentially expressed genes (DEG) were mostly up-regulated and that the repeated LPS treatment triggered a higher number of DEG compared with the single treatment (Fig. 3.9).

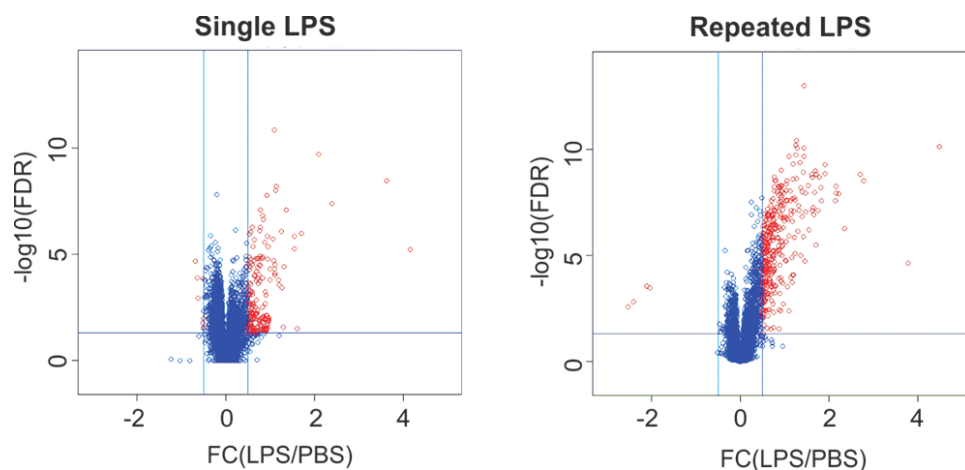


Figure 3.9 – Volcano plots display of differentially expressed genes (DEG) in the brain reveal increased DEG levels in repeated LPS challenged mice on day 5. Each circle represents a gene. The genes corresponding to significant DEG (fold change (FC) ≥ 0.5 , false discovery rate (FDR) < 0.05) depicted in red. Blue circles above the horizontal line represent genes with significant differences in expression between LPS and PBS but with weak fold changes. $n = 6$; data analysed in collaboration with Dr. Sinkkonen, University of Luxembourg.

An Ingenuity Pathway Analysis (IPA) for exploring the general significant biological functions related to the array data (FDR < 0.05) was performed. The top ten pathways are presented in Fig. 3.11. The IPA analysis revealed that many of the DEG up-regulated in the brain by LPS treatment were immune-related (e.g. enrichment of the immune cell trafficking pathway, inflammatory response pathway, inflammatory disease pathway). Other enriched pathways were represented by cellular movement, cellular function or maintenance pathways (Fig. 3.11). However, the biological functions analyzed by IPA generally proved a stronger enrichment by the repeated LPS treatment compared with the single LPS treatment.

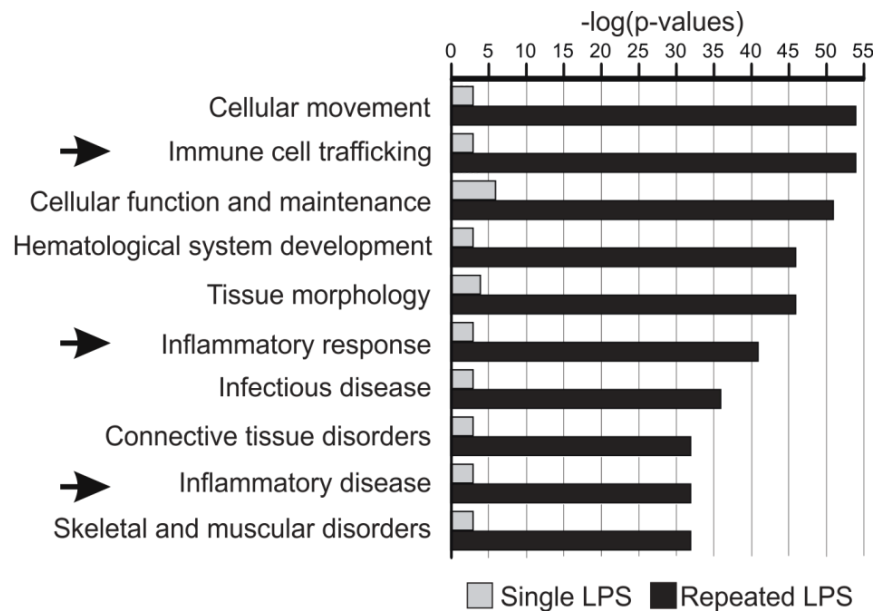


Figure 3.11 – Ingenuity Pathway Analysis of differentially expressed genes (FDR < 0.05) in whole mouse brain on experimental day 5 after single or repeated LPS challenge. Top ten most enriched functions after single or repeated LPS treatment represented. Arrows are pointing to immune-related pathways. n = 6 animals; data analysed in collaboration with Dr. Sinkkonen, University of Luxembourg.

3.2.5 Phagosome- and Complement-related Pathways Enriched by Systemic LPS Challenges

To get further insights on the difference between the single and the repeated LPS treatment mechanisms, a more detailed analysis of DEG was performed. In Fig. 3.12a, a Venn diagram summary of the number of genes selectively and significantly (FDR < 0.05; FC ≥ 2) up-regulated in the brain tissue on day 5 after single or repeated LPS treatment compared to the PBS is presented (for a comprehensive list of the genes, see Appendix).

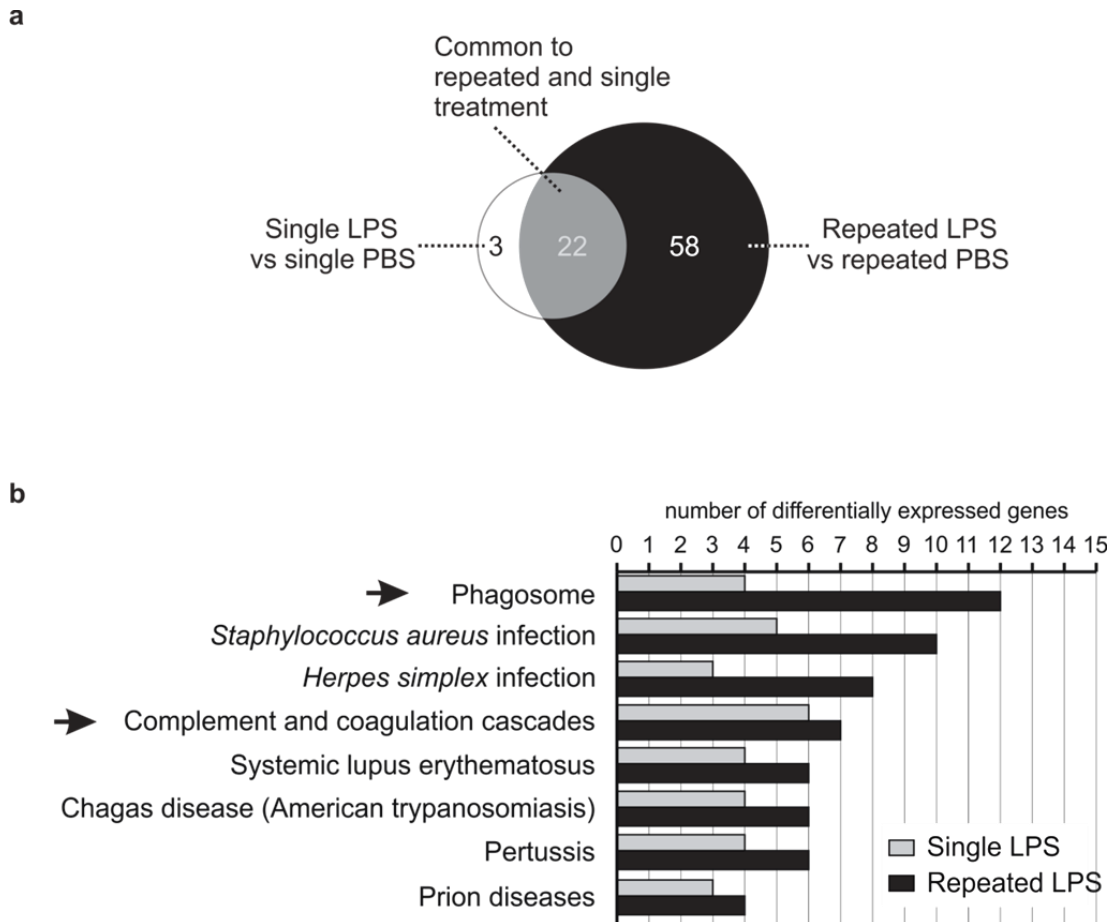


Figure 3.12 – Higher number of DEGs and associated pathways in the repeated LPS treatment group compared with the single treatment group. a – Venn diagram depicting DEG (FDR < 0.05, FC ≥ 2) distribution per treatment group. Only 3 DEG are specific to the single treatment, whereas 58 DEG are specific to the repeated treatment. A common single and repeated group of 22 DEG was observed. **b** - Kyoto Encyclopedia of Genes and Genomes (KEGG)-based pathway comparison of the 80 genes up-regulated after the repeated LPS treatment and the 25 genes up-regulated by the single LPS treatment. The phagosome pathway ranked as the most selectively up-regulated pathway in the repeated LPS challenge, whereas complement and coagulation cascade was found to be enriched in the brains after both single and repeated treatments. n = 6 animals; data analysed in collaboration with Dr. Sinkkonen, University of Luxembourg.

Only 3 DEG are specifically up-regulated by the single treatment, of which which two are indirectly linked to immune function (Fig. 3.12a, Appendix). A number of 22 DEG are common to both single and repeated LPS treatments, most of them being immune-related genes, e.g. complement components, chemokines and major histocompatibility (MHC) molecules (Fig. 3.12a, Appendix). A total number of 58 DEG were uniquely up-regulated by the repeated treatment, also mainly immune-related genes, e.g. complement components, Fc-receptors and MHC molecules (Fig. 3.12a, Appendix). Next, a Kyoto Encyclopedia of Genes and Genomes (KEGG) pathway analysis of all the 80 (58 specific and 22 common) genes up-regulated after repeated LPS treatment in comparison to single dose treatment was performed (Fig. 3.12b).

The most prominently up-regulated pathway emerging in the KEGG analysis after repeated LPS application was represented by the phagosome pathway (12 DEG after repeated challenge vs. 4 DEG after single LPS challenge; Fig. 3.12b). Interestingly, the complement cascade was the strongest commonly enriched pathway by both single and repeated LPS challenge (7 DEG after the repeated LPS challenge vs. 6 DEG after the single LPS challenge; Fig. 3.12b). Among these pathways, elements specific to a certain type of infectious agents were found (e.g. to *Staphylococcus aureus* infection, Chagas disease or *Herpes simplex* infections), but they were improbable in the experimental set-up used (Fig. 3.12b).

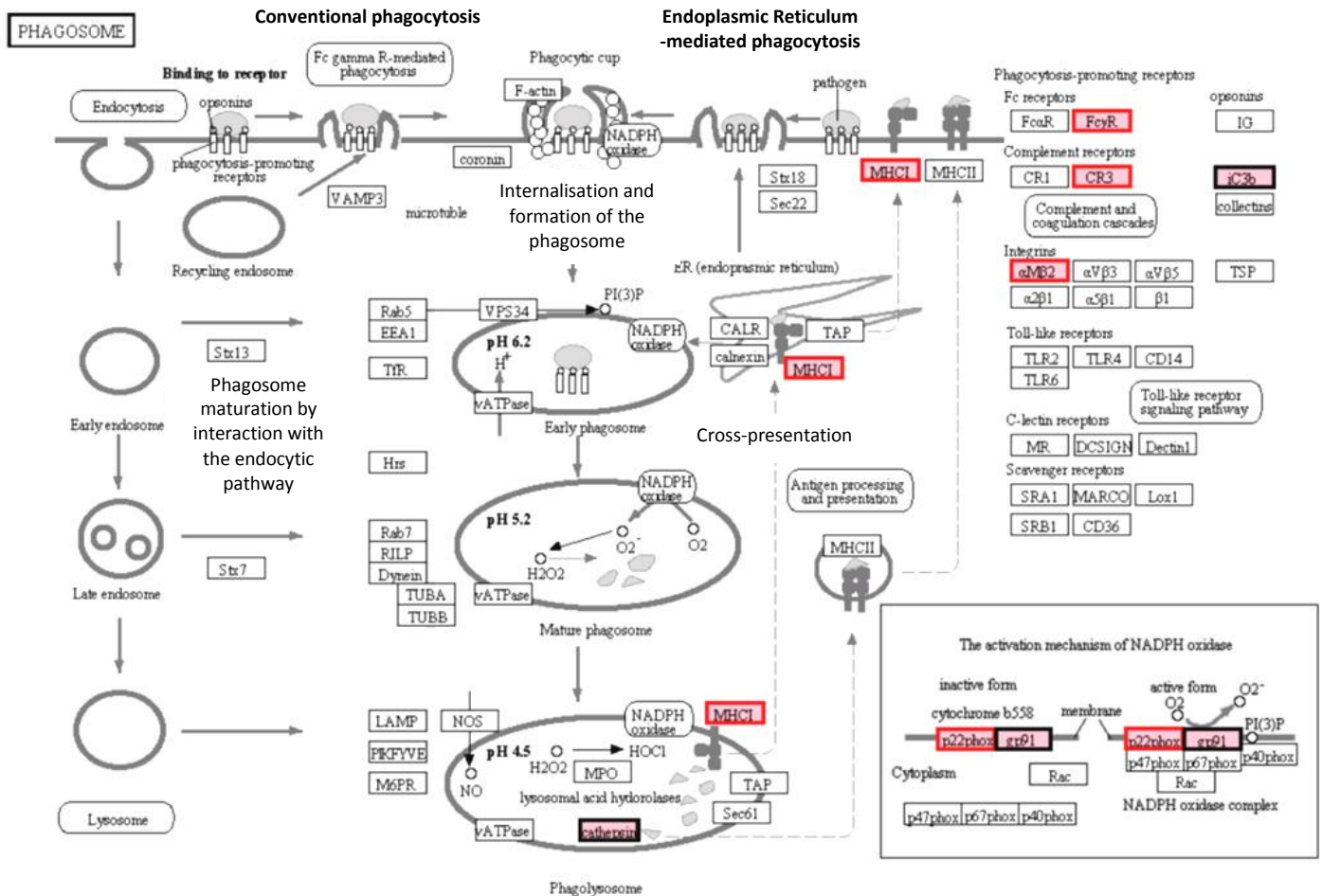


Figure 3.13 – Specific and common DEG of the phagosome pathway enriched by the LPS treatments. Specific DEG of the endoplasmic reticulum-mediated phagocytosis after the repeated LPS challenges (shown within red framed pink boxes) were: major histocompatibility complex I members (here depicted as *MHCI*), complement cascade members (*CR3* and its subunit *αMβ2*), targeted phagocytosis receptors (*FcγR*) and NADPH components (*p22phox*). Members of the same phagocytosis pathway common to both single and repeated LPS treatment groups (shown in black framed pink boxes) were represented by lysosomal proteases (*cathepsin S*), NADPH components (*gp91*) and complement cascade members (*iC3b*). No members of the endoplasmic reticulum-mediated phagocytes were found up-regulated specifically after single LPS challenge. n=6; data analysed in collaboration with Dr. Sinkkonen, University of Luxembourg.

A more detailed KEGG analysis of the phagosome pathway in whole brain mRNA of mice systemically challenged with LPS and analyzed on experimental day 5, was performed to identify common and specific DEG contributing to the pathway (Fig. 3.13). In the KEGG analysis, elements common to both acute and repeated LPS challenge were represented by the complement cascade member *C3*, the lysosomal protease Cathepsin S (*Ctss*), and the gp91 subunit (*Cybb*) of the nicotinamide adenine dinucleotide phosphate-oxidase (NADPH) complex (Fig. 3.13 and Appendix). Elements unique to the repeated LPS challenges were composed of MHC class I members (*H2-d1*, *H2-q6*, *H2-q7*), complement cascade members (*C3* and Integrin $\alpha_M\beta_2$, *Itgam* - part of the complement receptor 3, *CR3*), phagocytosis-related molecules (*Fcer2b*, *Fcgr3*, *Fcgr4*) or p22phox (*Cyba*), member of the NADPH complex (Fig. 3.13 and Appendix).

Next, a validating sqRT-PCR of representative elements of the array was performed (Fig. 3.14). The mRNA level of two common key adaptor molecules implicated in phagocytosis (DAP12 encoded by the *TYRO protein tyrosine binding protein* - *Tyrobp* gene and the common γ chain encoded by *Fcer1g* gene), together with the mRNA level of two phagosome-related NADPH oxidase members (p22phox – *Cyba* and gp91 – *Cybb*) were chosen to be further investigated.

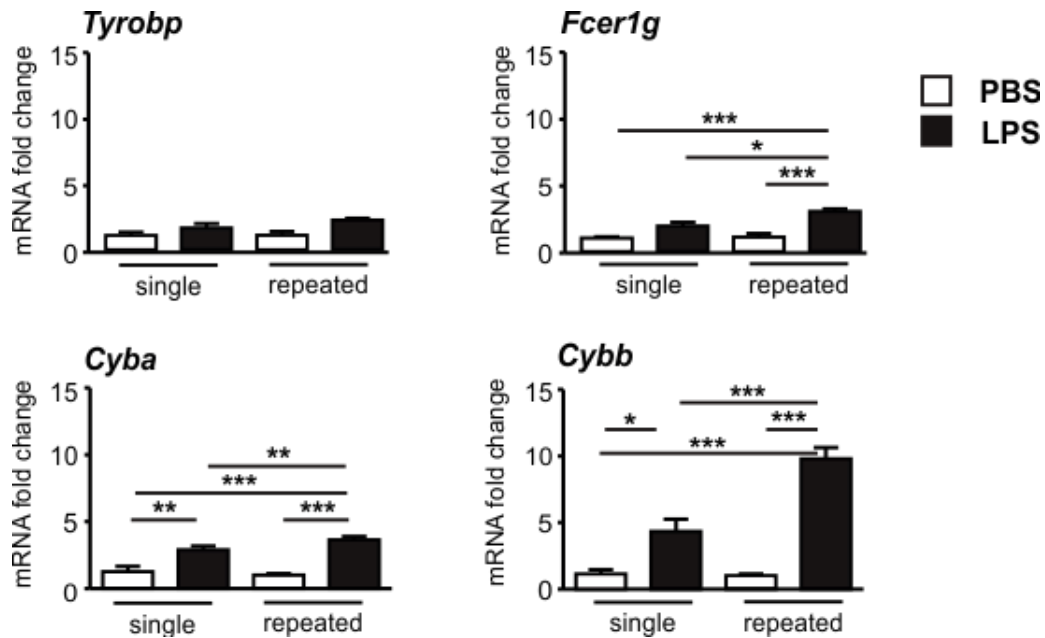


Figure 3.14 - mRNA levels of elements involved in phagocytosis (*Tyrobp*, *Fcer1g*) or phagocytosis-related oxidative stress (*Cyba*, *Cybb*) in whole mouse brain on day 5 after single or repeated LPS treatment. *TYRO protein tyrosine kinase-binding protein* (*Tyrobp*, encoding the DAP12 protein) mRNA was slightly increased by the repeated LPS treatment, whereas *high-affinity IgE receptor γ polypeptide* (*Fcer1g*, encoding the common Fc γ chain protein) was significantly increased by the repeated LPS challenges. NADPH oxidase components *cytochrome b-245, α polypeptide* (*Cyba*, encoding the p22phox protein) and *cytochrome b-245, β polypeptide* (*Cybb*, encoding gp91phox) mRNA levels were significantly up-regulated already by the single LPS treatment. After the repeated LPS challenges, the mRNA level of *Fcer1g*, *Cyba* and *Cybb* was further significantly increased. n = 6 animals.

Whole brain mRNA of mice systemically challenged with LPS after the single or repeated treatment paradigms were analyzed on experimental day 5. *Tyrobp* and *Fcer1g* led to a similar pattern of up-regulation in the mRNA levels after both LPS treatment paradigms, with a higher increase after the repeated challenge. *Fcer1g* reached significance after the repeated treatment, from 1.91 ± 0.28 FC, after single LPS challenge, to 3.1 ± 0.19 FC after repeated LPS challenge, $p < 0.05$; Fig 3.14. Both *Cyba* and *Cybb* mRNA levels were significantly increased by the single treatment and even significantly further increased by the repeated LPS challenge. Thus, *Cyba* gene transcription was increased from 2.91 ± 0.26 FC (single LPS) to 3.64 ± 0.24 FC (repeated LPS; $p < 0.01$; Fig. 3.14) and *Cybb* from 4.33 ± 0.94 FC (single LPS) to 9.8 ± 0.83 FC (repeated LPS; $p < 0.001$; Fig 3.14).

3.2.6 C3 Deficiency Abrogates Dopaminergic Neuronal Loss after Repeated LPS Challenges

To elucidate the mechanism of dopaminergic neuronal loss, the cDNA array data and related pathways analysis obtained on day 5 after single or repeated LPS treatment of mice (see sections 3.2.4-5) were analyzed thoroughly.

Complement cascade was found highly represented in the brain within the common elements of the single and repeated LPS treated animals (Fig. 3.12b, 3.13, Appendix). Thus the complement pathway was analyzed in more detail (Fig. 3.15). The array data provided evidence on the enrichment of the first components of the classical/alternate pathway (*C1q*, *SerpinG1*, *C4*, *C3*, *HF1*), with *C3* being a critical key element on day 5 after LPS challenge (Fig 3.15).

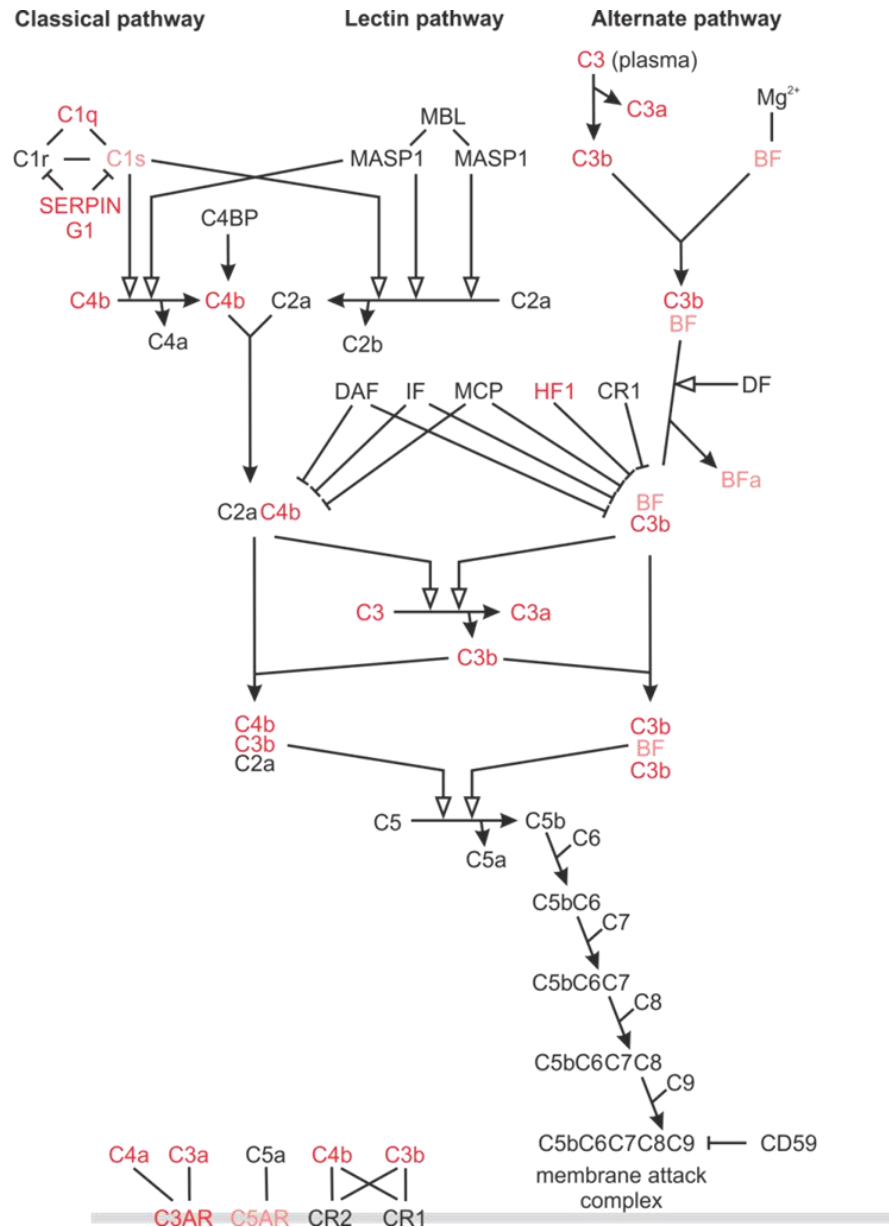


Figure 3.15 – DEG in the complement system pathway in mice after single or repeated treatments with LPS vs. PBS on experimental day 5. Ingenuity Pathway Analysis performed on significantly DEG (FDR < 0.05) in each condition (single and repeated LPS treatment). The canonical complement pathway showed a significant enrichment in both conditions ($p < 0.05$). The overlay corresponds to repeated treatment and significant up-regulated genes are shown in red color. $n = 6$; data analysed in collaboration with Dr. Sinkkonen, University of Luxembourg.

To confirm the array results, sqRT-PCR was performed. The sqRT-PCR analysis showed that *C1q* was not modulated by the LPS challenges (Fig 3.16). *C3* and *C4* responded to the single LPS application with a slight increase in the mRNA level, whereas *Itgam* levels remained unmodified compared with the PBS control (Fig. 3.16). However, the repeated LPS application led to a

significant increase in mRNA above the single challenge levels for *C3* (from 5.58 ± 1.02 in the single LPS treated group, to 7.75 ± 0.82 FC in the repeated treated group, $p < 0.001$), *C4* (from 2.26 ± 0.45 – single LPS, to 9.84 ± 2.60 FC – repeated LPS, $p < 0.01$) and *Itgam* (from 0.98 ± 0.2 FC – single LPS, to 4.32 ± 0.14 FC, $p < 0.001$; Fig. 3.16).

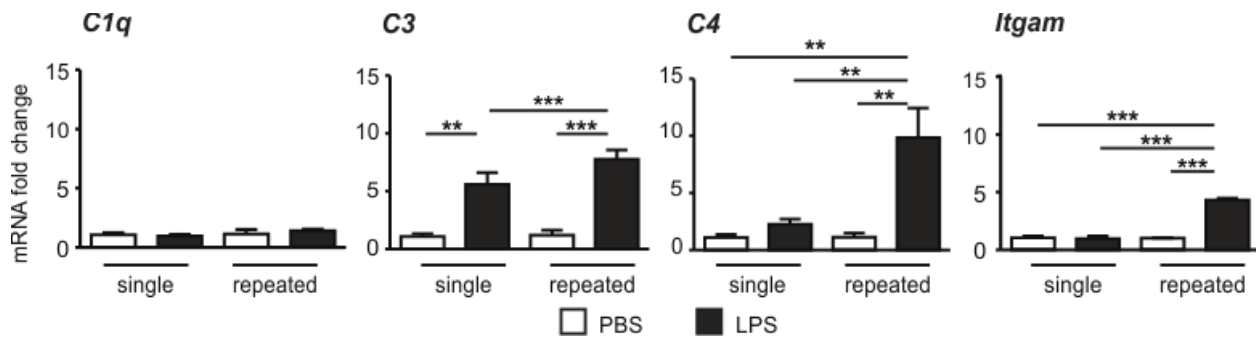


Figure 3.16 - Transcription levels of complement cascade members *C3*, *C4* and *Itgam* in whole mouse brain on experimental day 5 are significantly increased after repeated LPS treatment. The classical pathway initiator *C1q* is irresponsive to the LPS challenge, whereas *C3* and *C4* transcripts of the alternate pathway are showing an up-regulation induced by repeated LPS treatment. *Itgam* (CR3) transcripts were up-regulated only by the repeated LPS treatment. $n=6$.

C3 was identified as causal factor of dopaminergic degeneration triggered by repeated systemic LPS application, thus it was hypothesized that the absence of *C3* should block the dopaminergic neuronal loss. For this *C3* KO and WT controls were challenged using the repeated LPS treatment paradigm and analyzed on day 19 (Fig. 3.17).

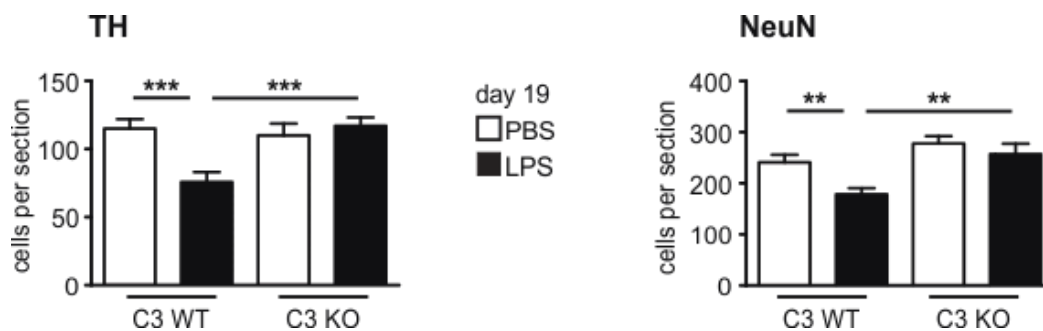


Fig 3.17 – *C3* KO mice are resistant to dopaminergic neuronal loss after repeated LPS challenges compared with *C3* WT controls. Quantification of TH and NeuN positive cells shows induced loss of TH and NeuN positive neurons after systemic repeated LPS application. $n = 3$ animals.

As expected, in C3 WT mice lower number of TH and NeuN positive neurons on experimental day 19 after the LPS treatment was registered, whereas C3 KO animals were unresponsive to the repeated LPS challenges (Fig. 3.17). In detail, the WT animals showed decreased neuronal numbers from 115.1 ± 6.86 cells per section after PBS treatment to 75.76 ± 7.27 cells per section after LPS treatment ($p < 0.001$), whereas the C3 KO mice presented 110.1 ± 8.63 cells per section after PBS treatment and 117.0 ± 6.22 cells per section after repeated LPS treatment (Fig. 3.17).

3.3 DAP12/*TYROBP* Acts as Causal Regulator in Late Onset AD (LOAD)

3.3.1 Microglial Cluster Enriched in Transcripts of LOAD Brains

In collaboration with the groups of Dr. Chris Gaiteri (Sage Bionetworks, USA), Prof. Dr. Erick Schadt (Icahn Institute of Genomics and Multiscale Biology, USA) and Prof. Valur Emilsson (University of Iceland), a gene regulatory networks in 1647 post-mortem brain tissue samples from late onset Alzheimer's disease (LOAD) patients and non-demented subjects was constructed via an integrative network-based approach. Within the LOAD network, DAP12 (encoded by the *TYROBP* gene) was identified as key regulator enriched in an immune/microglia-specific module (Zhang, Gaiteri, Bodea et al., 2013).

DAP12/*Tyrobp* as key regulator in the brain immune module is further confirmed by its strategic position inside the microglial phagocytosis-related signaling pathway. A more detailed analysis of the immune/microglia module in the LOAD brains revealed that many of the phagocytosis pathway members are enriched, with DAP12/*Tyrobp* being the first member in the pathway (Fig. 3.23; Zhang, Gaiteri, Bodea et al., 2013). Among the enriched elements in the immune/microglia module in the LOAD brains, were found members of the phagocytosis-related actin reorganization pathway (e.g. *Lat*, *Vav*, *Rac*), together with members of the phagocytosis-related oxidative burst (e.g. *Ncf2*, *Ncf4*, *Cyba*, *Cybb*; Fig. 3.23; Zhang, Gaiteri, Bodea et al., 2013).

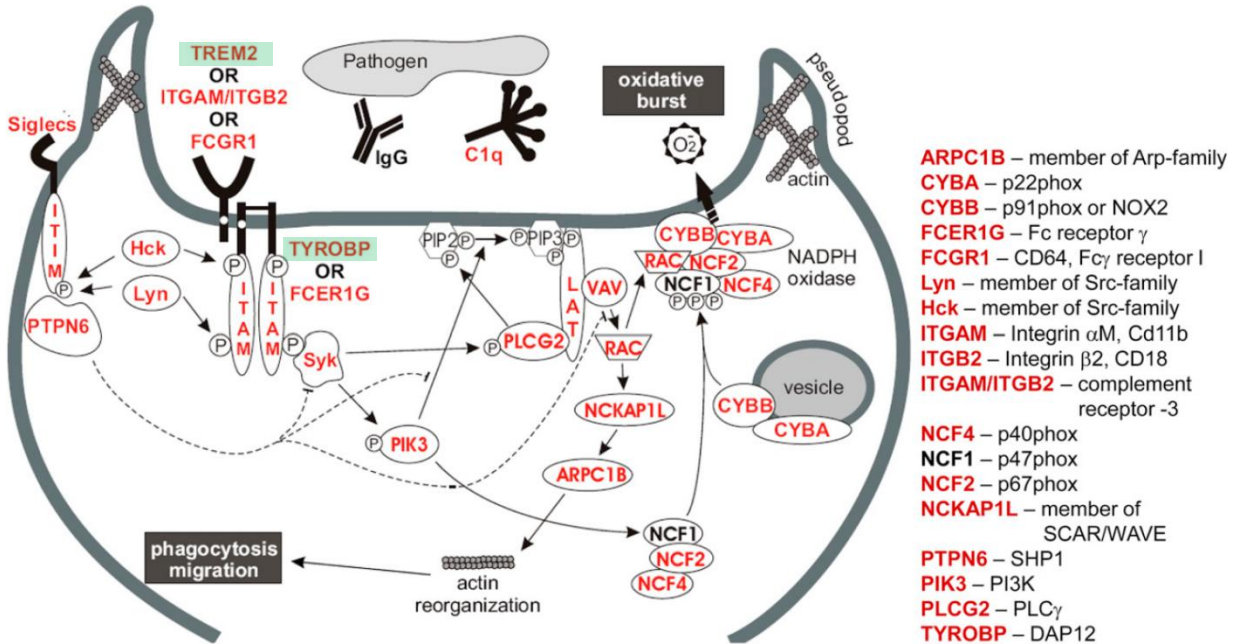


Figure 3.18 – Phagocytosis pathway of the immune/microglia cluster in late onset Alzheimer’s disease (LOAD) gene-expression analysis. Members of the pathway found DE marked in red, TREM2 and DAP12/*Tyrobp* position highlighted in green (analysis based on the data provided by Dr. Chris Gaiteri, Sage Bionetworks, Seattle, USA; published in Zhang, Gaiteri, Bodea et al., 2013).

3.3.2 Features of LOAD Recapitulated by DAP12 Overexpressing Microglial Cells

To verify the results obtained in the LOAD gene-expression analysis, full length mouse *Tyrobp*, truncated mouse *Tyrobp* (with both ITAM signaling motifs deleted) or a control vector were inserted in lentiviral expression plasmids containing an internal ribosome entry site (IRES) – enhanced green fluorescence protein (eGFP) sequence downstream of the *Tyrobp* expressing cassette (Fig. 2.3). Murine embryonic stem cell derived microglia (ESdM) were lentivirally transduced to overexpress Dap12/*Tyrobp* variants together with GFP or only GFP positive control vector, and then fluorescence-activated cell sorted (FACS) based on their GFP expression (Fig. 3.19).

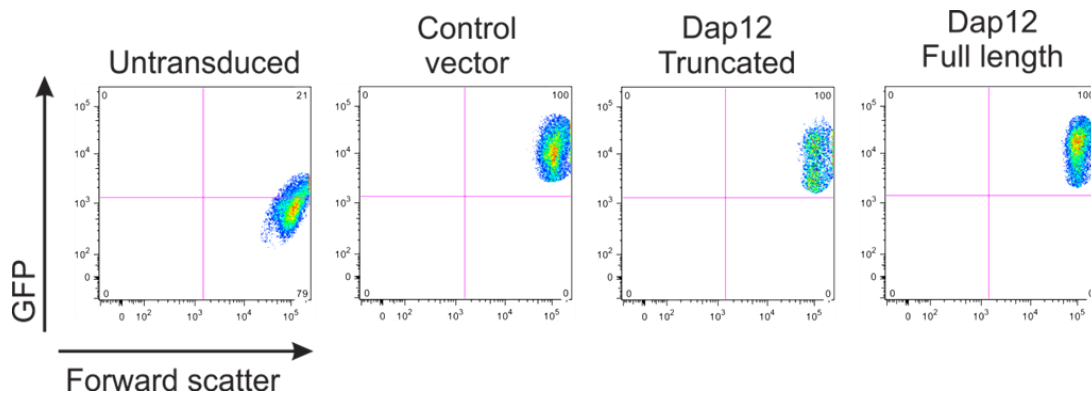
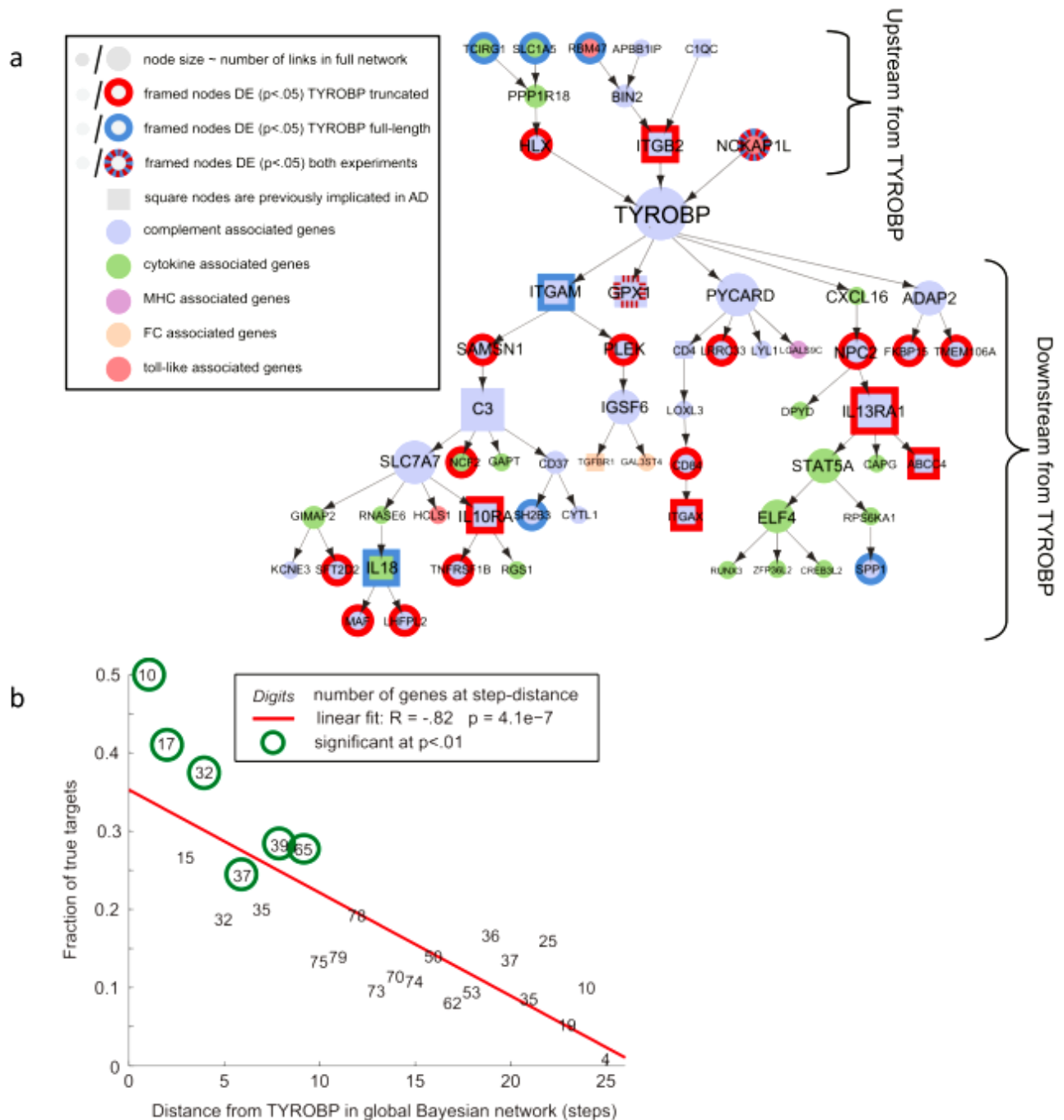


Figure 3.19 – Mouse embryonic stem cell derived microglia (ESdM) were successfully transduced to overexpress full length mouse Dap12, truncated Dap12 or control vector. Cells were transduced using a vector containing expressing enhanced green fluorescent protein (eGFP) sequence downstream of the *Tyrobp* expressing cassette (encoding Dap12 variants). Fluorescence-activated cell sorting (FACS) of the successfully transduced ESdM cells was performed based on the GFP signal (analysis performed by Jens Kopatz, modified from Zhang, Gaiteri, Bodea et al., 2013).

The mRNA expression profile of full length or truncated Dap12 overexpressing ESdM cells was compared with the results obtained in control cells and LOAD genome-wide gene-expression study (Fig. 3.20; Zhang, Gaiteri, Bodea et al., 2013). Several thousand DEG were identified in the Dap12 overexpressing ESdM cells (2638 DEG in full length Dap12 and 3415 DEG in truncated Dap12 overexpressing cells, FDR < 0.025). When compared with the LOAD brain tissue array data, approx. 1000 of these genes were found highly enriched ($p < 10^{-15}$), recapitulating also previous AD features (Fig. 3.20a, Zhang, Gaiteri, Bodea et al., 2013). Elements enriched in full length Dap12 overexpressing ESdM were represented by *Igam*, *I18* (both already described as LOAD-related) or by *Spp1* (secreted phosphoprotein 1; Fig. 3.20a). The elements enriched in truncated Dap12 overexpressing cells were more numerous and represented by already described LOAD-related genes (e.g. interleukin 10 receptor α , *I10ra*, or interleukin receptor 13 $\alpha 1$, *I13a1*) or by new elements (e.g. *Cd84*; Fig 3.20a; Zhang, Gaiteri, Bodea et al., 2013).

Next, a large Bayesian network (approx. 8000 nodes) was created based on the mRNA sequencing results, revealing that the highest predictive power for DEG is found in close pathway proximity to Dap12/*Tyrobp* (Fig. 3.20b, Zhang, Gaiteri, Bodea et al., 2013).



The study of functional categories enriched in the overexpressing Dap12 cells showed that approx 99% of the DEG from full length Dap12 cells were downregulated compared with the control vector cells, with an enrichment of genes involved in RNA metabolism ($p < 10^{-4}$) and cell-cycle mitosis ($p < 10^{-2}$). The cells overexpressing truncated Dap12 were presenting enriched up-regulated genes of vacuole/autophagy ($p < 10^{-7}$) and mitochondrion ($p < 10^{-3}$), and down-regulated genes of the histone assembly pathway ($p < 10^{-30}$). Among these results, 658 genes of the vacuole/autophagy pathway were down-regulated in the full length Dap12 overexpressing cells and up-regulated in the truncated Dap12 overexpressing cells (Zhang, Gaiteri, Bodea et al., 2013).

3.3.3 Amyloid- β (A β) Internalization by Functional Dap12 Overexpressing Microglial Cells

AD pathology is characterized by the presence of amyloid- β (A β) plaques in the brains and it is hypothesized that microglial cells might be involved in the up-take and removals of A β via ITAM-related receptors (Gaikwad et al., 2009; Melchior et al., 2010). However, the possible role of the ITAM-bearing Dap12 adaptor molecule in this process was not analysed so far.

Transduced ESdM cells were used to test the Dap12 involvement in the up-take of fibrillar A β . ESdM cells overexpressing full length Dap12, truncated Dap12 or a control vector were cultured in the presence of fibrillar A β or albumin as control and the up-take level was visualized via confocal microscopy (Fig. 3.21a). The internalized A β level was found significantly higher in the full length Dap12 overexpressing cells when compared with the A β up-take in the control cells (from 1.00 ± 0.07 relative units in the control cells to 1.28 ± 0.07 relative units in the full length Dap12 overexpressing cells, $p < 0.01$). The level of A β in the truncated Dap12 cells was significantly lower when compared with the A β up-take in the control cells (from 1.00 ± 0.07 relative units in the control cells to 0.61 ± 0.06 in the truncated Dap12 overexpressing cells, $p < 0.001$) (Fig. 3.21b). The albumin up-take was unaffected by the Dap12 overexpression, proving the up-take specificity of A β (Fig. 3.21c).

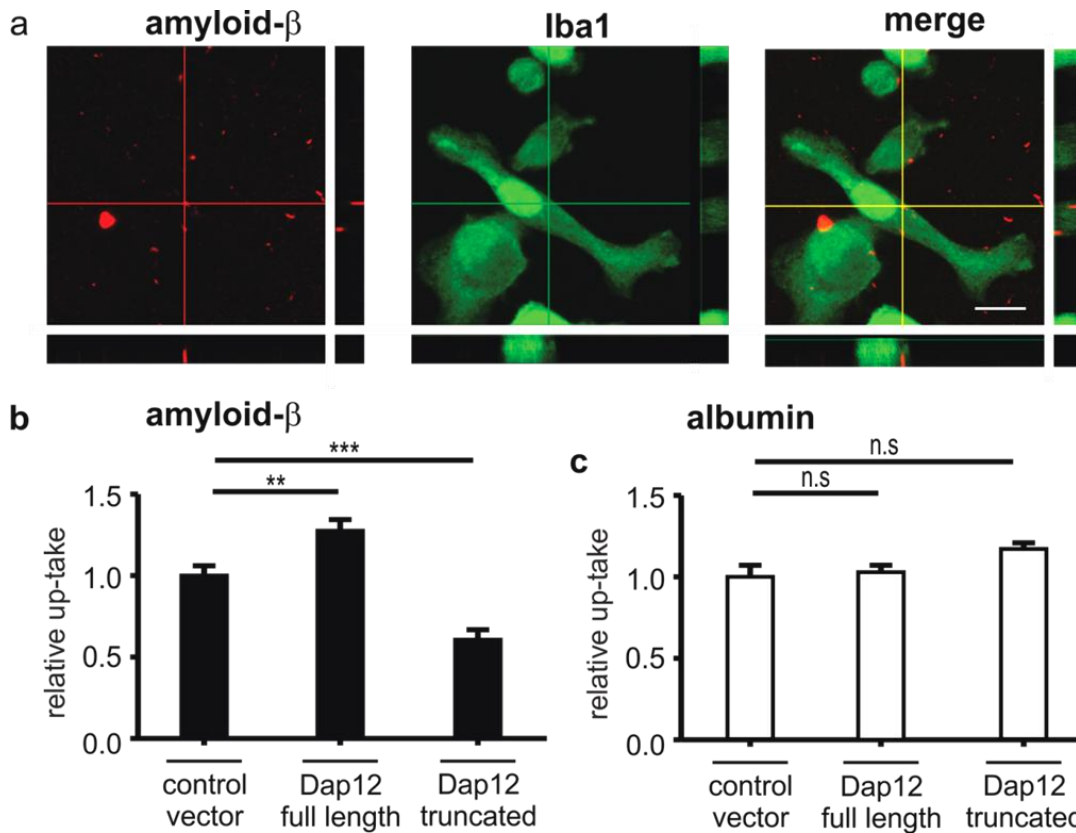


Figure 3.21 – Dap12 is required for amyloid- β (A β) phagocytosis by ESdM cells. **a** – Representative Z-stack confocal images of amyloid- β (red) and microglia marker Iba1 (green) immunostaining showing A β internalization. Scale bar: 10 μ m; **b** – Full length Dap12 overexpressing cells present a higher level of A β internalization compared with control vector transduced cells, whereas truncated Dap12 overexpressing cells show an inhibition of A β up-take; **c** - Albumin up-take by transduced ESdM presents similar levels. n=3.

The involvement of the ITAM signaling pathway in the up-take of A β was proven by measuring the phosphorylation level of spleen tyrosine kinase (Syk), an enzyme that is phosphorylated after recognizing activated ITAM motifs (C. Lowell, 2010). In this regard, Syk from Dap12 transduced cells treated with fibrillar A β was immunoprecipitated and used for western blot detection (Fig. 3.22a). The western blot quantification revealed a significantly increased level of Syk phosphorylation of full length Dap12 overexpressing cells in the presence of A β (from 0.45 ± 0.07 to 1.72 ± 0.33 relative units, $p < 0.001$), similar with the level reached in the control vector cells (1.62 ± 0.26 relative units; Fig. 3.22b). However, the level of Syk phosphorylation in the truncated Dap12 treated with A β was not changed compared with the same cell type treated with PBS as control, and, moreover, significantly reduced compared with the other cell types ($p < 0.05$ vs. control cell treated with A β and $p < 0.01$ vs. full length Dap12 cells treated with A β (Fig. 3.22b).

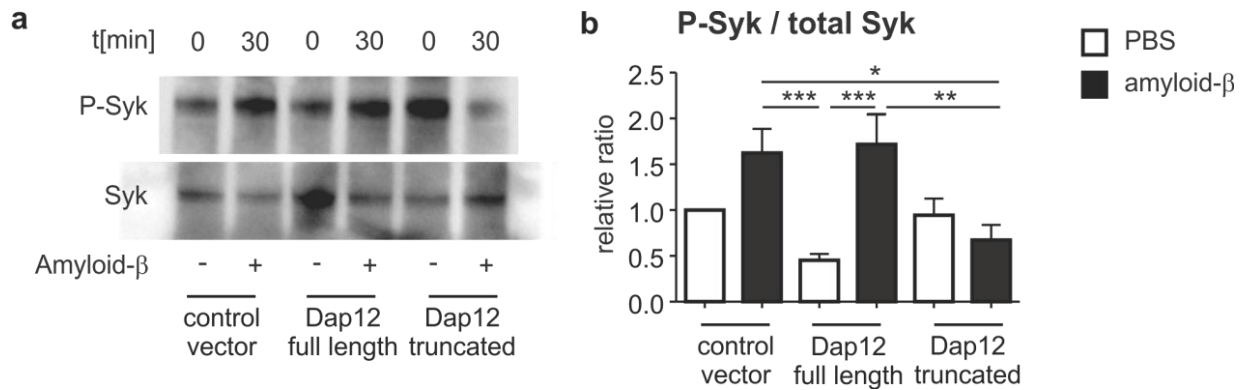


Figure 3.22 – Amyloid-β (Aβ) leads to phosphorilation of spleen tyrosine kinase (Syk) via functional Dap12. **a** – Representative immunoblot picture of Syk (bottom) and phosphorylated-Syk (P-Syk; top) with or without 30 minutes (min) incubation with Aβ; **b** – Quantification of the immunoblot signal shows significant higher ratios of P-Syk/Syk in the presence of Aβ for the full length Dap12 overexpressing cells, the truncated Dap12 cells being irresponsive to the treatment. n=3.

3.3.4 Neuron Degeneration by Functional Dap12 Overexpressing Microglial Cells

To explore possible ITAM-triggered effects on neuronal cells after Aβ up-take by microglia, transduced ESdM cells were co-cultured with primary mouse neurons in the presence or absence of Aβ (Fig. 3.23). First, analyzing the neurites length as neurotoxicity marker showed that primary neuronal cultures in the absence of microglia were irresponsive to Aβ (Fig. 3.23b). However, neurons were presenting shorter processes when microglia were added to the culture (from 1.05 ± 0.05 relative units reduced to 0.86 ± 0.03 relative units in the presence of microglia, $p < 0.01$; Fig. 3.23b). When Aβ is incubated together with the microglia-neurons co-culture, the neurites length is further significantly decreased (from 0.86 ± 0.03 relative units in co-culture, to 0.57 ± 0.02 relative units when Aβ is added to the co-culture, $p < 0.001$; Fig. 3.23b), supporting the idea of a microglia related neuronal toxicity.

To investigate further the involvement of microglial ITAM-bearing Dap12 in neuronal toxicity in the presence of Aβ, primary neuronal cultures were incubated with Dap12 overexpressing cells (full length or truncated) or with control cells. Data showed that the control vector ESdM (expressing the constitutive functional Dap12) underwent a decrease in neurites length from 0.86 ± 0.03 relative units to 0.57 ± 0.02 relative units in the presence of Aβ ($p < 0.001$) and the full length Dap12 overexpressing cells – from 0.92 ± 0.05 to 0.58 ± 0.04 relative units in the presence of Aβ ($p < 0.001$; Fig. 3.23c). The primary neurons co-cultured with truncated Dap12 were irresponsive to Aβ presence (Fig. 3.23c).

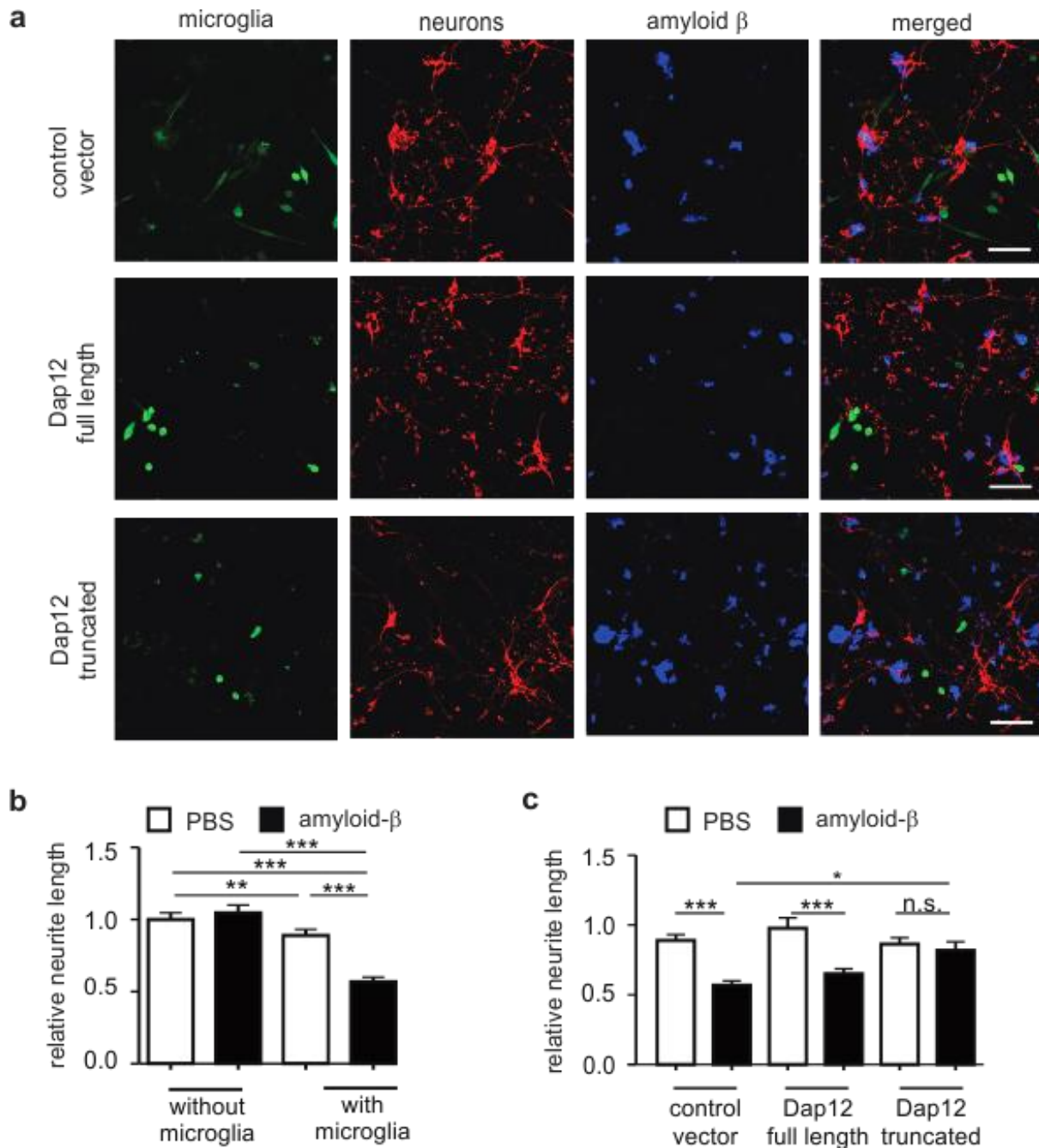


Figure 3.23 – Neuronal processes integrity is compromised by ESdM overexpressing functional Dap12, in the presence of A β . **a** – Representative immunocytochemistry images of primary neurons and transduced ESdM (control vector, Dap12 full length, Dap12 truncated) co-cultures in the presence of A β . Scale bar: 50 μ m; **b** – The lengths of neuronal processes are shortened in co-culture with microglia only in the presence of A β ; **c** – The neurites damage is increased in the presence of A β and control vector or full length Dap12 overexpressing ESdM. The neurotoxic effect is abolished in truncated Dap12 overexpressing ESdM. n.s. – not significant; n = 3.

3.3.5 Superoxide Release by Functional Dap12 Overexpressing Microglial Cells

One of the microglia-related proposed pathways arising from the LOAD genome-expression analysis was having as endpoint members of the NADPH oxidase complex (Fig. 3.18). NADPH oxidase is an enzyme implicated in superoxide production as response to pathogen recognition by phagocytes, like microglia (Block, 2008). Therefore, the reactive oxygen species production in Dap12 overexpressing ESdM cells was assayed in the presence or absence of A β (Fig. 3.24a). Signal intensity quantification of DHE-labeled superoxide showed that control vector ESdM cells expressing the constitutive Dap12 were able to elicit a significant level of superoxide production (from 1.00 ± 0.09 to 1.43 ± 0.10 relative units in the presence of A β , $p < 0.001$; Fig. 3.24a). The full length Dap12 cells presented constitutively an increased level of superoxide production, thus the increase caused by A β presence was not significant compared with PBS treated cells, however the increase was significant in comparison with the PBS treated control cells (from 1.00 ± 0.09 relative units in the control cells, to 1.55 ± 0.04 relative units in the A β treated full length Dap12 cells, $p < 0.001$; Fig 3.24a). The truncated Dap12 overexpressing ESdM cells were not presenting a constitutively increased level of superoxide production, nor were they able to produce additional superoxide in response to A β presence compared with PBS treated cells (Fig. 3.24a). To prove the specificity of superoxide production to the A β , transduced cells were incubated with zymosan, as superoxide inducing reagent. Zymosan was able to increase the superoxide production in all the cell lines, proving that the NADPH functions were not altered in the Dap12 variants overexpressing cells (Fig 3.24b). Albumin was used as additional negative control, without having any effect on the superoxide production in all the transduced cell lines (Fig 3.24b).

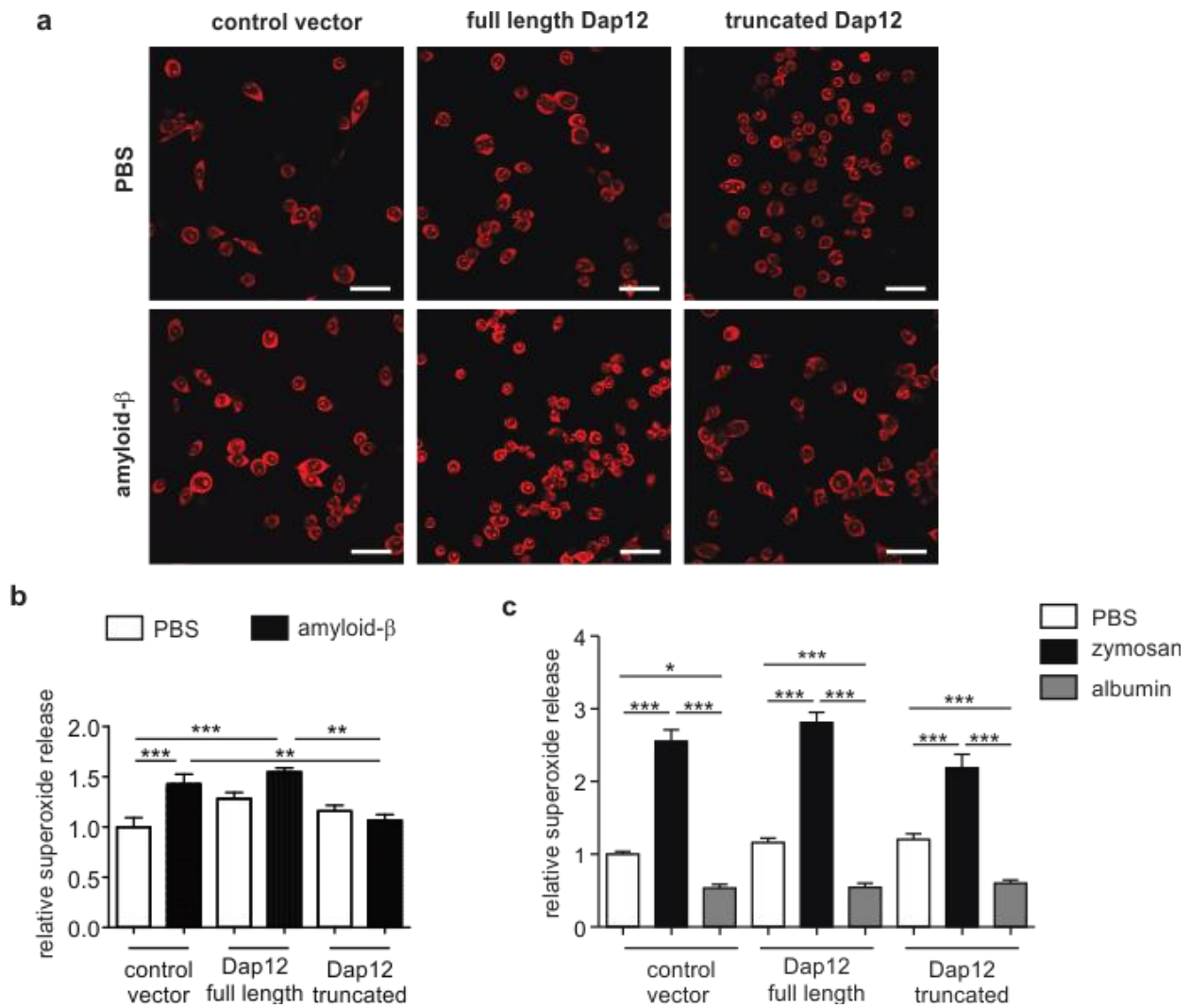


Figure 3.24 – Dap12 increases superoxide production specifically in the presence of A β . **a** – Representative pictures of control vector, full length or truncated Dap12 overexpressing ESdM cells in the presence or absence of amyloid- β and stained by the superoxide recognition agent dihydroethidium (DHE). Scale bar: 50 μ m; **b** – Functional Dap12 increases the superoxide production of ESdM in the presence of A β , whereas truncated Dap12 is irresponsive to the A β presence; **c** – Release of superoxide is independent of Dap12 (full length or truncated) overexpressing ESdM in the presence of zymosan or albumin. n = 3.

4. Discussions

The involvement of immunity in the neurodegenerative process mediated by brain microglial cells has been reported in many studies (Carson et al., 2006; Cunningham, 2013; Perry et al., 2010). However, a detailed mechanism to explain the microglia-mediated neurodegeneration is still far from reach. Within this study, the involvement of the microglial TREM2/DAP12 pathway in two neurodegenerative disease was evaluated using *in vitro* and *in vivo* models. The TREM2 receptor deficient mouse model of NHD was characterized in regard to microglial capacity to elicit a detrimental effect in the brain parenchyma, as reported in human NHD brains (Bianchin et al., 2010). Systemic inflammation was described as contributing to the increase of neurodegenerative susceptibility and/or cognitive decline in already diseased patients (Perry et al., 2007). To facilitate a better understanding of the involvement of systemic inflammation in the neurodegenerative process, two LPS treatment paradigms of mice were compared, proving the microglial involvement in dopaminergic degeneration, as found in PD (Miller et al., 2009). Based on a GWAS analysis of AD brains, DAP12 was identified as a key regulator of LOAD and its involvement in A β -related neurotoxicity was evaluated *in vitro*. The present study brings new evidences on the involvement of immunity in the neurodegenerative process, proposing mechanisms by which microglial DAP12 expression can correlate with neurotoxicity.

4.1 The Effects of Microglial TREM2 Deficiency

Loss of function mutations in TREM2 or its adaptor molecule DAP12 are associated in humans with the Nasu-Hakola disease (Paloneva et al., 2002, 2000). Within the present thesis, a mouse deficient of TREM2 was characterized in the absence or presence of inflammatory stimulation. The results revealed changes in microglial morphology in adult TREM2 KO mice together with alterations of transcripts levels in aged TREM2 KO animals without additional inflammatory stimulation. After intraperitoneal LPS application in mice, microglial morphological changes were more pronounced in adult TREM2 KO vs. WT controls. However, no changes in the proinflammatory mRNA levels were detected between TREM2 KO animals compared with WT controls. Integrating these results within the literature associated with TREM2 deficiency, it

seems that there is a different TREM2-related response mechanism in the CNS compared with the periphery.

4.1.1 Involvement of TREM2/DAP12 Complex in Nasu-Hakola Disease

Within this study, the characterization of the TREM2 KO mouse model of NHD was performed in regard to the brain microglial cell population. Since the TREM2 adaptor molecule DAP12 was discovered before TREM2, a higher amount of data on DAP12 was available, with many of the previous studies related to DAP12 deficiency.

DAP12 protein was first reported as being expressed in NKs (Lanier et al., 1998) and shortly afterwards the group of Prof. Peltonen identified loss of function mutations in the *DAP12* gene as being associated with the recessive autosomal disease NHD (Paloneva et al., 2000). The same study observed transcripts of *DAP12* in microglial cells (Paloneva et al., 2000). The immune receptors TREM family was discovered in the same year by the group of Prof. Colonna and was proven to be expressed together with DAP12 in neutrophils and monocytes (Bouchon et al., 2000). The correlation between loss of function mutations in *TREM2* gene and NHD was observed two years later, when a study on macrophages and dendritic cells (DCs) expressing TREM2 confirmed the association between TREM2 and DAP12 proteins (Paloneva et al., 2002). Since then, the TREM2 and DAP12 molecules were studied in different *in vitro* and *in vivo* models, increasing the level of knowledge on microglial cells physiology both in healthy and pathological conditions. Today, NHD is considered to be the prototype of primary microglial disorder inside CNS (Bianchin et al., 2010).

The main features of NHD are neuroinflammation and bone cysts (Bianchin et al., 2010; Kaneko et al., 2010a; Satoh et al., 2011a). As a result, some of the initial studies on DAP12 have focused on osteoclasts, cells of myeloid origin that are associated with bone resorption function. Continuing their pursuit, the group of Prof. Peltonen reported impaired differentiation and function of DAP12 or TREM2 deficient osteoclasts derived from peripheral blood mononuclear cells (PBMCs; Paloneva et al., 2003). These results were confirmed by other groups examining TREM2 or DAP12 KO osteoclasts differentiated from PBMCs or bone marrow derived monocytes/macrophages (BMDMs; Cella et al., 2003; Humphrey et al., 2006).

Initial studies on DAP12 KO mice showed dysfunctions in the normal function of NKs and DCs (Tomasello et al., 2000) and inability of animals to develop autoimmunity due to impaired antigen priming (Bakker et al., 2000). After connecting NHD pathology with mutations in the *DAP12* gene, evaluation of DAP12 KO mice reported features like osteopetrosis, thalamus hypoplasia with synaptic degeneration and sensorimotor-related behavioral dysfunction

(Kaifu et al., 2003). However, these *in vivo* DAP12 KO mice data could not be confirmed by another group (Lanier, 2009).

Unlike DAP12, the effects of TREM2 deficiency were initially studied to a lesser extent. In immature human DCs the crosslinking of TREM2 with antibodies led to increased MHC class II, CD86, CD40 and CCR7 expression (Bouchon et al., 2001). In primary mouse microglia cells only upregulation of CCR7, but not of MHC class II, CD86 or CD40 molecules was reported (Takahashi et al., 2005). CCR7 upregulation led to increased chemotaxis towards CCL19 and CCL21, both being ligands of CCR7 (Takahashi et al., 2005). Additionally, the same study reported the involvement of microglial TREM2/DAP12 complex in phagocytosis of apoptotic neurons without inflammation (Takahashi et al., 2005). The capacity of microglial phagocytosis inside CNS in the absence of inflammation is a crucial feature of nervous tissue homeostasis (Neumann et al., 2008). Knock-down of TREM2 in microglia increased the transcription of proinflammatory genes like *Tnfa*, *Nos2* and *Il12p40*, whereas overexpression of TREM2 did not change the normal expression pattern of these genes (Takahashi et al., 2005). These results are in concordance with another study that reported enhanced TLR responses in Dap12 KO animals (Hamerman et al., 2005). Based on these results, it was concluded that TREM2 is involved in suppressing the microglial proinflammatory reaction.

4.1.2 TREM2 Deficient Mouse Characterization

4.1.2.1 Age-related Changes in the mRNA of TREM2 Deficient Mice

Within the present thesis, the previously described TREM2 KO mouse line (Turnbull et al., 2006) was used to explore the TREM2 deficiency inside CNS. It was shown previously that TLR stimulation of BMDMs from TREM2 KO and DAP12 KO mice increased the proinflammatory cytokine response (Turnbull et al., 2006). These findings confirmed previous results on DAP12 KO BMDMs (Hamerman et al., 2005) and on TREM2 KD microglial cells (Takahashi et al., 2005). Moreover, *in vivo* studies of TREM2 KO mice, showed increased proinflammatory response in the periphery (Correale et al., 2013; Seno et al., 2009), whereas in WT animals, TREM2 expression was increased on macrophages as response to challenge with the anti-inflammatory IL4 cytokine (Turnbull et al., 2006).

Based on the above data, within this thesis the transcription levels of inflammatory-related genes were first evaluated in the brain of adult TREM2 KO and WT control mice. The chosen microglia-related genes were represented by *Aif1* that encodes the microglial marker Iba1 reported as being enriched in NHD brains (Satoh et al., 2011a), *Tnfa* and *Il1b* encoding typical

proinflammatory molecules released by activated immune cells and found also enriched in PBMCs from blood of NHD patients (Kiialainen et al., 2007). Additionally, since NHD pathology is also characterized by astrogliosis (Sato et al., 2011a), transcription of astroglial marker *Gfap* was assayed. Intriguingly, 3 months old TREM2 KO animals showed no differences in the transcription of the above mentioned gene compared with matched WT controls. The same hold true for animals of 6 and 12 months. Only 24 months old animals showed differences between KO and WT controls mRNA levels in *Aif* and *I1b*, indicating a slow progression of microglial dysfunction (Luo et al., 2010).

It is known that NHD symptoms debut in the 20s or 30s (Kaneko et al., 2010a), thus it can be supposed that the mechanisms of *in vivo* microglia-related dysfunctions require a long time be triggered and the mouse model is not adequate for these experiments. Indeed, there are known human physiological processes in neurodegenerative diseases that cannot be fully mimicked by mouse models (Gilley et al., 2011; Götz and Ittner, 2008).

4.1.2.2 Altered Microglial Morphology in TREM2 KO Mice

In previous studies, dysfunctions of cellular activation due to either TREM2 or DAP12 deficiency were studied in the presence of inflammatory stimuli like IL1 β (Paloneva et al., 2002) or LPS (Turnbull et al., 2006). In humans, NHD symptoms were initially observed in the 3rd decade of life (Kaneko et al., 2010a), thus it is tempting and plausible to presume that the NHD patients had suffered common inflammatory episodes before the onset of the disease. Moreover, systemic infections and inflammation were reported to correlate with chronic neurodegeneration (Perry et al., 2007). Therefore it was hypothesized that the TREM2 KO mice require an inflammatory stimulation to trigger similar microglial cytokine release as reported in NHD. For this, systemic intraperitoneal LPS challenges were administered to adult TREM2 KO and WT animals and the level of expression of several immune-related genes were measured in the mouse brains. Data showed that LPS elicited a normal response in WT animals, however no difference between TREM2 KO and WT animals was observed after LPS treatment.

Upon stimulation, microglia undergo morphological changes that correlate with cellular activation (Kettenmann and Hanisch, 2011; Ransohoff and Perry, 2009). In human NHD brains, microglial are described only as being activated (Bianchin et al., 2010). However, no detailed study was performed on this aspect of the disease. Sato and colleagues tried to tackle this aspect, but their results were inconclusive (Sato et al., 2011a). Thus, within this thesis an in-depth study of microglial phenotype in TREM2 KO vs. WT mice was performed. To evaluate the effects of systemic inflammation, groups of i.p. LPS treated TREM2 KO mice and appropriate

WT controls were used. In this regard, microglial cells within *SNpr* were fluorescently immunostained with the specific marker Iba1 and quantified. *SNpr* is a substructure of the basal ganglia which were reported to be affected in NHD (Kaneko et al., 2010a). Moreover, *SNpr* was described as normally having an increased density of microglial cells (Lawson et al., 1990), thus *SNpr* is a good area for exploring putative changes in microglial morphology.

In TREM2 KO animals, microglial morphology was found to be altered compared with WT and vehicle treated animals. The microglial cell body area was smaller in TREM2 KO vs. WT mice, however, the number of microglial soma processes was found unchanged in TREM2 KO and WT mice as well as the branching number. A previous common concept of microglial physiology stated that activated microglia present a phenotype in which the number of microglial processes is decreased peaking with the amoebal morphology (Kreutzberg, 1996). Perry and colleagues improved this linear model of activation, proposing a more comprehensive model of microglial activation (Perry et al., 2007). In this model microglia can discriminate between different parameters of stimulation (e.g. intensity, interval of stimulation) eliciting different responses that can correlate with microglial morphology, although difficult to assess. One of these phenotypic states might be the one observed in the TREM2 KO vehicle treated animals. This 'primed' state of microglia was described as being a consequence of detection of changes in the parenchymal microenvironment, a common process in aged or diseased brain (Perry, 2010). Systemic inflammation can trigger the switch of primed microglial physiology, tipping from a relatively benign phenotype towards a proinflammatory aggressive state (Perry, 2010). Indeed, in TREM2 KO and WT microglia, LPS treatment further increased the differences between the two genotypes. Microglial soma area in the LPS treated animals showed significant decrease in relation to the absence of TREM2, whereas Iba1 staining intensity increased, proving a shift towards a more activated microglial phenotype. Moreover, the number of soma processes in LPS TREM2 KO group was significantly decreased compared with the vehicle treated group of the same genotype further proving TREM2 deficiency-related microglial shift towards activation after inflammatory stimulation. These differences seen in microglial morphology after LPS treatment are in disagreement with a study in which the same LPS treatment protocol was used on WT animals and that claims an increase of microglial area accompanied by increase in number of processes after treatment (Chen et al., 2012). However, different anatomical areas were studied by Chen and colleagues (cortex and hippocampus) and moreover, on the experimental day 5 (Chen et al., 2012). Within this thesis, microglial cells were assayed in *SNpr* area at a later time point (experimental day 19). It can be hypothesised that microglia can adopt different morphological phenotypes subsequent to LPS treatment according to the brain localization. Evidences supporting this theory have come from other studies that identified different microglial subpopulations based on marker expression and response to activation (Chen et al., 2010; Scheffel et al., 2012).

The microglial morphological changes in LPS-treated TREM2 KO mice however, were not supported by upregulation of microglia-related proinflammatory genes (e.g. *Tnfa* or *Il1b*) above the level normally observed in LPS-treated WT mice. The incapacity of TREM2 KO mice to induce an increase of proinflammatory molecules transcription is in contradiction with previous *in vitro* reports on TREM2-related dysfunction (Takahashi et al., 2005; Turnbull et al., 2006) or GWAS of NHD PBMC derived DCs (Kiialainen et al., 2007; Satoh et al., 2011a). Besides the type and origin of the material mentioned in these studies, it has to be noted that no study on cytokines profile of NHD brains was reported and generally all NHD brain data are post-mortem analysis. This includes the fact that no transcriptomic or proteomic data are available throughout NHD development and thus interpreting the results obtained in TREM2 deficient mice might be difficult to correlate with the previous *in vitro* and human post-mortem data.

As a potential additional readout of the TREM2-mediated microglial immunosuppression, neuronal integrity of the dopaminergic system was investigated in TREM2 KO mice after i.p. LPS stimulation. Of note, *SNpr* is adjacent to the *SNpc* structure in which the somas of dopaminergic neurons are found. Many studies report LPS-triggered dopaminergic degeneration *in vivo*, as described in detail in the next subchapter of the thesis. It was hypothesised that the LPS-triggered neurotoxicity could be elevated in microglia of TREM2 deficient mice due to absence of proinflammatory inhibition exercised by the TREM2 receptor (Takahashi et al., 2005). Data obtained revealed that all the LPS treatment groups were responsive to the LPS treatment by decrease in the number of TH positive cells in *SNpc* (data not shown). However, there was no difference observed between TREM2 KO and WT mice. These results might prove a TREM2 independent neurotoxicity mechanism. In fact, in literature, TREM2 is considered to be part of the alternative (M2) activation markers (Ydens et al., 2012), thus it can be presumed that the expression of TREM2 is actually downregulated after the LPS treatment of WT mice towards levels encountered in the TREM2 KO animals.

Many of the initial reports of TREM2 involvement in cytokines release come from either *in vitro* differentiated cells that might suffer expression changes due to the manipulation (Cella et al., 2003; Hamerman et al., 2006; Paloneva et al., 2003; Turnbull et al., 2006) or primary mouse microglia cell cultures (Takahashi et al., 2005). On top of this, it is known that *in vitro* studies present only a snapshot of the entire complexity of the *in vivo* process and that *in vivo* genetic/functional compensation is an important mechanism in maintaining a stable condition. As reviewed by Barbaric and colleagues, mechanisms of genetic compensation were reported in mice in various loss of function studies, bringing forth the theory of genetic and functional robustness (Barbaric et al., 2007).

In another line of *in vivo* studies, the involvement of TREM2 in ameliorating neuropathological conditions was shown. TREM2-mediated removal of apoptotic material and the capacity of

TREM2 to restrict the microglial proinflammatory cytokines release (Takahashi et al., 2005) led to inquiries on the capacity of TREM2 receptor to participate in ameliorating neurodegenerative diseases. MS is a human neurodegenerative disease characterized by axonal degeneration, demyelination and microglial activation (Compston and Coles, 2008). The mouse model of MS, the EAE model, was used to test the hypothesis of TREM2 involvement in ameliorating the disease (Takahashi et al., 2007). The study was able to recapitulate previous results by TREM2 overexpression in murine BMDMs and to present a non-invasive way of grafting the TREM2 positive myeloid cells at the site of lesion by intravenous administration (Takahashi et al., 2007). Additionally, TREM2 involvement in debris clearance *in vivo*, together with the active production of an anti-inflammatory milieu at the site of injury generally contributing to EAE disease amelioration were reported (Takahashi et al., 2007). The results of this study were further enforced by a simultaneous study presenting exacerbated pathology of EAE by antibody-mediated blocking of TREM2 (Piccio et al., 2007). However, in these studies, manipulation of TREM2 was performed either *in vitro* or pharmaceutically, thus potentially masking or exacerbating an otherwise undetected TREM2-related effect.

TREM2 KO mice were successfully used in acute models of colon injury, evidentiating the involvement of TREM2 in mucosal wound repair (Correale et al., 2013; Seno et al., 2009). In the study of Seno and colleagues, absence of TREM2 receptor on macrophages led to diminished epithelial proliferation as response to experimental colon injury together with increase of *Ifn γ* and *Tnfa* proinflammatory gene expression and decrease of *Il4* and *Il13* genes for cytokines implicated in alternative activation (Seno et al., 2009). In the analysis of Correale and colleagues, TREM2 deficiency conferred relative protection against colitis with less associated body weight loss, but also with lower levels of proinflammatory cytokine production and bacterial killing capacity (Correale et al., 2013). Another *in vivo* proof of TREM2 implication in tissue repair came from an acute peripheral nerve injury study in which proinflammatory markers (*Nos2*, *Ifn γ* or *Il12p40*) were absent, but an increased level of tissue repair markers (*arginase 1* and *Ym1*) were associated with an upregulation of *TREM2* transcription (Ydens et al., 2012).

In agreement with the colon wound repair study of Seno and colleagues (Seno et al., 2009), another study observed increased *TREM2* transcription after injury, this time presented by stroke (Sieber et al., 2013a). However, when TREM2 KO mice were used, the acute inflammatory response (12 h after reperfusion) was very similar between TREM2 KO mice and littermate controls (Sieber et al., 2013a). Moreover, in the subacute phase (7 days reperfusion) and more evidently later (28 days) following stroke, TREM2 KO mice showed normal transcription of proinflammatory cytokines *Tnfa*, *Il1a* and *Il1b* (Sieber et al., 2013a). These results are in concordance with the present thesis in which no increase of microglial activation-associated genes was observed. In view of these results, it is tempting to speculate on a

different response to TREM2 deficiency in the periphery vs. CNS, a phenomenon that might also explain the previous apparently contradictory *in vitro* data (Hamerman et al., 2005; Takahashi et al., 2005; Turnbull et al., 2006).

4.2 Mechanisms of Neurodegeneration Triggered by Systemic LPS Application

Systemic inflammation was associated with neurodegeneration in clinical studies (Perry et al., 2007). *In vitro* and *in vivo* models of LPS challenges reported dopaminergic sensitivity via a process in which microglial cells play an important role (Cunningham, 2013; Miller et al., 2009). Here, two different systemic LPS treatment paradigms were compared to help identifying the specific microglial role within the neuronal dopaminergic loss. Transcriptome analysis revealed functions altered by LPS challenges, such as phagocytosis and complement-related immunity. By using a C3 deficient mouse line, the effects observed in LPS treated WT animals were abrogated, proving that the microglial involvement in dopaminergic loss is mediated via the complement system.

4.2.1 Contribution of Systemic Inflammation to Neurodegeneration

The application of inflammatory stimuli to trigger a response in TREM2 KO mice led to the search for a fast and reliable treatment paradigm of microglial activation.

Microglial cells express a wide range of PRRs required for recognition of potentially dangerous molecules (Hanisch and Kettenmann, 2007). Bacterial LPS is one of the most common inflammatory molecules used in experiments and is known to be recognized by PRRs, namely by TLR4 found also on microglia where it induces a strong activation both *in vitro* and *in vivo* (Kettenmann, 2006; Perry, 2004; Rivest, 2003). Recently, Sceffel and colleagues observed that murine microglia reorganizes their response to TLR-mediated activation postnatally and that this process correlates with maturation of TLR4-organized functions (Sceffel et al., 2012). LPS recognition elicits convergent signaling cascades mediated by MAPK, NF κ B or IRF to induce proinflammatory cytokines (e.g. TNF α , IL1 β) or IFN extracellular release (Kawai and Akira, 2006). Of note is that inflammation was correlated with neurodegeneration in various studies, as reviewed in Cunningham, 2013; Perry et al., 2007; Wyss-Coray and Rogers, 2012.

Different models of microglial activation induced by LPS are widely used, many reporting specific degeneration of dopaminergic neurons as a result inside CNS (reviewed by Dutta et al., 2008). Important aspects related with LPS administration is the route of administration and the

dosage. Based on previous studies (Cardona et al., 2006; Czapski et al., 2007), i.p. administration of LPS was used within this thesis in either repeated treatments over 4 consecutive days with low dose of LPS (1 µg/gbw) or in a single treatment of a cumulative dose of LPS (4 µg/gbw).

Peripheral immune system can communicate with the CNS via parallel direct and indirect routes (Dantzer et al., 2008; Perry et al., 2007; Skelly et al., 2013). The direct route follows the afferent vagal and trigeminal nerves or by molecules reaching brain parenchyma via BBB or physiological open brain structures, like the circumventricular organs (Dantzer et al., 2008; Perry et al., 2007). The indirect route is intermediated by the perivascular macrophages that recognize blood-carried stimuli, eliciting an adequate response inside the brain parenchyma (Ek et al., 2001; Perry et al., 2007). However, if the BBB structure is altered, blood cells or molecules from periphery can enter the brain, affecting its normal function and activating microglia. This is the case for example in the EAE model, where macrophages and other immune cells from the periphery invade the CNS (Constantinescu et al., 2011), or serum molecules entering brain after injury (Adams et al., 2007).

Yet the route of LPS communication with the CNS is debated (Cunningham, 2013). A study using radioactively-labeled LPS reported little evidence of BBB penetration (Banks and Robinson, 2010). These findings were confirmed by another group that additionally observed increased LPS-related molecules in brain endothelial cells (Singh and Jiang, 2004), correlating with the indirect pathway of communication between brain and periphery. However, based on extravasation labeling with Texas red-conjugated dextran of 70 kDa, another study reported that BBB was disrupted after intravenous administration of LPS in mice (Ruiz-Valdepeñas et al., 2011).

Patients suffering from neurodegenerative diseases showed that episodes of peripheral inflammation triggered by infections lead to worsening of the clinical pathology (Combrinck et al., 2002; Perry et al., 2007). Moreover, the PD risk was significantly reduced by non-steroid anti-inflammatory drugs usage (Chen et al., 2005). Indeed, these observations were backed up by studies on dopaminergic neuronal loss triggered by experimental inflammation. LPS applied to mice has been reported to lead to dopaminergic degeneration with kinetics dependent on dosage and mode of administration (Dutta et al., 2008; Tufekci et al., 2011). A single injection of LPS directly within SN led to neuronal loss paralleled by dopamine decrease 21 days after injection (Castaño et al., 1998), together with the release of microglial cytokines (Arai et al., 2004) and ROS production (Qin et al., 2004). The level of dopaminergic degeneration reached a plateau phase in ca. 8 weeks, whereas microglial activation gradually subsided (Liu, 2006). Systemic application of LPS, however, was reported to require longer time to achieve dopaminergic neuronal loss (7 months), but the process was progressive (Qin et al., 2007).

However, by using a repeated treatment paradigm (4 daily doses of 1 µg/gbw LPS), Cardona and colleagues observed fast microglial activation and neuronal loss in Cx3cr1 deficient mice (Cardona et al., 2006).

4.2.2 Complement Involvement in Dopaminergic Neurodegeneration

4.2.2.1 Microglial Activation and Dopaminergic Degeneration Triggered by Systemic LPS Application in Mice

The results of Cardona and colleagues (Cardona et al., 2006) were successfully replicated within the present thesis by systemically injecting LPS in adult mice. Data showed significantly decreased numbers of TH positive cells after 19 days, but only by using repeated i.p. treatments of low dose LPS (1 µg/gbw) over 4 consecutive days. A single cumulative dose of LPS (4 µg/gbw) was not able to reach the same level of dopaminergic loss within 19 days. However, it is probable that the single treatment paradigm requires a longer time period to achieve dopaminergic degeneration, as reported previously (Qin et al., 2007). In conformity with other studies (Nguyen et al., 2013; Qin et al., 2007), the decrease in TH specific marker accurately described dopaminergic loss and not only a decrease of TH production, as proven by using another neuronal specific marker (NeuN) that led to the same pattern of neuronal loss.

Brain inflammatory response to peripheral LPS application was assayed initially by investigating microglial specific gene *Aif1*. Data showed a fast microglial response by upregulation of *Aif1* gene mRNA on the experimental day 5 after the initiation of repeated or single LPS treatment. However, when assayed on day 19, *Aif1* mRNA was found to be decreased to similar levels as registered in vehicle controls. These results were confirmed at protein level by IHC analysis, when Iba1 reactivity was observed to be increased initially and returned to basal level on experimental day 19. A similar pattern of microglial activation was observed in the mRNA levels of other microglia activation markers, like *Tnfa*, *Il1b* and *Nos2*. Of note, the only gene that presented a significant increased expression level on day 19 was *Il1b*, but only after repeated treatment. A possible explanation for this outcome would be the autocrine properties of Il1β (Toda et al., 2002) that could contribute to its further release for a longer period of time. Il1β has higher potency compared with other cytokine: experimentally Il1β is required in a much lower amount for reaching similar effects as the ones observed for example after LPS treatment (Skelly et al., 2013).

To further prove the differences between the LPS treatment paradigms, $Tnf\alpha$ and $Il1\beta$ proteins were measured inside the brain on experimental day 5 and were significantly increased in the repeated compared to single treatment. The transient activation of microglia, similar to the acute-phase response in the periphery, with fast increase of activation markers directly after LPS treatment which were lost in several days, was also reported in several other studies, as reviewed by Liu (Liu, 2006). Tolerance to subsequent LPS challenges was previously observed in the periphery (Nomura et al., 2000). To investigate this aspect, $Tnf\alpha$ and $Il1\beta$ in blood plasma were quantified after LPS challenges and were found to be similar after both single and repeated treatments, in concordance with the study of Nomura and colleagues (Nomura et al., 2000). Altogether, these data evidentiate brain vs. periphery differences in the induction of tolerance after successive LPS challenges, in accordance with older studies (Faggioni et al., 1995; Püntener et al., 2012).

4.2.2.2 Enriched Immune-related Transcripts in Mice Systemically Treated with LPS

To identify key players in the mechanism of microglial activation subsequent to repeated LPS i.p. application involved in dopaminergic degeneration, a microarray study of brains of LPS treated mice was performed. The array analysis showed higher gene enrichment after the repeated treatment paradigm compared with the single treatment paradigm. The majority of the genes were found to be upregulated. Interestingly, *Hbb-a1* and *Hbb-a2* (encoding for α - and β -hemoglobin) were the only significantly downregulated genes and they were specific to the repeated treatment paradigm. It was previously proven in mice, rats and humans that dopaminergic neurons express hemoglobin, with a role in mitochondrial and oxygen related functions within the neurons (Biagioli et al., 2009). Differences between the time-span of the last LPS challenge and the time of tissue collection (4 days for the single treatment and 1 day for the repeated treatment) might explain the variation observed in the number of DE genes between the treatment paradigms. However, the identification of specific DE genes elicited by the LPS treatment can provide an insight on the mechanism of dopaminergic degeneration.

To identify significant biological functions related with the array data, pathway analysis was performed with a higher stringency on the DE genes. The most enriched pathways were found to be microglia-related (e.g. enrichment of the immune cell trafficking pathway, inflammatory response pathway, inflammatory disease pathway). Within these pathways, the majority of genes were found to be DE in the repeated treatment paradigm (58 genes) compared with the single treatment paradigm (3 genes). Only 22 genes were found to be common to both treatment paradigms. A more detailed analysis of the DE genes identified the phagosome

together with the complement and coagulation cascades as being the most prevalent functions activated by the LPS challenges.

Indeed, under both healthy and pathological conditions, one of the main functions of microglia is phagocytosis (Brown and Neher, 2012; Neumann et al., 2008; Sierra et al., 2013). In the phagosome-related genes, the array data identified the complement component C3, the integrin subunit *Itgam* of the CR3, the common γ -chain (encoded by the *Fcer1g* gene), and the NADPH members p22phox (coded by the *Cyba* gene) and gp91phox (coded by the *Cybb* gene). The array data were also confirmed by sqRT-PCR. Interestingly, all these genes and/or proteins were previously correlated individually with different neurodegenerative processes or dysfunctions. Deficiency in CR3 leads to abnormalities in the normal development of the optic nerve due to an absence of microglia-mediated phagocytosis (Schafer et al., 2012). Interestingly, CR3 signals via DAP12 to induce phagocytosis followed by respiratory burst (Ivashkiv, 2009), however *Tyrobp* was not found significantly increased. On the other hand, *Fcer1g* mRNA of the common γ -chain, which is also an adaptor protein containing an ITAM motif and very similar in structure with DAP12, was increased by the LPS treatment. The involvement of *Fcer1g* in neurodegeneration was previously described (Lunnon et al., 2011). Other studies have also reported partial protection of *Fcer1g* KO animals against dopaminergic degeneration (Cao et al., 2010) or even irresponsiveness to the application of dopaminergic-specific toxin MPTP (Lira et al., 2011). The involvement of NADPH in dopaminergic degeneration was previously reported (Choi et al., 2012; Qin et al., 2013; Wu et al., 2002). Interestingly, the organisation and activation of NADPH is also downstream of ITAM bearing molecules (Colonna, 2003; Ivashkiv, 2008).

4.2.1.3 The Contribution of Complement Component 3 in LPS-induced Dopaminergic Degeneration

The complement system involvement in neurodegeneration was vastly investigated in previous studies. Complement proteins are produced mostly in the liver and are present at high levels in serum, but glial cells and neurons in the CNS can synthesize these proteins as well (Wyss-Coray and Rogers, 2012). Moreover, levels of complement molecules are increased after brain injury or neurodegeneration (Gasque, 2004). In PD, C1q was associated with labeling and clearance of neuromelanin (Depboylu et al., 2011). Another study observed intraneuronal and extraneuronal Lewy bodies and dendritic spheroid bodies stained for C3d, C4d, C7, and C9 in the SNpc of PD brains (Yamada et al., 1992).

Within this thesis, a careful analysis of the complement pathway after repeated LPS treatment revealed the important role played by C3. Thus, it was hypothesised that in the absence of C3 the effects of microglial activation on neuronal degeneration might be inhibited. For this, C3 KO animals were injected with LPS using the repeated treatment paradigm and the loss of SNpc dopaminergic neurons was evaluated. The results confirmed the hypothesis. In C3 KO mice neuronal loss was significantly less compared with WT animals. In previous studies, C3 was demonstrated to contribute to microglial priming towards a proinflammatory state (Ramaglia et al., 2012). Additionally, deficiency in another complement-related protein, the C3 convertase regulator complement receptor 1-related protein (Crry), leads to increased cleavage of C3 into the active products C3b and iC3b sensitizing microglia to systemic LPS (Ramaglia et al., 2012). Interestingly, in a mouse model of AD, Crry-mediated inhibition of C3 activation of microglia increased the amyloid plaques deposition and neuronal degeneration (Wyss-Coray and Yan, 2002), providing another evidence of microglial implication in neurodegenerative diseases.

4.3 DAP12/TYROBP Involvement in LOAD

Different genes, together with epidemiological and psychosocial factors were previously correlated with LOAD (Bettens et al., 2013; Qiu et al., 2010). Within this thesis, a broad GWAS on LOAD brain and non-demented controls was conducted, identifying TYROBP (the gene encoding for DAP12) as a key regulator of LOAD. Overexpression of functional or non-functional DAP12 variants in microglial cells recapitulated LOAD-associated transcriptomic features and revealed its implications in A β -related pathology. *In vitro* results pointed out the requirement of functional DAP12 for A β internalization by microglia and for subsequent release of intracellular signaling cascades. A β -associated neurotoxicity was evidenced on neurons in cocultures only when functional microglial DAP12 was present. Release of toxic superoxide, one of the functions downstream of DAP12, was proven to be abolished in non-functional DAP12 overexpressing cells. Results propose an A β -related neurotoxic pathway mediated by microglial DAP12.

4.3.1 The Genetic Background of LOAD

Many of the potential disease mechanisms reported in AD, and particularly in sporadic LOAD, were centered on A β -related pathology. Recently, multidisciplinary studies in epidemiology, neuropathology and neuroimaging have provided evidences which support the role of vascular factors and related disorders (like high blood pressure, obesity, diabetes, cerebral microvascular lesions and smoking) as risk factors and the possible role of psychosocial factors (like high educational achievements, mentally-stimulating activity, social engagement and

physical exercise) as protective factors in the development and clinical manifestation of the dementia syndrome, including AD (Qiu et al., 2010). However, before this multidisciplinary approach, other groups reported genetics that are involved in LOAD debut and progression with the highest odds ratio gene being found for the *APOE* (Corder et al., 1993). As the GWAS technique advanced, a multitude of additional susceptible risk loci were identified (Bettens et al., 2013).

4.3.2 Mechanisms of DAP12 Mediated Neurotoxicity in LOAD

4.3.2.1 DAP12 Revealed as Key Regulator by Transcriptome Analysis of LOAD

Excepting the *APOE* gene that accounts for at least 30% of genetic variance (Corder et al., 1993), the correlation of these susceptible loci with LOAD is very small. It can be hypothesized that other fraction of the genetic variance might be implicated in the development of the disease. Based on this, within this thesis, a GWAS was performed on more than 1500 brains of patients suffering from LOAD or non-demented controls. These GWAS results were found to be correlated with known dysfunctions of the cell cycle, mitochondrion and autophagy, as reported previously in LOAD (Coskun et al., 2004; Webber et al., 2005). Additionally, present GWAS network revealed the immune/microglia cluster to be predominate in the LOAD brains, in agreement with previous results (Bettens et al., 2013).

Indeed, microglial involvement in AD was investigated by many groups using different techniques (El Khoury and Luster, 2008; González-Scarano and Baltuch, 1999; Perry et al., 2010, 2007; Wyss-Coray and Rogers, 2012). The GWAS presented in this thesis, reported an immune/microglia related cluster found among others of *ITGAM*, *FCGR1* and *TREM2* genes encoding for receptors that were correlated previously with AD. Thus, *ITGAM* gene encodes the $\alpha_M\beta_2$ -integrin, part of the CR3. Complement was reported to be activated in the AD brain (Shen et al., 2001) and a more recent transcriptome analysis have also identified enrichments of the complement genes in AD (Blalock et al., 2004; Katsel et al., 2009). Of note, C1q, the initiator of the classical complement pathway was found to be associated with plaques in AD brains (Fonseca et al., 2004) and was also found enriched within the present LOAD GWAS. *FCGR1* gene encodes the immunoglobulin G Fc receptor (CD64) and was recently implicated in the development of hypercholesterolaemia-associated features of AD (Fernandez-Vizarra et al., 2012). *TREM2* receptor was also reported as being found in the proximity of A β plaques, raising questions regarding its function in AD (Frank et al., 2008; Melchior et al., 2010). Recently, *TREM2* was associated with LOAD in two individual system biology studies with odds ratios similar with the ones of *APOE* (Guerreiro et al., 2013; Jonsson et al., 2013).

4.3.2.2 DAP12 Modified Microglial Cells Recapitulate Features of LOAD

TREM2 relies on DAP12 for intracellular signaling (Colonna, 2003). Within the GWAS analysis of the thesis, *TYROBP* (encoding DAP12) was identified as key regulator of the immune/microglia cluster in LOAD brains. Moreover, most of the major proteins downstream of DAP12 were also found to be enriched. Since DAP12 is involved in signaling towards actin reorganisation (related with process of phagocytosis and migration) and NADPH oxidase activation (related with the oxidative-burst), these functions were hypothesized to be altered in the LOAD brain.

ESdM cells are a microglial cell line generated *in vitro* from mouse embryonic stem cells via a five step protocol of differentiation (Beutner et al., 2010). ESdM were fully characterized and they showed a microglial phenotype and transcriptome similar with mouse primary microglia and clearly different from other brain cell types or macrophages (Beutner et al., 2013, 2010). Transcriptome analysis of the ESdM overexpressing DAP12 variants showed a highly similar pattern with the results of LOAD brain, thus validating the working system. To identify possible DAP12-related dysfunctions in AD brains, ESdM cells were lentivirally transduced to overexpress either full length functional DAP12, truncated non-functional DAP12 (in which the ITAM signaling motif was deleted) or a control vector. The backbone vector was designed to present a GFP expressing cassette, thus the overexpressing cells were selected based on the GFP signal.

4.3.2.3 DAP12-mediated Mechanism of A β -triggered Neurotoxicity

Among the variety of PRRs expressed by microglia, a number of them were reported as implicated in microglial recognition and/or phagocytosis of A β , like TLRs, RAGE, scavenger receptor A, signal regulatory protein β 1 (SIRP β 1), CR3, or a multicomplex structure formed of CD36, α 6 β 1-integrin and CD47 (Gaikwad et al., 2009; Mandrekar and Landreth, 2010; Wyss-Coray and Rogers, 2012). DAP12 is an adaptor molecule for at least two of the receptors implicated in A β recognition and/or internalization, as it was demonstrated *in vitro* for SIRP β 1 (Gaikwad et al., 2009) and *in vivo* for CR3 (Fu et al., 2012). Based on these informations, it was hypothesised that Dap12 might be of vital importance for intracellular signaling after A β engagement. Indeed, by using Dap12 variants overexpressing cells it was proved that the level of A β was upregulated in microglial cells when functional Dap12 was present, whereas dysfunction in Dap12 signaling led to decreased internalization. Moreover, full length overexpression of Dap12 increased the phagocytosis level of A β in microglial cells. When using

albumin as control, the level of internalisation was similar between all the cell types, proving Dap12 specificity in the microglial uptake of A β .

After Dap12 activation, Syk is phosphorylated, releasing intracellular activatory signaling cascades, one of them increasing the capacity of cellular phagocytosis (Ivashkiv, 2009; Mócsai et al., 2010; Turnbull and Colonna, 2007). Thus, as additional proof of Dap12 involvement in A β uptake, the level of Syk activation in the A β treated microglial cells was explored. Results confirmed the activated Syk after A β application to the microglial culture in cells overexpressing functional Dap12, whereas Syk activation was not detected in truncated Dap12 overexpressing cells. Syk activation was previously correlated with AD (McDonald et al., 1997) and recent reports evidenciat Syk involvement also in tau protein hyperphosphorylation (Lebouvier et al., 2009). Of note, Syk is crucial for initiation of ITAM-signaling receptors (Lowell, 2010) and thus it can be presumed that DAP12 is not the only molecule enhancing Syk activation in AD. Additionally, due to its position within the signaling pathway, Syk is another bottleneck molecule that can modulate the activity of immune cells (Lowell, 2010). Recent studies reported Syk involvement in adaptive immunity, cellular adhesion, innate immune recognition, osteoclast maturation, platelet activation and vascular development (Mócsai et al., 2010).

The overactivated microglial neurotoxicity was reported by many studies (Kettenmann and Hanisch, 2011; Ransohoff and Perry, 2009) as being closely related also with the presence of amyloid plaques inside the AD brain (Wyss-Coray and Rogers, 2012). Microglia are known to be more abundant in the white matter of brain (Lawson et al., 1990), thus an overactivation of microglia can easily lead to associated neurodegenerative dysfunctions (Cunningham, 2013). The effect of A β on Dap12 overexpressing ESdMs was assayed in mouse primary neuronal culture. First the effect of microglia, amyloid or a combination of both was investigated, observing that only when all are added to the culture, a significant change in the length of neurites can be detected. This result provides evidence of microglial mediated neurotoxicity in the presence of A β , a process that was previously described also by other studies (Maezawa et al., 2011; Murgas et al., 2012; von Bernhardt et al., 2007; Zhang et al., 2011). However, when microglia overexpressing Dap12 variants were added to the neuronal culture, a reduction of neurite lengths correlated with the presence of A β together with a functional Dap12 in microglial cells was detected. Non-functional truncated Dap12 abrogated the neurotoxic effects of A β treated micriglia, proving the involvement of Dap12 signaling pathway in microglial neurotoxicity. Indeed, the signaling pathway related with A β induced neurotoxicity was previously reported to involve CR3 and PI3K (Zhang et al., 2011), LPS receptor component CD14 (Liu et al., 2005), scavenger receptors (Bamberger et al., 2003; Murgas et al., 2012), caspase (Burguillos et al., 2011) and NADPH (Block, 2008). Many of these molecules were found within or close proximity of the DAP12 signaling cascade.

One of the processes activated by the DAP12 pathway is superoxide production via NADPH oxidase complex recruitment (Colonna, 2003; Ivashkiv, 2009). Microglia, like all phagocytic cells, can provide host defense by ingesting microbes and destroying them by different mechanisms, including the generation of NADPH oxidase-mediated ROS (Block et al., 2007). However, many studies reported dysfunctions or side-effects of this process, when microglial NADPH oxidase exceeds its protective effect and becomes detrimental for brain parenchyma (Block, 2008). Thus, NADPH-related oxidative stress was described in diseases like PD (Choi et al., 2012; Hunot et al., 1996) or AD (Block, 2008; Zhang et al., 2011), but as well in the normal process of ageing (Qin et al., 2013). Based on these reports, the release of superoxide mediated by Dap12 was investigated next in microglial cells overexpressing variants of Dap12 in the presence or absence of A β . The results show that indeed ROS production is increased in microglial cells in the presence of A β only when a functional Dap12 is present in the system, the truncated overexpression of Dap12 presenting no effect on superoxide release. To verify the specificity of the Dap12-mediated pathway in superoxide release after A β stimulation, the cells were incubated with another potent superoxide inductor zymosan (agonist of TLR2) or albumin, which was proven previously to be internalized by microglial cells independent of Dap12. Under these stimuli, the production of superoxide is not influenced by the presence of different Dap12 variants overexpressed in microglial cells.

Thus, it can be concluded that microglial release of superoxide after A β stimulation is mediated via activation of the Dap12 adaptor molecules.

4.4 Summary

Microglia, the resident immune cells of the CNS, were described as presenting both neuroprotective and neurotoxic functions, depending on stimulation and/or brain physiological condition (Biber et al., 2007; Ransohoff and Perry, 2009). Nasu-Hakola disease (NHD) is considered to be the prototype of primary microglial disorder inside brain (Bianchin et al., 2010), but microglial involvement has been described in essentially all the major neurodegenerative diseases (Cunningham, 2013; Minghetti, 2005; Perry et al., 2010). However, the intimate physiology that drives microglial changes from a beneficial to a detrimental cell type for the brain parenchyma is not fully understood.

Within the present thesis, microglial physiology was assessed in models of different neurodegenerative diseases such as NHD, Parkinson's disease (PD) or late onset Alzheimer's disease (LOAD).

NHD is known to be caused by loss of function mutation in either triggering receptor expressed on myeloid cells 2 (TREM2) or its associated molecule DNAX-activating protein of molecular mass 12 kDa (DAP12) (Paloneva et al., 2002, 2000). By using a NHD mouse model to assess the implications of microglial TREM2 deficiency for the brain parenchyma, here was observed for the first time age-dependent changes in microglia-related gene expressions. Data obtained in this thesis identified an increase of immune-related genes like *I11b* and *Aif1* in 24 months old TREM2 knock-out (KO) vs. wild type (WT) mice. However, when bacterial toxin lipopolysaccharide (LPS) was applied to the TREM2 KO mice, the obtained response was similar with the one elicited in normal WT control mice. These results are contradictory at first sight with previous *in vitro* studies (Hamerman et al., 2005; Takahashi et al., 2005) or *in vivo* studies on macrophages or models of experimental colitis (Correale et al., 2013; Seno et al., 2009; Turnbull et al., 2006). These studies report an increase of cytokines in TREM2 deficient models. However, until present, only one other study has assessed TREM2 deficiency inside the brain (Sieber et al., 2013b). Sieber and colleagues used TREM2 KO mice in a model of stroke, confirming the results obtained in this thesis (Sieber et al., 2013b). Thus, based on these data, it can be hypothesized that TREM2 is presenting a different response in CNS compared with the periphery, where TREM2 deficiency seem to lead to increase of proinflammatory cytokines after inflammatory stimulation (Correale et al., 2013; Seno et al., 2009).

Microglial cells present an important contribution to LPS-induced dopaminergic degeneration both *in vitro* and *in vivo*, but the exact mechanism of degeneration is not fully known (Cunningham, 2013; Dutta et al., 2008). To bring more data on the microglial-mediated neurodegeneration, two models of systemic LPS application in mice were compared here, one based on a repeated intraperitoneal (i.p.) application and the other on a single i.p. application of the same total cumulative dose of LPS. Only the repeated LPS treatment paradigm was able to produce fast dopaminergic degeneration. To characterize the mechanism involved in this process, transcriptome array was performed, comparing the two treatment paradigms. Further pathway analysis showed enrichment of the microglial phagosome, oxidative burst and complement cascade-related functions after the repeated LPS treatment of mice. To explore the complement involvement in the dopaminergic neurons loss, C3 KO animals were challenged according to the LPS treatment paradigm and proved to be resistant to neuronal loss. The results presented in the thesis bring further insights into microglia-mediated dopaminergic degeneration, providing ground for possible future treatment strategies.

Complex multifactorial diseases as LOAD require careful analysis for the identification of causal factors (Bettens et al., 2013; Qiu et al., 2010). Within the present thesis, a genome wide association study was performed on a group of more than 1500 LOAD brains and non-demented controls. *TYROBP* (encoding DAP12) was identified as key regulator of the disease. Overexpression of functional or non-functional DAP12 (without signaling motif) in microglial

cells recapitulated features of LOAD in an array analysis. Studies on the DAP12-associated microglial functions evidenced the involvement of DAP12 in previously described aspects of LOAD pathology such as microglial A β phagocytosis, neuronal toxicity in the presence of A β and release of superoxide. The present thesis proposes a microglial DAP12-mediated neurotoxicity triggered by the presence of A β that can contribute to the development LOAD neuropathology.

Thus, the present thesis proposes a microglial-related mechanism in which different immune-related pathways are converging and thus contributing to the neurodegenerative processes.

Appendix

Specific genes enriched by the repeated (4x) LPS challenges of mice. $FC \geq 2$, $FDR < 0.05$.

Symbol	Gene	Symbol	Gene
Al607873	expressed sequence Al607873	H2-Q6	histocompatibility 2, Q region locus 1; histocompatibility 2, Q region locus 9; similar to H-2 class I histocompatibility antigen, L-D alpha chain precursor; histocompatibility 2, Q region locus 8; histocompatibility 2, Q region locus 2; similar to MHC class Ib antigen; histocompatibility 2, Q region locus 7; histocompatibility 2, Q region locus 6; hypothetical protein LOC100044307; similar to H-2 class I histocompatibility antigen, Q7 alpha chain precursor (QA-2 antigen); RIKEN cDNA 0610037M15 gene
AW112010	expressed sequence AW112010	H2-Q7	histocompatibility 2, Q region locus 1; histocompatibility 2, Q region locus 9; similar to H-2 class I histocompatibility antigen, L-D alpha chain precursor; histocompatibility 2, Q region locus 8; histocompatibility 2, Q region locus 2; similar to MHC class Ib antigen; histocompatibility 2, Q region locus 7; histocompatibility 2, Q region locus 6; hypothetical protein LOC100044307; similar to H-2 class I histocompatibility antigen, Q7 alpha chain precursor (QA-2 antigen); RIKEN cDNA 0610037M15 gene
Acer2	alkaline ceramidase 2	Ifi204	interferon activated gene 204
Aoah	acyloxyacyl hydrolase	Ifi30	interferon gamma inducible protein 30
Apobec3	apolipoprotein B mRNA editing enzyme, catalytic polypeptide 3	Ifit1	interferon-induced protein with tetratricopeptide repeats 1
C1qb	complement component 1, q subcomponent, beta polypeptide	Ifit3	interferon-induced protein with tetratricopeptide repeats 3
Cav1	caveolin 1, caveolae protein	Igfbp7	insulin-like growth factor binding protein 7
Ccl3	chemokine (C-C motif) ligand 3	Il2rg	predicted gene 614; interleukin 2 receptor, gamma chain
Cd33	CD33 antigen	Itgam	integrin alpha M
Cd53	CD53 antigen	Lcp1	lymphocyte cytosolic protein 1
Cd68	CD68 antigen	Lcp2	lymphocyte cytosolic protein 2
Cd72	CD72 antigen	Lgals3bp	lectin, galactoside-binding, soluble, 3 binding protein
Cd93	CD93 antigen		
Clec4a1	C-type lectin domain family 4, member a1		
Clec4a3	C-type lectin domain family 4, member a3		
Cp	ceruloplasmin		
Ctsc	cathepsin C		
Ctsh	cathepsin H		
Cxcl13	chemokine (C-X-C motif) ligand 13		
Cyba	cytochrome b-245, alpha polypeptide		
Eltf1	EGF, latrophilin seven transmembrane domain containing 1		
Eng	endoglin		
Fcgr1g	Fc receptor, IgE, high affinity I, gamma polypeptide		
Fcgr2b	Fc receptor, IgG, low affinity IIb		
Fcgr3	Fc receptor, IgG, low affinity III		
Fcgr4	Fc receptor, IgG, low affinity IV		
Fn1	fibronectin 1		
Gbp2	guanylate binding protein 2		
H2-D1	histocompatibility 2, D region; histocompatibility 2, D region locus 1		

Lilrb4	glycoprotein 49 A; leukocyte immunoglobulin-like receptor, subfamily B, member 4
Ly6a	lymphocyte antigen 6 complex, locus A
Ly86	lymphocyte antigen 86
Mpeg1	macrophage expressed gene 1
Ms4a6b	membrane-spanning 4-domains, subfamily A, member 6B
Ms4a6d	membrane-spanning 4-domains, subfamily A, member 6D
Ms4a7	membrane-spanning 4-domains, subfamily A, member 7
Pglyrp1	peptidoglycan recognition protein 1; similar to peptidoglycan recognition protein
Pilra	paired immunoglobulin-like type 2 receptor alpha

Prg4	proteoglycan 4 (megakaryocyte stimulating factor, articular superficial zone protein)
Ptprc	protein tyrosine phosphatase, receptor type, C
Stab1	stabilin 1
Tgtp1	T-cell specific GTPase 2; T-cell specific GTPase
Tlr13	toll-like receptor 13
Trim30	tripartite motif-containing 30
Tyrobp	TYRO protein tyrosine kinase binding protein
Unc93b1	unc-93 homolog B1 (C. elegans)

Common genes enriched by the repeated (4x) and single (1x) LPS challenge of mice. FC ≥ 2, FDR < 0.05

Symbol	Gene
C1qa	complement component 1, q subcomponent, alpha polypeptide
C1qc	complement component 1, q subcomponent, C chain
C3	complement component 3; similar to complement component C3 prepropeptide, last
C3ar1	complement component 3a receptor 1
C4b	similar to Complement C4 precursor; complement component 4A (Rodgers blood group); similar to complement C4; complement component 4B (Childo blood group)
Ccl5	chemokine (C-C motif) ligand 5
Cd52	CD52 antigen
Ctss	cathepsin S
Cybb	cytochrome b-245, beta polypeptide

Symbol	Gene
Emr1	EGF-like module containing, mucin-like, hormone receptor-like sequence 1
Fyb	FYN binding protein
Wfdc17	WAP four-disulfide core domain 17
H2-K1	histocompatibility 2, K1, K region; similar to H-2K(d) antigen
Ifitm3	interferon induced transmembrane protein 3
Igsf6	immunoglobulin superfamily, member 6
Lcn2	lipocalin 2
Lyz2	lysozyme 2
Ms4a6c	membrane-spanning 4-domains, subfamily A, member 6C
Pld4	phospholipase D family, member 4
Saa3	serum amyloid A 3
Serpina3n	serine (or cysteine) peptidase inhibitor, clade A, member 3N
Vwf	Von Willebrand factor homolog

Specific genes enriched by the single (1x) LPS challenge of mice. FC ≥ 2, FDR < 0.05

Symbol	Gene
Gh	growth hormone
Gpx3	glutathione peroxidase 3
Ngp	neutrophilic granule protein

References

- Adams, R. a, Bauer, J., Flick, M.J., Sikorski, S.L., Nuriel, T., Lassmann, H., Degen, J.L., Akassoglou, K., 2007. The fibrin-derived gamma377-395 peptide inhibits microglia activation and suppresses relapsing paralysis in central nervous system autoimmune disease. *J. Exp. Med.* 204, 571–82.
- Ajami, B., Bennett, J.L., Krieger, C., McNagny, K.M., Rossi, F.M. V, 2011. Infiltrating monocytes trigger EAE progression, but do not contribute to the resident microglia pool. *Nat. Neurosci.* 14, 1142–9.
- Allcock, R.J.N., Barrow, A.D., Forbes, S., Beck, S., Trowsdale, J., 2003. The human TREM gene cluster at 6p21.1 encodes both activating and inhibitory single IgV domain receptors and includes NKp44. *Eur. J. Immunol.* 33, 567–77.
- Allinson, T.M.J., Parkin, E.T., Turner, A.J., Hooper, N.M., 2003. ADAMs family members as amyloid precursor protein alpha-secretases. *J. Neurosci. Res.* 74, 342–52.
- Alliot, F., Godin, I., Pessac, B., 1999. Microglia derive from progenitors, originating from the yolk sac, and which proliferate in the brain. *Brain Res. Dev. Brain Res.* 117, 145–52.
- Arai, H., Furuya, T., Yasuda, T., Miura, M., Mizuno, Y., Mochizuki, H., 2004. Neurotoxic effects of lipopolysaccharide on nigral dopaminergic neurons are mediated by microglial activation, interleukin-1beta, and expression of caspase-11 in mice. *J. Biol. Chem.* 279, 51647–53.
- Bakker, A.B., Hoek, R.M., Cerwenka, A., Blom, B., Lucian, L., McNeil, T., Murray, R., Phillips, L.H., Sedgwick, J.D., Lanier, L.L., 2000. DAP12-deficient mice fail to develop autoimmunity due to impaired antigen priming. *Immunity* 13, 345–53.
- Ballatore, C., Lee, V.M.-Y., Trojanowski, J.Q., 2007. Tau-mediated neurodegeneration in Alzheimer’s disease and related disorders. *Nat. Rev. Neurosci.* 8, 663–72.
- Bamberger, M.E., Harris, M.E., McDonald, D.R., Husemann, J., Landreth, G.E., 2003. A cell surface receptor complex for fibrillar beta-amyloid mediates microglial activation. *J. Neurosci.* 23, 2665–74.
- Banks, W.A., Robinson, S.M., 2010. Minimal penetration of lipopolysaccharide across the murine blood-brain barrier. *Brain. Behav. Immun.* 24, 102–9.
- Baquet, Z.C., Williams, D., Brody, J., Smeyne, R.J., 2009. A comparison of model-based (2D) and design-based (3D) stereological methods for estimating cell number in the substantia nigra pars compacta (SNpc) of the C57BL/6J mouse. *Neuroscience* 161, 1082–90.
- Barbaric, I., Miller, G., Dear, T.N., 2007. Appearances can be deceiving: phenotypes of knockout mice. *Brief. Funct. Genomic. Proteomic.* 6, 91–103.
- Barron, K.D., 1995. The microglial cell. A historical review. *J. Neurol. Sci.* 134 Suppl, 57–68.
- Barrow, A.D., Trowsdale, J., 2006. You say ITAM and I say ITIM, let’s call the whole thing off: the ambiguity of immunoreceptor signalling. *Eur. J. Immunol.* 36, 1646–53.
- Barrow, C.J., Zagorski, M.G., 1991. Solution structures of beta peptide and its constituent fragments: relation to amyloid deposition. *Science* 253, 179–82.
- Batchelor, P., 2002. Macrophages and Microglia Produce Local Trophic Gradients That Stimulate Axonal Sprouting Toward but Not beyond the Wound Edge. *Mol. Cell. Neurosci.* 21, 436–453.
- Bauer, J., Sminia, T., Wouterlood, F.G., Dijkstra, C.D., 1994. Phagocytic activity of macrophages and microglial cells during the course of acute and chronic relapsing experimental autoimmune encephalomyelitis. *J. Neurosci. Res.* 38, 365–75.
- Benilova, I., Karran, E., De Strooper, B., 2012. The toxic A β oligomer and Alzheimer’s disease: an emperor in need of clothes. *Nat. Neurosci.* 15, 349–57.
- Bertram, L., McQueen, M.B., Mullin, K., Blacker, D., Tanzi, R.E., 2007. Systematic meta-analyses of Alzheimer disease genetic association studies: the AlzGene database. *Nat. Genet.* 39, 17–23.
- Bertram, L., Tanzi, R.E., 2008. Thirty years of Alzheimer’s disease genetics: the implications of systematic meta-analyses. *Nat. Rev. Neurosci.* 9, 768–78.
- Bettens, K., Sleegers, K., Van Broeckhoven, C., 2013. Genetic insights in Alzheimer’s disease. *Lancet Neurol.* 12, 92–104.
- Beutner, C., Linnartz-Gerlach, B., Schmidt, S. V, Beyer, M., Mallmann, M.R., Staratschek-Jox, A., Schultze, J.L., Neumann, H., 2013. Unique transcriptome signature of mouse microglia. *Glia* 1–14.

- Beutner, C., Roy, K., Linnartz, B., Napoli, I., Neumann, H., 2010. Generation of microglial cells from mouse embryonic stem cells. *Nat. Protoc.* 5, 1481–1494.
- Bezard, E., Yue, Z., Kirik, D., Spillantini, M.G., 2013. Animal models of Parkinson's disease: limits and relevance to neuroprotection studies. *Mov. Disord.* 28, 61–70.
- Biagioli, M., Pinto, M., Cesselli, D., Zaninello, M., Lazarevic, D., Roncaglia, P., Simone, R., Vlachouli, C., Plessy, C., Bertin, N., Beltrami, A., Kobayashi, K., Gallo, V., Santoro, C., Ferrer, I., Rivella, S., Beltrami, C.A., Carninci, P., Raviola, E., Gustincich, S., 2009. Unexpected expression of alpha- and beta-globin in mesencephalic dopaminergic neurons and glial cells. *J. Neurosci. Res.* 106, 15454–9.
- Bianchin, M.M., Martin, K.C., de Souza, A.C., de Oliveira, M. a, Rieder, C.R.D.M., 2010. Nasu-Hakola disease and primary microglial dysfunction. *Nat. Rev. Neurol.* 6, 2 p following 523.
- Biber, K., Neumann, H., Inoue, K., Boddeke, H.W.G.M., 2007. Neuronal “On” and “Off” signals control microglia. *Trends Neurosci.* 30, 596–602.
- Blalock, E.M.E., Geddes, J.W.J., Chen, K.C., Porter, N.M., Markesbery, W.R., Landfield, P.W., 2004. Incipient Alzheimer's disease: Microarray correlation analyses reveal major transcriptional and tumor suppressor responses. *Proc. Natl. Acad. Sci. U. S. A.* 101, 2173–2178.
- Block, M., Hong, J., 2005. Microglia and inflammation-mediated neurodegeneration: Multiple triggers with a common mechanism. *Prog. Neurobiol.* 76, 77–98.
- Block, M.L., 2008. NADPH oxidase as a therapeutic target in Alzheimer's disease. *BMC Neurosci.* 9 Suppl 2, S8.
- Block, M.L., Zecca, L., Hong, J.S., 2007. Microglia-mediated neurotoxicity: uncovering the molecular mechanisms. *Nat. Rev. Neurosci.* 8, 57–69.
- Bolmont, T., Haiss, F., Eicke, D., Radde, R., Mathis, C. a, Klunk, W.E., Kohsaka, S., Jucker, M., Calhoun, M.E., 2008. Dynamics of the microglial/amyloid interaction indicate a role in plaque maintenance. *J. Neurosci.* 28, 4283–92.
- Bouchon, A., Dietrich, J., Colonna, M., 2000. Cutting edge: inflammatory responses can be triggered by TREM-1, a novel receptor expressed on neutrophils and monocytes. *J. Immunol.* 164, 4991–5.
- Bouchon, A., Hernández-Munain, C., Cella, M., Colonna, M., 2001. A DAP12-mediated pathway regulates expression of CC chemokine receptor 7 and maturation of human dendritic cells. *J. Exp. Med.* 194, 1111–22.
- Braak, H., Braak, E., 1991. Neuropathological staging of Alzheimer-related changes. *Acta Neuropathol.* 82, 239–259.
- Braak, H., Del, K., Rüb, U., Vos, R.A.I. De, Jansen, E.N.H., Braak, E., 2003. Staging of brain pathology related to sporadic Parkinson's disease. *Neurobiol. Aging* 24, 197–211.
- Brown, G.C., Neher, J.J., 2012. Eaten alive! Cell death by primary phagocytosis: “phagoptosis”. *Trends Biochem. Sci.* 37, 325–332.
- Burguillos, M. a, Deierborg, T., Kavanagh, E., Persson, A., Hajji, N., Garcia-Quintanilla, A., Cano, J., Brundin, P., Englund, E., Venero, J.L., Joseph, B., 2011. Caspase signalling controls microglia activation and neurotoxicity. *Nature* 472, 319–24.
- Cao, S., Theodore, S., Standaert, D.G., 2010. Fcγ receptors are required for NF-κB signaling, microglial activation and dopaminergic neurodegeneration in an AAV-synuclein mouse model of Parkinson's disease. *Mol. Neurodegener.* 5, 42.
- Cardona, A.E., Piro, E.P., Sasse, M.E., Kostenko, V., Cardona, S.M., Dijkstra, I.M., Huang, D., Kidd, G., Dombrowski, S., Dutta, R., Lee, J.-C., Cook, D.N., Jung, S., Lira, S. a, Littman, D.R., Ransohoff, R.M., 2006. Control of microglial neurotoxicity by the fractalkine receptor. *Nat. Neurosci.* 9, 917–24.
- Carson, M.J., Doose, J.M., Melchior, B., Schmid, C.D., Ploix, C.C., 2006. CNS immune privilege: hiding in plain sight. *Immunol. Rev.* 213, 48–65.
- Castañó, A., Herrera, A.J., Cano, J., Machado, A., 1998. Lipopolysaccharide intranigral injection induces inflammatory reaction and damage in nigrostriatal dopaminergic system. *J. Neurochem.* 70, 1584–92.
- Cella, M., Buonsanti, C., Strader, C., Kondo, T., Salmaggi, A., Colonna, M., 2003. Impaired differentiation of osteoclasts in TREM-2-deficient individuals. *J. Exp. Med.* 198, 645–51.
- Chan, W.Y., Kohsaka, S., Rezaie, P., 2007. The origin and cell lineage of microglia—New concepts. *Brain Res. Rev.* 53, 344–354.
- Chen, H., Jacobs, E., Schwarzschild, M. a, McCullough, M.L., Calle, E.E., Thun, M.J., Ascherio, A., 2005. Nonsteroidal antiinflammatory drug use and the risk for Parkinson's disease. *Ann. Neurol.* 58, 963–7.

- Chen, S.-K., Tvrdik, P., Peden, E., Cho, S., Wu, S., Spangrude, G., Capecchi, M.R., 2010. Hematopoietic origin of pathological grooming in Hoxb8 mutant mice. *Cell* 141, 775–85.
- Chen, Z., Jalabi, W., Shpargel, K.B., Farabaugh, K.T., Dutta, R., Yin, X., Kidd, G.J., Bergmann, C.C., Stohlman, S. a, Trapp, B.D., 2012. Lipopolysaccharide-induced microglial activation and neuroprotection against experimental brain injury is independent of hematogenous TLR4. *J. Neurosci.* 32, 11706–15.
- Choi, D.-H., Cristóvão, A.C., Guhathakurta, S., Lee, J., Joh, T.H., Beal, M.F., Kim, Y.-S., 2012. NADPH oxidase 1-mediated oxidative stress leads to dopamine neuron death in Parkinson's disease. *Antioxid. Redox Signal.* 16, 1033–45.
- Citron, M., 2004. Strategies for disease modification in Alzheimer's disease. *Nat. Rev. Neurosci.* 5, 677–85.
- Colonna, M., 2003. TREMs in the immune system and beyond. *Nat. Rev. Immunol* 3, 445–453.
- Colonna, Marco, 2003. DAP12 signaling : from immune cells to bone modeling and brain myelination. *J. Clin. Invest.* 111, 1–2.
- Combrinck, M., Perry, V., Cunningham, C., 2002. Peripheral infection evokes exaggerated sickness behaviour in pre-clinical murine prion disease. *Neuroscience* 112, 7–11.
- Compston, A., Coles, A., 2008. Multiple sclerosis. *Lancet* 372, 1502–1517.
- Constantinescu, C.S., Farooqi, N., O'Brien, K., Gran, B., 2011. Experimental autoimmune encephalomyelitis (EAE) as a model for multiple sclerosis (MS). *Br. J. Pharmacol.* 164, 1079–106.
- Corder, E., Saunders, A., Strittmatter, W., Schmechel, D., Gaskell, P., Small, G., Roses, A., Haines, J., Pericak-Vance, M., 1993. Gene dose of apolipoprotein E type 4 allele and the risk of Alzheimer's disease in late onset families. *Science* (80-). 261, 921–923.
- Correale, C., Genua, M., Vetrano, S., Mazzini, E., Martinoli, C., Spinelli, A., Arena, V., Peyrin-Biroulet, L., Caprioli, F., Passini, N., Panina-Bordignon, P., Repici, A., Malesci, A., Rutella, S., Rescigno, M., Danese, S., 2013. Bacterial sensor triggering receptor expressed on myeloid cells-2 regulates the mucosal inflammatory response. *Gastroenterology* 144, 346–356.e3.
- Coskun, P.P.E., Beal, M.F., Wallace, D.C., 2004. Alzheimer's brains harbor somatic mtDNA control-region mutations that suppress mitochondrial transcription and replication. *Proc. Natl. Acad. Sci. U. S. A.* 101, 10726–31.
- Coull, J. a M., Beggs, S., Boudreau, D., Boivin, D., Tsuda, M., Inoue, K., Gravel, C., Salter, M.W., De Koninck, Y., 2005. BDNF from microglia causes the shift in neuronal anion gradient underlying neuropathic pain. *Nature* 438, 1017–21.
- Cunningham, C., 2013. Microglia and neurodegeneration: The role of systemic inflammation. *Glia* 61, 71–90.
- Cunningham, C., Wilcockson, D.C., Champion, S., Lunnon, K., Perry, V.H., 2005. Central and systemic endotoxin challenges exacerbate the local inflammatory response and increase neuronal death during chronic neurodegeneration. *J. Neurosci.* 25, 9275–84.
- Czapski, G.A., Cakala, M., Chalimoniuk, M., Gajkowska, B., Strosznajder, J.B., 2007. Role of nitric oxide in the brain during lipopolysaccharide-evoked systemic inflammation. *J. Neurosci. Res.* 85, 1694–703.
- D'Andrea, M.R., Cole, G.M., Ard, M.D., 2004. The microglial phagocytic role with specific plaque types in the Alzheimer disease brain. *Neurobiol. Aging* 25, 675–83.
- Dantzer, R., O'Connor, J.C., Freund, G.G., Johnson, R.W., Kelley, K.W., 2008. From inflammation to sickness and depression: when the immune system subjugates the brain. *Nat. Rev. Neurosci.* 9, 46–56.
- Dauer, W., Przedborski, S., 2003. Parkinson's disease: mechanisms and models. *Neuron* 39, 889–909.
- Davalos, D., Grutzendler, J., Yang, G., Kim, J. V, Zuo, Y., Jung, S., Littman, D.R., Dustin, M.L., Gan, W.-B., 2005. ATP mediates rapid microglial response to local brain injury in vivo. *Nat. Neurosci.* 8, 752–8.
- Daws, M.R., Lanier, L.L., Seaman, W.E., Ryan, J.C., 2001. Cloning and characterization of a novel mouse myeloid DAP12-associated receptor family. *Eur. J. Immunol.* 31, 783–91.
- Depboylu, C., Schäfer, M.K.-H., Arias-Carrión, O., Oertel, W.H., Weihe, E., Höglinger, G.U., 2011. Possible involvement of complement factor C1q in the clearance of extracellular neuromelanin from the substantia nigra in Parkinson disease. *J. Neuropathol. Exp. Neurol.* 70, 125–32.
- Di Giovanni, G., Pessia, M., Di Maio, R., 2012. Redox sensitivity of tyrosine hydroxylase activity and expression in dopaminergic dysfunction. *CNS Neurol Disord Drug Targets* 11, 419–29.
- Dickson, D.W., 2012. Parkinson's disease and parkinsonism: neuropathology. *Cold Spring Harb. Perspect. Med.* 2, 1–15.
- Dutta, G., Zhang, P., Liu, B., 2008. The lipopolysaccharide Parkinson's disease animal model: mechanistic studies and drug discovery. *Fundam. Clin. Pharmacol.* 22, 453–464.

- Ek, M., Engblom, D., Sipra, S., Blomqvist, A., Jakobsson, P.-J., Ericsson-Dahlstrand, A., 2001. Pathway across the blood–brain barrier. *Science* (80-.). 410, 430–431.
- El Khoury, J., Luster, A.D., 2008. Mechanisms of microglia accumulation in Alzheimer’s disease: therapeutic implications. *Trends Pharmacol. Sci.* 29, 626–32.
- Erridge, C., Bennett-Guerrero, E., Poxton, I.R., 2002. Structure and function of lipopolysaccharides. *Microbes Infect.* 4, 837–51.
- Faggioni, R., Fantuzzi, G., Villa, P.I.A., Buurman, W.I.M., 1995. Independent down-regulation of central and peripheral tumor necrosis factor production as a result of lipopolysaccharide tolerance in mice. *Infect. Immun.* 63, 1473–1477.
- Fernandez-Vizarrá, P., Lopez-Franco, O., Mallavia, B., Higuera-Matas, A., Lopez-Parra, V., Ortiz-Muñoz, G., Ambrosio, E., Egido, J., Almeida, O.F.X., Gomez-Guerrero, C., 2012. Immunoglobulin G Fc receptor deficiency prevents Alzheimer-like pathology and cognitive impairment in mice. *Brain* 135, 2826–37.
- Fonseca, M.I., Kawas, C.H., Troncoso, J.C., Tenner, A.J., 2004. Neuronal localization of C1q in preclinical Alzheimer’s disease. *Neurobiol. Dis.* 15, 40–46.
- Frank, S., Burbach, G.J., Bonin, M., Walter, M., Streit, W., Bechmann, I., Deller, T., 2008. TREM2 is upregulated in amyloid plaque-associated microglia in aged APP23 transgenic mice. *Glia* 56, 1438–47.
- Fu, H., Liu, B., Frost, J.L., Hong, S., Jin, M., Ostaszewski, B., Shankar, G.M., Costantino, I.M., Carroll, M.C., Mayadas, T.N., Lemere, C. a, 2012. Complement component C3 and complement receptor type 3 contribute to the phagocytosis and clearance of fibrillar A β by microglia. *Glia* 60, 993–1003.
- Gaikwad, S., Larionov, S., Wang, Y., Dannenberg, H., Matozaki, T., Monsonego, A., Thal, D.R., Neumann, H., 2009. Signal regulatory protein-beta1: a microglial modulator of phagocytosis in Alzheimer’s disease. *Am. J. Pathol.* 175, 2528–39.
- Galea, I., Bechmann, I., Perry, V.H., 2007. What is immune privilege (not)? *Trends Immunol.* 28, 12–8.
- Gao, H.-M., Jiang, J., Wilson, B., Zhang, W., Hong, J.-S., Liu, B., 2002. Microglial activation-mediated delayed and progressive degeneration of rat nigral dopaminergic neurons: relevance to Parkinson’s disease. *J. Neurochem.* 81, 1285–1297.
- Gasque, P., 2004. Complement: a unique innate immune sensor for danger signals. *Mol. Immunol.* 41, 1089–1098.
- Gilley, J., Adalbert, R., Coleman, M.P., 2011. Modelling early responses to neurodegenerative mutations in mice. *Biochem. Soc. Trans.* 39, 933–8.
- Ginhoux, F., Greter, M., Leboeuf, M., Nandi, S., See, P., Gokhan, S., Mehler, M.F., Conway, S.J., Ng, L.G., Stanley, E.R., Samokhvalov, I.M., Merad, M., 2010. Fate mapping analysis reveals that adult microglia derive from primitive macrophages. *Science* 330, 841–5.
- Glass, C.K., Saijo, K., Winner, B., Marchetto, M.C., Gage, F.H., 2010. Mechanisms underlying inflammation in neurodegeneration. *Cell* 140, 918–34.
- Glenner, G.G., Wong, C.W., 1984. Alzheimer’s disease: initial report of the purification and characterisation of a novel cerebrovascular amyloid protein. *Biochem. Biophys. Res. Commun.* 120, 885–890.
- González-Scarano, F., Baltuch, G., 1999. Microglia as mediators of inflammatory and degenerative diseases. *Annu. Rev. Neurosci.* 22, 219–40.
- Götz, J., Ittner, L.M., 2008. Animal models of Alzheimer’s disease and frontotemporal dementia. *Nat. Rev. Neurosci.* 9, 532–44.
- Griffin, W.S., Stanley, L.C., Ling, C., White, L., MacLeod, V., Perrot, L.J., White, C.L., Araoz, C., 1989. Brain interleukin 1 and S-100 immunoreactivity are elevated in Down syndrome and Alzheimer disease. *Proc. Natl. Acad. Sci. U. S. A.* 86, 7611–5.
- Grundke-Iqbal, I., Iqbal, K., Tung, Y.C., Quinlan, M., Wisniewski, H.M., Binder, L.I., 1986. Abnormal phosphorylation of the microtubule-associated protein tau (tau) in Alzheimer cytoskeletal pathology. *Proc. Natl. Acad. Sci. U. S. A.* 83, 4913–7.
- Guerreiro, R., Wojtas, A., Bras, J., Carrasquillo, M., Rogaeva, E., Majounie, E., Cruchaga, C., Sassi, C., Kauwe, J.S.K.K., Younkin, S., Hazrati, L., Collinge, J., Pocock, J., Lashley, T., Williams, J., Lambert, J., Amouyel, P., Goate, A., Rademakers, R., Morgan, K., Powell, J., St George-Hyslop, P., Singleton, A., Hardy, J., Ph, D., George-hyslop, P.S., St. George-Hyslop, P., 2013. TREM2 variants in Alzheimer’s disease. *N. Engl. J. Med.* 368, 117–27.
- Guerreiro, R.J., Lohmann, E., Brás, J.M., Gibbs, J.R., Rohrer, J.D., Gurunlian, N., Dursun, B., Bilgic, B., Hanagasi, H., Gurvit, H., Emre, M., Singleton, A., Hardy, J., 2013. Using Exome Sequencing to Reveal Mutations in TREM2

- Presenting as a Frontotemporal Dementia-like Syndrome Without Bone Involvement. *JAMA Neurol.* 70, 78–84.
- Haass, C., Hung, A., 1993. beta-Amyloid peptide and a 3-kDa fragment are derived by distinct cellular mechanisms. *J. Biol. Chem.* 268, 3021–3024.
- Hamerman, J. a, Jarjoura, J.R., Humphrey, M.B., Nakamura, M.C., Seaman, W.E., Lanier, L.L., 2006. Cutting edge: inhibition of TLR and FcR responses in macrophages by triggering receptor expressed on myeloid cells (TREM)-2 and DAP12. *J. Immunol.* 177, 2051–5.
- Hamerman, J. a, Ni, M., Killebrew, J.R., Chu, C.-L., Lowell, C. a, 2009. The expanding roles of ITAM adapters FcRgamma and DAP12 in myeloid cells. *Immunol. Rev.* 232, 42–58.
- Hamerman, J. a, Tchao, N.K., Lowell, C. a, Lanier, L.L., 2005. Enhanced Toll-like receptor responses in the absence of signaling adaptor DAP12. *Nat. Immunol.* 6, 579–86.
- Hanisch, U.-K., Kettenmann, H., 2007. Microglia: active sensor and versatile effector cells in the normal and pathologic brain. *Nat. Neurosci.* 10, 1387–94.
- Hasegawa, T., Takagi, K., Kitaichi, K., 1999. Effects of bacterial endotoxin on drug pharmacokinetics. *Nagoya J. Med. Sci.* 62, 11–28.
- Hayashi, Y., Ishibashi, H., Hashimoto, K., Nakanishi, H., 2006. Potentiation of the NMDA receptor-mediated responses through the activation of the glycine site by microglia secreting soluble factors. *Glia* 668, 660–668.
- Hernández-Romero, M.C., Delgado-Cortés, M.J., Sarmiento, M., de Pablos, R.M., Espinosa-Oliva, A.M., Argüelles, S., Bández, M.J., Villarán, R.F., Mauriño, R., Santiago, M., Venero, J.L., Herrera, A.J., Cano, J., Machado, A., 2012. Peripheral inflammation increases the deleterious effect of Cns inflammation on the nigrostriatal dopaminergic system. *Neurotoxicology* 1–14.
- Hickey, W.F., Kimura, H., 1988. Perivascular microglial cells of the CNS are bone marrow-derived and present antigen in vivo. *Science* 239, 290–2.
- Hirsch, E.C., Vyas, S., Hunot, S., 2012. Neuroinflammation in Parkinson’s disease. *Parkinsonism Relat. Disord.* 18 Suppl 1, S210–2.
- Hsieh, C.L., Koike, M., Spusta, S.C., Niemi, E.C., Yenari, M., Nakamura, M.C., Seaman, W.E., 2009. A role for TREM2 ligands in the phagocytosis of apoptotic neuronal cells by microglia. *J. Neurochem.* 109, 1144–56.
- Humphrey, M.B., Daws, M.R., Spusta, S.C., Niemi, E.C., Torchia, J.A., Lanier, L.L., Seaman, W.E., Nakamura, M.C., 2006. TREM2, a DAP12-associated receptor, regulates osteoclast differentiation and function. *J. Bone Miner. Res.* 21, 237–45.
- Hunot, S., Boissière, F., Faucheux, B., Brugg, B., Mouatt-Prigent, A., Agid, Y., Hirsch, E.C., 1996. Nitric oxide synthase and neuronal vulnerability in Parkinson’s disease. *Neuroscience* 72, 355–363.
- Iravani, M.M., Leung, C.C.M., Sadeghian, M., Haddon, C.O., Rose, S., Jenner, P., 2005. The acute and the long-term effects of nigral lipopolysaccharide administration on dopaminergic dysfunction and glial cell activation. *Eur. J. Neurosci.* 22, 317–30.
- Ivashkiv, L.B., 2008. A signal-switch hypothesis for cross-regulation of cytokine and TLR signalling pathways. *Nat. Rev. Immunol.* 8, 816–22.
- Ivashkiv, L.B., 2009. Cross-regulation of signaling by ITAM-associated receptors. *Nat. Immunol.* 10, 340–7.
- Jinno, S., Fleischer, F., Eckel, S., Schmidt, V., Kosaka, T., 2007. Spatial arrangement of microglia in the mouse hippocampus: a stereological study in comparison with astrocytes. *Glia* 1334–1347.
- Jonsson, T., Stefansson, H., Steinberg, S., Jonsdottir, I., Jonsson, P. V., Snaedal, J., Bjornsson, S., Huttenlocher, J., Levey, A.I., Lah, J.J., Rujescu, D., Hampel, H., Giegling, I., Andreassen, O. a., Engedal, K., Ulstein, I., Djurovic, S., Ibrahim-Verbaas, C., Hofman, A., Ikram, M.A., van Duijn, C.M., Thorsteinsdottir, U., Kong, A., Stefansson, K., Ph.D., S.S., 2013. Variant of TREM2 associated with the risk of Alzheimer’s disease. *N. Engl. J. Med.* 368, 107–16.
- Kaifu, T., Nakahara, J., Inui, M., Mishima, K., Momiyama, T., Kaji, M., Sugahara, A., Koito, H., Ujike-asai, A., Nakamura, A., Kanazawa, K., Tan-takeuchi, K., Iwasaki, K., Yokoyama, W.M., Kudo, A., Fujiwara, M., Asou, H., Takai, T., 2003. Osteopetrosis and thalamic hypomyelinosis with synaptic degeneration in DAP12-deficient mice. *J. Clin. Invest.* 111, 323–332.
- Kaneko, M., Sano, K., Nakayama, J., Amano, N., 2010a. Nasu-Hakola disease: The first case reported by Nasu and review. *Neuropathology*.
- Kaneko, M., Sano, K., Nakayama, J., Amano, N., 2010b. Nasu-Hakola disease: The first case reported by Nasu and review. *Neuropathology*.

- Kaneko, M., Stellwagen, D., Malenka, R.C., Stryker, M.P., 2008. Tumor necrosis factor-alpha mediates one component of competitive, experience-dependent plasticity in developing visual cortex. *Neuron* 58, 673–80.
- Katsel, P., Tan, W., Haroutunian, V., 2009. Gain in brain immunity in the oldest-old differentiates cognitively normal from demented individuals. *PLoS One* 4, e7642.
- Kaushal, V., Schlichter, L.C., 2008. Mechanisms of microglia-mediated neurotoxicity in a new model of the stroke penumbra. *J. Neurosci.* 28, 2221–30.
- Kawai, T., Akira, S., 2006. TLR signaling. *Cell Death Differ.* 13, 816–25.
- Kettenmann, H., 2006. Triggering the brain pathology sensor. *Nat. Neurosci.* 578, 233–47.
- Kettenmann, H., Hanisch, U., 2011. Physiology of microglia. *Physiol. ...* 91, 461–553.
- Kierdorf, K., Erny, D., Goldmann, T., Sander, V., Schulz, C., Perdiguero, E.G., Wieghofer, P., Heinrich, A., Riemke, P., Hölscher, C., Müller, D.N., Luckow, B., Brocker, T., Debowski, K., Fritz, G., Opdenakker, G., Diefenbach, A., Biber, K., Heikenwalder, M., Geissmann, F., Rosenbauer, F., Prinz, M., 2013. [Microglia emerge from erythromyeloid precursors via Pu.1- and Irf8-dependent pathways. *Nat. Neurosci.* 16, 273–80.
- Kiialainen, A., Veckman, V., Saharinen, J., Paloneva, J., Gentile, M., Hakola, P., Hemelsoet, D., Ridha, B., Kopra, O., Julkunen, I., Peltonen, L., 2007. Transcript profiles of dendritic cells of PLOSL patients link demyelinating CNS disorders with abnormalities in pathways of actin bundling and immune response. *J. Mol. Med. (Berl).* 85, 971–83.
- Kim, W.G., Mohny, R.P., Wilson, B., Jeohn, G.H., Liu, B., Hong, J.S., 2000. Regional difference in susceptibility to lipopolysaccharide-induced neurotoxicity in the rat brain: role of microglia. *J. Neurosci.* 20, 6309–16.
- Koenigsknecht, J., Landreth, G., 2004. Microglial phagocytosis of fibrillar beta-amyloid through a beta1 integrin-dependent mechanism. *J. Neurosci.* 24, 9838–46.
- Koenigsknecht-Talboo, J., Landreth, G.E., 2005. Microglial phagocytosis induced by fibrillar beta-amyloid and IgGs are differentially regulated by proinflammatory cytokines. *J. Neurosci.* 25, 8240–9.
- Koizumi, S., Shigemoto-Mogami, Y., Nasu-Tada, K., Shinozaki, Y., Ohsawa, K., Tsuda, M., Joshi, B. V., Jacobson, K. a, Kohsaka, S., Inoue, K., 2007. UDP acting at P2Y6 receptors is a mediator of microglial phagocytosis. *Nature* 446, 1091–5.
- Kreutzberg, G.W., 1996. Microglia: a sensor for pathological events in the CNS. *Trends Neurosci.* 19, 312–8.
- Kumar, K.R., Lohmann, K., Klein, C., 2012. Genetics of Parkinson disease and other movement disorders. *Curr. Opin. Neurol.* 25, 466–74.
- Kuroda, R., Satoh, J., Yamamura, T., Anezaki, T., Terada, T., Yamazaki, K., Obi, T., Mizoguchi, K., 2007. A novel compound heterozygous mutation in the DAP12 gene in a patient with Nasu-Hakola disease. *J. Neurol. Sci.* 252, 88–91.
- LaFerla, F.M., Green, K.N., Oddo, S., 2007. Intracellular amyloid-beta in Alzheimer's disease. *Nat. Rev. Neurosci.* 8, 499–509.
- Lanier, L.L., Corliss, B.C., Wu, J., Leong, C., Phillips, J.H., 1998. Immunoreceptor DAP12 bearing a tyrosine-based activation motif is involved in activating NK cells. *Nature* 391, 703–7.
- Lanier, L.L.L., 2009. DAP10- and DAP12-associated receptors in innate immunity. *Immunol. Rev.* 227, 150–160.
- Lassmann, H., Schmied, M., Vass, K., Hickey, W.F., 1993. Bone marrow derived elements and resident microglia in brain inflammation. *Glia* 7, 19–24.
- Lawson, L.J., Perry, V.H., Dri, P., Gordon, S., 1990. Heterogeneity in the distribution and morphology of microglia in the normal adult mouse brain. *Neuroscience* 39, 151–70.
- Lebouvier, T., Scales, T.M.E., Williamson, R., Noble, W., Duyckaerts, C., Hanger, D.P., Reynolds, C.H., Anderton, B.H., Derkinderen, P., 2009. The microtubule-associated protein tau is also phosphorylated on tyrosine. *J. Alzheimers. Dis.* 18, 1–9.
- Lee, B.D., Shin, J.-H., VanKampen, J., Petrucelli, L., West, A.B., Ko, H.S., Lee, Y.-I., Maguire-Zeiss, K. a, Bowers, W.J., Federoff, H.J., Dawson, V.L., Dawson, T.M., 2010. Inhibitors of leucine-rich repeat kinase-2 protect against models of Parkinson's disease. *Nat. Med.* 16, 998–1000.
- Lee, J.-H., Yu, W.H., Kumar, A., Lee, S., Mohan, P.S., Peterhoff, C.M., Wolfe, D.M., Martinez-Vicente, M., Massey, A.C., Sovak, G., Uchiyama, Y., Westaway, D., Cuervo, A.M., Nixon, R. a, 2010. Lysosomal Proteolysis and Autophagy Require Presenilin 1 and Are Disrupted by Alzheimer-Related PS1 Mutations. *Cell* 1, 1–13.
- Lee, Y., Dawson, V.L., Dawson, T.M., 2012. Animal models of Parkinson's disease: vertebrate genetics. *Cold Spring Harb. Perspect. Med.* 2.

- Liberatore, G.T., Jackson-Lewis, V., Vukosavic, S., Mandir, a S., Vila, M., McAuliffe, W.G., Dawson, V.L., Dawson, T.M., Przedborski, S., 1999. Inducible nitric oxide synthase stimulates dopaminergic neurodegeneration in the MPTP model of Parkinson disease. *Nat. Med.* 5, 1403–9.
- Ling, Z., Chang, Q. a, Tong, C.W., Leurgans, S.E., Lipton, J.W., Carvey, P.M., 2004. Rotenone potentiates dopamine neuron loss in animals exposed to lipopolysaccharide prenatally. *Exp. Neurol.* 190, 373–83.
- Ling, Z., Zhu, Y., Tong, C.W., Snyder, J. a, Lipton, J.W., Carvey, P.M., 2006. Progressive dopamine neuron loss following supra-nigral lipopolysaccharide (LPS) infusion into rats exposed to LPS prenatally. *Exp. Neurol.* 199, 499–512.
- Lira, A., Kulczykcki, J., Slack, R., Anisman, H., Park, D.S., 2011. Involvement of the Fc gamma receptor in a chronic N-methyl-4-phenyl-1,2,3,6-tetrahydropyridine mouse model of dopaminergic loss. *J. Biol. Chem.* 286, 28783–93.
- Liu, B., 2006. Modulation of microglial pro-inflammatory and neurotoxic activity for the treatment of Parkinson's disease. *AAPS J.* 8, 606–621.
- Liu, B., Gao, H.-M., Wang, J.-Y., Jeohn, G.-H., Cooper, C.L., Hong, J.-S., 2002. Role of nitric oxide in inflammation-mediated neurodegeneration. *Ann. N. Y. Acad. Sci.* 962, 318–31.
- Liu, B., Jiang, J.W., Wilson, B.C., Du, L., Yang, S.N., Wang, J.Y., Wu, G.C., Cao, X.D., Hong, J.S., 2000. Systemic infusion of naloxone reduces degeneration of rat substantia nigral dopaminergic neurons induced by intranigral injection of lipopolysaccharide. *J. Pharmacol. Exp. Ther.* 295, 125–32.
- Liu, Y., Walter, S., Stagi, M., Cherny, D., Letiembre, M., Schulz-Schaeffer, W., Heine, H., Penke, B., Neumann, H., Fassbender, K., 2005. LPS receptor (CD14): a receptor for phagocytosis of Alzheimer's amyloid peptide. *Brain* 128, 1778–89.
- Loeffler, D., DeMaggio, A., Juneau, P., Havaich, M., LeWitt, P., 1994. Effects of enhanced striatal dopamine turnover in vivo on glutathione oxidation.pdf. *Clin. Neuropharmacol.* 17, 370–379.
- Lowell, C., 2010. Src-family and Syk kinases in activating and inhibitory pathways in innate immune cells: signaling cross talk. *Cold Spring Harb. Perspect. Biol.*
- Lowell, C.C.A., 2010. Src-family and Syk kinases in activating and inhibitory pathways in innate immune cells: signaling cross talk. *Cold Spring Harb. Perspect. Biol.*
- Lunnon, K., Teeling, J.L., Tutt, A.L., Cragg, M.S., Glennie, M.J., Perry, V.H., 2011. Systemic inflammation modulates Fc receptor expression on microglia during chronic neurodegeneration. *J. Immunol.* 186, 7215–24.
- Luo, X.-G., Ding, J.-Q., Chen, S.-D., 2010. Microglia in the aging brain: relevance to neurodegeneration. *Mol. Neurodegener.* 5, 12.
- Maezawa, I., Zimin, P.I., Wulff, H., Jin, L.-W., 2011. Amyloid-beta protein oligomer at low nanomolar concentrations activates microglia and induces microglial neurotoxicity. *J. Biol. Chem.* 286, 3693–706.
- Majumdar, A., Cruz, D., Asamoah, N., Buxbaum, A., Sohar, I., Lobel, P., Maxfield, F.R., 2007. Activation of Microglia Acidifies Lysosomes and Leads to Degradation of Alzheimer Amyloid Fibrils. *Mol. Biol. Cell* 18, 1490–1496.
- Mandrekar, S., Jiang, Q., Lee, C.Y.D., Koenigsnecht-Talboo, J., Holtzman, D.M., Landreth, G.E., 2009. Microglia mediate the clearance of soluble Abeta through fluid phase macropinocytosis. *J. Neurosci.* 29, 4252–62.
- Mandrekar, S., Landreth, G., 2010. Microglia and inflammation in Alzheimer's disease. *CNS Neurol. Disord. Drug Targets* 9, 156–167.
- Mantovani, A., Sozzani, S., Locati, M., Allavena, P., Sica, A., 2002. Macrophage polarization: tumor-associated macrophages as a paradigm for polarized M2 mononuclear phagocytes. *Trends Immunol.* 23, 549–55.
- Marín-Teva, J.L., Dusart, I., Colin, C., Gervais, A., van Rooijen, N., Mallat, M., 2004. Microglia promote the death of developing Purkinje cells. *Neuron* 41, 535–47.
- McCormack, A.L., Thiruchelvam, M., Manning-Bog, A.B., Thiffault, C., Langston, J.W., Cory-Slechta, D. a., Di Monte, D. a., 2002. Environmental Risk Factors and Parkinson's Disease: Selective Degeneration of Nigral Dopaminergic Neurons Caused by the Herbicide Paraquat. *Neurobiol. Dis.* 10, 119–127.
- McDonald, D.R., Brunden, K.R., Landreth, G.E., 1997. Amyloid fibrils activate tyrosine kinase-dependent signaling and superoxide production in microglia. *J. Neurosci.* 17, 2284–94.
- McGowan, E., Pickford, F., Kim, J., Onstead, L., Eriksen, J., Yu, C., Skipper, L., Murphy, M.P., Beard, J., Das, P., Jansen, K., Delucia, M., Lin, W., Dolios, G., Wang, R., Eckman, C.B., Dickson, D.W., Hutton, M., Hardy, J., Golde, T., 2005. Abeta42 is essential for parenchymal and vascular amyloid deposition in mice. *Neuron* 47, 191–9.

- Melchior, B., Garcia, A.E., Hsiung, B.-K., Lo, K.M., Doose, J.M., Thrash, J.C., Stalder, A.K., Staufenbiel, M., Neumann, H., Carson, M.J., 2010. Dual induction of TREM2 and tolerance-related transcript, *Tmem176b*, in amyloid transgenic mice: implications for vaccine-based therapies for Alzheimer's disease. *ASN Neuro* 2, e00037.
- Meyer-Luehmann, M., Spiess-Jones, T.L., Prada, C., Garcia-Alloza, M., de Calignon, A., Rozkalne, A., Koenigsnecht-Talboo, J., Holtzman, D.M., Bacskai, B.J., Hyman, B.T., 2008. Rapid appearance and local toxicity of amyloid-beta plaques in a mouse model of Alzheimer's disease. *Nature* 451, 720–4.
- Mildner, A., Schmidt, H., Nitsche, M., Merkler, D., Hanisch, U.-K., Mack, M., Heikenwalder, M., Brück, W., Priller, J., Prinz, M., 2007. Microglia in the adult brain arise from Ly-6ChiCCR2+ monocytes only under defined host conditions. *Nat. Neurosci.* 10, 1544–53.
- Miller, R.L., James-Kracke, M., Sun, G.Y., Sun, A.Y., 2009. Oxidative and inflammatory pathways in Parkinson's disease. *Neurochem. Res.* 34, 55–65.
- Miller, S.I., Ernst, R.K., Bader, M.W., 2005. LPS, TLR4 and infectious disease diversity. *Nat. Rev. Microbiol.* 3, 36–46.
- Minghetti, L., 2005. Role of inflammation in neurodegenerative diseases. *Curr. Opin. Neurol.* 18, 315–21.
- Minten, C., Terry, R., Deffrasnes, C., King, N.J.C., Campbell, I.L., 2012. IFN Regulatory Factor 8 Is a Key Constitutive Determinant of the Morphological and Molecular Properties of Microglia in the CNS. *PLoS One* 7, e49851.
- Mócsai, A., Ruland, J., Tybulewicz, V.L.J., 2010. The SYK tyrosine kinase: a crucial player in diverse biological functions. *Nat. Rev. Immunol.* 10, 387–402.
- Mogi, M., Harada, M., Kondo, T., Riederer, P., Inagaki, H., Minami, M., Nagatsu, T., 1994a. Interleukin-1 beta, interleukin-6, epidermal growth factor and transforming growth factor-alpha are elevated in the brain from parkinsonian patients. *Neurosci. Lett.* 180, 147–150.
- Mogi, M., Harada, M., Riederer, P., Narabayashi, H., Fujita, K., Nagatsu, T., Riedere, R., 1994b. Tumor necrosis factor-alpha (TNF-alpha) increases both in the brain and in the cerebrospinal fluid from parkinsonian patients. *Neurosci. Lett.* 165, 208–10.
- Monje, M.L., Toda, H., Palmer, T.D., 2003. Inflammatory blockade restores adult hippocampal neurogenesis. *Science* 302, 1760–5.
- Murgas, P., Godoy, B., von Bernhardt, R., 2012. Aβ potentiates inflammatory activation of glial cells induced by scavenger receptor ligands and inflammatory mediators in culture. *Neurotox. Res.* 22, 69–78.
- N'Diaye, E.-N., Branda, C.S., Branda, S.S., Nevarez, L., Colonna, M., Lowell, C., Hamerman, J. a, Seaman, W.E., 2009. TREM-2 (triggering receptor expressed on myeloid cells 2) is a phagocytic receptor for bacteria. *J. Cell Biol.* 184, 215–23.
- Neumann, H., Daly, M., 2013. Variant TREM2 as risk factor for Alzheimer's disease. *N. Engl. J. Med* 1–3.
- Neumann, H., Kotter, M.R., Franklin, R.J.M., 2008. Debris clearance by microglia: an essential link between degeneration and regeneration. *Brain* 132, 288–95.
- Nguyen, T. a, Frank-Cannon, T., Martinez, T.N., Ruhn, K. a, Marvin, M., Casey, B., Treviño, I., Hong, J.J., Goldberg, M.S., Tansey, M.G., 2013. Analysis of inflammation-related nigral degeneration and locomotor function in DJ-1-/- mice. *J. Neuroinflammation* 10, 50.
- Nimmerjahn, A., Kirchhoff, F., Helmchen, F., 2005. Resting microglial cells are highly dynamic surveillants of brain parenchyma in vivo. *Science* 308, 1314–8.
- Nomura, F., Akashi, S., Sakao, Y., Sato, S., Kawai, T., Matsumoto, M., Nakanishi, K., Kimoto, M., Miyake, K., Takeda, K., Akira, S., 2000. Cutting edge: endotoxin tolerance in mouse peritoneal macrophages correlates with down-regulation of surface toll-like receptor 4 expression. *J. Immunol.* 164, 3476–9.
- Nuber, S., Petrasch-Parwez, E., Winner, B., Winkler, J., von Hörsten, S., Schmidt, T., Boy, J., Kuhn, M., Nguyen, H.P., Teismann, P., Schulz, J.B., Neumann, M., Pichler, B.J., Reischl, G., Holzmann, C., Schmitt, I., Bornemann, A., Kuhn, W., Zimmermann, F., Servadio, A., Riess, O., 2008. Neurodegeneration and motor dysfunction in a conditional model of Parkinson's disease. *J. Neurosci.* 28, 2471–84.
- O'Neill, L.A.J., Golenbock, D., Bowie, A.G., 2013. The history of Toll-like receptors - redefining innate immunity. *Nat. Rev. Immunol.* 13, 453–60.
- Olson, J.K., Miller, S.D., 2004. Microglia initiate central nervous system innate and adaptive immune responses through multiple TLRs. *J. Immunol.* 173, 3916–24.
- Paloneva, J., Kestilä, M., Wu, J., Salminen, a, Böhling, T., Ruotsalainen, V., Hakola, P., Bakker, a B., Phillips, J.H., Pekkarinen, P., Lanier, L.L., Timonen, T., Peltonen, L., 2000. Loss-of-function mutations in TYROBP (DAP12) result in a presenile dementia with bone cysts. *Nat. Genet.* 25, 357–61.

- Paloneva, J., Mandelin, J., Kiialainen, A., Bohling, T., Prudlo, J., Hakola, P., Haltia, M., Konttinen, Y.T., Peltonen, L., 2003. DAP12/TREM2 deficiency results in impaired osteoclast differentiation and osteoporotic features. *J. Exp. Med.* 198, 669–75.
- Paloneva, J., Manninen, T., Christman, G., Hovanes, K., Mandelin, J., Adolfsson, R., Bianchin, M., Bird, T., Miranda, R., Salmaggi, A., Tranebjaerg, L., Konttinen, Y., Peltonen, L., 2002. Mutations in two genes encoding different subunits of a receptor signaling complex result in an identical disease phenotype. *Am. J. Hum. Genet.* 71, 656–62.
- Paolicelli, R.C., Bolasco, G., Pagani, F., Maggi, L., Scianni, M., Panzanelli, P., Giustetto, M., Ferreira, T.A., Guiducci, E., Dumas, L., Ragozzino, D., Gross, C.T., 2011. Synaptic Pruning by Microglia Is Necessary for Normal Brain Development. *Science*.
- Park, B.S., Song, D.H., Kim, H.M., Choi, B.-S., Lee, H., Lee, J.-O., 2009. The structural basis of lipopolysaccharide recognition by the TLR4-MD-2 complex. *Nature* 458, 1191–5.
- Pascual, O., Ben Achour, S., Rostaing, P., Triller, A., Bessis, A., 2012. Microglia activation triggers astrocyte-mediated modulation of excitatory neurotransmission. *Proc. Natl. Acad. Sci. U. S. A.* 109, E197–205.
- Peng, Q., Malhotra, S., Torchia, J.A., Kerr, W.G., Coggeshall, K.M., Humphrey, M.B., Activation, D., Dap, P.I.K.R., Mark, K., 2010. TREM2- and DAP12-dependent activation of PI3K requires DAP10 and is inhibited by SHIP1. *Sci. Signal.* 3, ra38.
- Perlmutter, L., Barron, E., Chui, H., 1990. Morphologic association between microglia and senile plaque amyloid in Alzheimer's disease. *Neurosci. Lett.* 119, 32–36.
- Perry, V.H., 2004. The influence of systemic inflammation on inflammation in the brain: implications for chronic neurodegenerative disease. *Brain. Behav. Immun.* 18, 407–13.
- Perry, V.H., 2010. Contribution of systemic inflammation to chronic neurodegeneration. *Acta Neuropathol.* 120, 277–86.
- Perry, V.H., 2012. Innate inflammation in Parkinson's disease. *Cold Spring Harb. Perspect. Med.* 2, a009373.
- Perry, V.H., Cunningham, C., Holmes, C., 2007. Systemic infections and inflammation affect chronic neurodegeneration. *Nat. Rev. Immunol.* 7, 161–7.
- Perry, V.H., Nicoll, J. a R., Holmes, C., 2010. Microglia in neurodegenerative disease. *Nat. Rev. Neurol.* 6, 193–201.
- Piccio, L., Buonsanti, C., Mariani, M., Cella, M., Gilfillan, S., Cross, A.H., Colonna, M., Panina-Bordignon, P., 2007. Blockade of TREM-2 exacerbates experimental autoimmune encephalomyelitis. *Eur. J. Immunol.* 37, 1290–301.
- Pickrell, A.M., Pinto, M., Moraes, C.T., 2013. Mouse models of Parkinson's disease associated with mitochondrial dysfunction. *Mol. Cell. Neurosci.* 55, 87–94.
- Püntener, U., Booth, S.G., Perry, V.H., Teeling, J.L., 2012. Long-term impact of systemic bacterial infection on the cerebral vasculature and microglia. *J. Neuroinflammation* 9, 146.
- Qin, L., Liu, Y., Hong, J.-S., Crews, F.T., 2013. NADPH oxidase and aging drive microglial activation, oxidative stress, and dopaminergic neurodegeneration following systemic LPS administration. *Glia* 61, 855–868.
- Qin, L., Liu, Y., Wang, T., Wei, S.-J., Block, M.L., Wilson, B., Liu, B., Hong, J.-S., 2004. NADPH oxidase mediates lipopolysaccharide-induced neurotoxicity and proinflammatory gene expression in activated microglia. *J. Biol. Chem.* 279, 1415–21.
- Qin, L., Wu, X., Block, M.L., Liu, Y., Breese, G.R., Hong, J., Knapp, D.J., Crews, F.T., 2007. Systemic LPS Causes Chronic Neuroinflammation and Progressive Neurodegeneration. *Glia* 462, 453–462.
- Qiu, C., Xu, W., Fratiglioni, L., 2010. Vascular and psychosocial factors in Alzheimer's disease: Epidemiological evidence toward intervention [WWW Document]. *J. Alzheimers Dis.* URL <http://iospress.metapress.com/content/682028731u442p52/?genre=article&issn=1387-2877&volume=20&issue=3&spage=689>
- Quan, D.N., Cooper, M.D., Potter, J.L., Roberts, M.H., Cheng, H., Jarvis, G. a, 2008. TREM-2 binds to lipooligosaccharides of *Neisseria gonorrhoeae* and is expressed on reproductive tract epithelial cells. *Mucosal Immunol.* 1, 229–38.
- Ramaglia, V., Hughes, T.R., Donev, R.M., Ruseva, M.M., Wu, X., Huitinga, I., Baas, F., Neal, J.W., Morgan, B.P., 2012. C3-dependent mechanism of microglial priming relevant to multiple sclerosis. *Proc. Natl. Acad. Sci. U. S. A.* 109, 965–70.
- Ransohoff, R.M., Cardona, A.E., 2010. The myeloid cells of the central nervous system parenchyma. *Nature* 468, 253–262.

- Ransohoff, R.M., Engelhardt, B., 2012. The anatomical and cellular basis of immune surveillance in the central nervous system. *Nat. Rev. Immunol.* 12, 623–35.
- Ransohoff, R.M., Perry, V.H., 2009. Microglial physiology: unique stimuli, specialized responses. *Annu. Rev. Immunol.* 27, 119–45.
- Rappert, A., Bechmann, I., Pivneva, T., Mahlo, J., Biber, K., Nolte, C., Kovac, A.D., Gerard, C., Boddeke, H.W.G.M., Nitsch, R., Kettenmann, H., 2004. CXCR3-dependent microglial recruitment is essential for dendrite loss after brain lesion. *J. Neurosci.* 24, 8500–9.
- Ravetch, J. V., 2000. Immune Inhibitory Receptors. *Science* (80-). 290, 84–89.
- Ravichandran, K.S., Lorenz, U., 2007. Engulfment of apoptotic cells: signals for a good meal. *Nat. Rev. Immunol.* 7, 964–74.
- Richfield, E.K., Thiruchelvam, M.J., Cory-Slechta, D. a, Wuertzer, C., Gainetdinov, R.R., Caron, M.G., Di Monte, D. a, Federoff, H.J., 2002. Behavioral and neurochemical effects of wild-type and mutated human alpha-synuclein in transgenic mice. *Exp. Neurol.* 175, 35–48.
- Rivest, S., 2003. Molecular insights on the cerebral innate immune system. *Brain. Behav. Immun.* 17, 13–9.
- Roodveldt, C., Christodoulou, J., Dobson, C.M., 2008. Immunological features of alpha-synuclein in Parkinson's disease. *J. Cell. Mol. Med.* 12, 1820–9.
- Ruiz-Valdepeñas, L., Martínez-Orgado, J. a, Benito, C., Millán, A., Tolón, R.M., Romero, J., 2011. Cannabidiol reduces lipopolysaccharide-induced vascular changes and inflammation in the mouse brain: an intravital microscopy study. *J. Neuroinflammation* 8, 5.
- Saha, R., Pahan, K., 2006. Regulation of inducible nitric oxide synthase gene in glial cells. *Antioxid. Redox Signal.* 8, 929–947.
- Satoh, J.-I., Tabunoki, H., Ishida, T., Yagishita, S., Jinnai, K., Futamura, N., Kobayashi, M., Toyoshima, I., Yoshioka, T., Enomoto, K., Arai, N., Arima, K., 2011a. Immunohistochemical characterization of microglia in Nasu-Hakola disease brains. *Neuropathology* 31, 363–375.
- Satoh, J.-I., Tabunoki, H., Ishida, T., Yagishita, S., Jinnai, K., Futamura, N., Kobayashi, M., Toyoshima, I., Yoshioka, T., Enomoto, K., Arai, N., Arima, K., 2011b. Immunohistochemical characterization of microglia in Nasu-Hakola disease brains. *Neuropathology* 31, 363–375.
- Schafer, D.P., Lehrman, E.K., Kautzman, A.G., Koyama, R., Mardinly, A.R., Yamasaki, R., Richard, M., Ransohoff, R.M., Greenberg, M.E., Barres, B. a, Stevens, B., 2012. Microglia sculpt postnatal neural circuits in an activity and complement-dependent manner. *Neuron* 74, 691–705.
- Scheffel, J., Regen, T., Van Rossum, D., Seifert, S., Ribes, S., Nau, R., Parsa, R., Harris, R. a, Boddeke, H.W.G.M., Chuang, H.-N., Pukrop, T., Wessels, J.T., Jürgens, T., Merkler, D., Brück, W., Schnaars, M., Simons, M., Kettenmann, H., Hanisch, U.-K., 2012. Toll-like receptor activation reveals developmental reorganization and unmasks responder subsets of microglia. *Glia* 60, 1930–43.
- Seno, H., Miyoshi, H., Brown, S.L., Geske, M.J., Colonna, M., Stappenbeck, T.S., 2009. Efficient colonic mucosal wound repair requires Trem2 signaling. *Proc. Natl. Acad. Sci. U. S. A.* 106, 256–61.
- Shen, Y., Lue, L.-F., Yang, L.-B., Roher, A., Kuo, Y.-M., Strohmeyer, R., Goux, W.J., Lee, V., Johnson, G.V., Webster, S.D., Cooper, N.R., Bradt, B., Rogers, J., 2001. Complement activation by neurofibrillary tangles in Alzheimer's disease. *Neurosci. Lett.*
- Sieber, M.W., Jaenisch, N., Brehm, M., Guenther, M., Linnartz-Gerlach, B., Neumann, H., Witte, O.W., Frahm, C., 2013a. SIEBER 2013 Attenuated Inflammatory Response in Triggering Receptor Expressed on Myeloid Cells 2 (TREM2) Knock-Out Mice following Stroke [suppl2].pdf. *PLoS One* 8, e52982.
- Sieber, M.W., Jaenisch, N., Brehm, M., Guenther, M., Linnartz-Gerlach, B., Neumann, H., Witte, O.W., Frahm, C., 2013b. Attenuated Inflammatory Response in Triggering Receptor Expressed on Myeloid Cells 2 (TREM2) Knock-Out Mice following Stroke. *PLoS One* 8, e52982.
- Sierra, A., Abiega, O., Shahraz, A., Neumann, H., 2013. Janus-faced microglia: beneficial and detrimental consequences of microglial phagocytosis. *Front. Cell. Neurosci.* 7, 6.
- Sierra, A., Encinas, J.M., Deudero, J.J.P., Chancey, J.H., Enikolopov, G., Overstreet-Wadiche, L.S., Tsirka, S.E., Maletic-Savatic, M., 2010. Microglia shape adult hippocampal neurogenesis through apoptosis-coupled phagocytosis. *Cell Stem Cell* 7, 483–95.
- Silva, A., Simpson, E., Takahashi, J., 1997. Mutant mice and neuroscience: recommendations concerning genetic background. *Neuron* 19, 755–759.

- Singh, A.K., Jiang, Y., 2004. How does peripheral lipopolysaccharide induce gene expression in the brain of rats? *Toxicology* 201, 197–207.
- Sisodia, S.S., St George-Hyslop, P.H., 2002. gamma-Secretase, Notch, Abeta and Alzheimer's disease: where do the presenilins fit in? *Nat. Rev. Neurosci.* 3, 281–90.
- Skelly, D.T., Hennessy, E., Dansereau, M.-A., Cunningham, C., 2013. A Systematic Analysis of the Peripheral and CNS Effects of Systemic LPS, IL-1B, TNF- α and IL-6 Challenges in C57BL/6 Mice. *PLoS One* 8, e69123.
- Soulet, D., Rivest, S., 2008. Microglia. *Curr. Biol.* 18, R506–8.
- Staub, E., Rosenthal, A., Hinzmann, B., 2004. Systematic identification of immunoreceptor tyrosine-based inhibitory motifs in the human proteome. *Cell. Signal.* 16, 435–456.
- Stefano, L., Racchetti, G., Bianco, F., Passini, N., Gupta, R.S., Panina Bordignon, P., Meldolesi, J., 2009. The surface-exposed chaperone, Hsp60, is an agonist of the microglial TREM2 receptor. *J. Neurochem.* 110, 284–294.
- Stevens, B., Allen, N.J., Vazquez, L.E., Howell, G.R., Christopherson, K.S., Nouri, N., Micheva, K.D., Mehalow, A.K., Huberman, A.D., Stafford, B., Sher, A., Litke, A.M., Lambris, J.D., Smith, S.J., John, S.W.M., Barres, B. a, 2007. The classical complement cascade mediates CNS synapse elimination. *Cell* 131, 1164–78.
- Streit, W.J., 2002. Microglia as neuroprotective, immunocompetent cells of the CNS. *Glia* 40, 133–9.
- Takahashi, K., Prinz, M., Stagi, M., Chechneva, O., Neumann, H., 2007. TREM2-transduced myeloid precursors mediate nervous tissue debris clearance and facilitate recovery in an animal model of multiple sclerosis. *PLoS Med.* 4, e124.
- Takahashi, K., Rochford, C.D.P., Neumann, H., 2005. Clearance of apoptotic neurons without inflammation by microglial triggering receptor expressed on myeloid cells-2. *J. Exp. Med.* 201, 647–57.
- Takegahara, N., Takamatsu, H., Toyofuku, T., Tsujimura, T., Okuno, T., Yukawa, K., Mizui, M., Yamamoto, M., Prasad, D.V.R., Suzuki, K., Ishii, M., Terai, K., Moriya, M., Nakatsuji, Y., Sakoda, S., Sato, S., Akira, S., Takeda, K., Inui, M., Takai, T., Ikawa, M., Okabe, M., Kumanogoh, A., Kikutani, H., 2006. Plexin-A1 and its interaction with DAP12 in immune responses and bone homeostasis. *Nat. Cell Biol.* 8, 615–22.
- Taylor, D.L., Diemel, L.T., Pocock, J.M., 2003. Activation of microglial group III metabotropic glutamate receptors protects neurons against microglial neurotoxicity. *J. Neurosci.* 23, 2150–60.
- Thrash, J.C., Torbett, B.B.E.B., Carson, M.M.J., 2009. Developmental regulation of TREM2 and DAP12 expression in the murine CNS: implications for Nasu-Hakola disease. *Neurochem. Res.* 34, 38–45.
- Toda, Y., Tsukada, J., Misago, M., Kominato, Y., Auron, P.E., Tanaka, Y., 2002. Autocrine induction of the human pro-IL-1 β gene promoter by IL-1 β in monocytes. *J. Immunol.* 168, 1984–91.
- Tomasello, E., Desmoulin, P.O., Chemin, K., Guia, S., Cremer, H., Ortaldo, J., Love, P., Kaiserlian, D., Vivier, E., 2000. Combined natural killer cell and dendritic cell functional deficiency in KARAP/DAP12 loss-of-function mutant mice. *Immunity* 13, 355–64.
- Tomasello, E., Vivier, E., 2005. KARAP/DAP12/TYROBP: three names and a multiplicity of biological functions. *Eur. J. Immunol.* 35, 1670–7.
- Trapnell, C., Schatz, M., 2009. Optimizing data intensive GPGPU computations for DNA sequence alignment. *Parallel Comput.* 35, 429–440.
- Tremblay, M.-È., Lowery, R.L., Majewska, A.K., 2010. Microglial Interactions with Synapses Are Modulated by Visual Experience. *PLoS Biol.* 8, e1000527.
- Tufekci, K.U., Genc, S., Genc, K., 2011. The endotoxin-induced neuroinflammation model of Parkinson's disease. *Parkinsons. Dis.* 2011, 487450.
- Turnbull, I.R., Colonna, M., 2007. Activating and inhibitory functions of DAP12. *Nat. Rev. Immunol.* 7, 155–161.
- Turnbull, I.R., Gilfillan, S., Cella, M., Aoshi, T., Miller, M., Piccio, L., Hernandez, M., Colonna, M., 2006. Cutting edge: TREM-2 attenuates macrophage activation. *J. Immunol.* 177, 3520.
- Von Bernhardi, R., Ramirez, G., Toro, R., Eugenin, J., 2007. Pro-inflammatory conditions promote neuronal damage mediated by Amyloid Precursor Protein and decrease its phagocytosis and degradation by microglial cells in culture. *Neurobiol. Dis.* 26, 153–64.
- Wake, H., Moorhouse, A.J., Jinno, S., Kohsaka, S., Nabekura, J., 2009. Resting microglia directly monitor the functional state of synapses in vivo and determine the fate of ischemic terminals. *J. Neurosci.* 29, 3974–80.
- Wake, H., Moorhouse, A.J., Miyamoto, A., Nabekura, J., 2013. Microglia: actively surveying and shaping neuronal circuit structure and function. *Trends Neurosci.* 36, 209–17.
- Wang, Yiner, Neumann, H., 2010. Alleviation of neurotoxicity by microglial human Siglec-11. *J. Neurosci.* 30, 3482–8.

- Wang, Y, Neumann, H., 2010. Alleviation of neurotoxicity by microglial human Siglec-11. *J. Neurosci.*
- Waterston, R.H., Lindblad-Toh, K., Birney, E., Rogers, J., Abril, J.F., et al., 2002. Initial sequencing and comparative analysis of the mouse genome. *Nature* 420, 520–62.
- Webber, K.M., Raina, A.K., Marlatt, M.W., Zhu, X., Prat, M.I., Morelli, L., Casadesus, G., Perry, G., Smith, M.A., 2005. The cell cycle in Alzheimer disease: A unique target for neuropharmacology. *Mech. Ageing Dev.* 126, 1019–1025.
- Weinberg, J.B., 2000. Nitric oxide synthase 2 and cyclooxygenase 2 interactions in inflammation. *Immunol. Res.* 22, 319–41.
- Wu, D.C., Jackson-lewis, V., Vila, M., Tieu, K., Teismann, P., Vadseth, C., Choi, D., Ischiropoulos, H., Przedborski, S., 2002. Blockade of Microglial Activation Is Neuroprotective in the 1-Methyl-4-Phenyl-1, 2, 3, 6-Tetrahydropyridine Mouse Model of Parkinson Disease 22, 1763–1771.
- Wyss-Coray, T., Rogers, J., 2012. Inflammation in Alzheimer disease—a brief review of the basic science and clinical literature. *Cold Spring Harb. Perspect. Med.* 2, 1–23.
- Wyss-Coray, T., Yan, F., 2002. Prominent neurodegeneration and increased plaque formation in complement-inhibited Alzheimer’s mice. *Proc. Natl. Acad. Sci.* 99, 10837–10842.
- Yamada, T., McGeer, P.L., McGeer, E.G., 1992. Lewy bodies in Parkinson’s disease are recognized by antibodies to complement proteins. *Acta Neuropathol.* 84, 100–4.
- Ydens, E., Cauwels, A., Asselbergh, B., Goethals, S., Peeraer, L., Lornet, G., Almeida-Souza, L., Van Ginderachter, J.A., Timmerman, V., Janssens, S., 2012. Acute injury in the peripheral nervous system triggers an alternative macrophage response. *J. Neuroinflammation* 9, 176.
- Zelcer, N., Khanlou, N., Clare, R., 2007. Attenuation of neuroinflammation and Alzheimer’s disease pathology by liver x receptors. *Proc. ...* 104, 10601–6.
- Zhang, B., Gaiteri, C., Bodea, L.-G., Wang, Z., McElwee, J., Podtelezhnikov, A.A. a, Zhang, C., Xie, T., Tran, L., Dobrin, R., Fluder, E., Clurman, B., Melquist, S., Narayanan, M., Suver, C., Shah, H., Mahajan, M., Gillis, T., Mysore, J., MacDonald, M.E.E., Lamb, J.R.R., Bennett, D.A. a, Molony, C., Stone, D.J.J., Gudnason, V., Myers, A.J.J., Schadt, E.E.E., Neumann, H., Zhu, J., Emilsson, V., 2013. Integrated Systems Approach Identifies Genetic Nodes and Networks in Late-Onset Alzheimer’s Disease. *Cell* 153, 707–720.
- Zhang, D., Hu, X., Qian, L., Chen, S.-H., Zhou, H., Wilson, B., Miller, D.S., Hong, J.-S., 2011. Microglial MAC1 receptor and PI3K are essential in mediating β -amyloid peptide-induced microglial activation and subsequent neurotoxicity. *J. Neuroinflammation* 8, 3.
- Zhang, J., Stanton, D.M., Nguyen, X. V, Liu, M., Zhang, Z., Gash, D., Bing, G., 2005. Intrapallidal lipopolysaccharide injection increases iron and ferritin levels in glia of the rat substantia nigra and induces locomotor deficits. *Neuroscience* 135, 829–38.
- Zhang, W.W., Wang, T., Pei, Z., Miller, D.S., Wu, X., Block, M.L., Wilson, B., Zhou, Y., Hong, J.-S., Zhang, J., 2005. Aggregated alpha-synuclein activates microglia: a process leading to disease progression in Parkinson’s disease. *FASEB J.* 19, 533–42.
- Ziegenfuss, J.S., Biswas, R., Avery, M.A., Hong, K., Sheehan, A.E., Yeung, Y.G., Stanley, E.R., Freeman, M.R., 2008. Draper-dependent glial phagocytic activity is mediated by Src and Syk family kinase signalling. *Nature* 453, 935–939.
- Zusso, M., Methot, L., Lo, R., Greenhalgh, A.D., David, S., Stifani, S., 2012. Regulation of postnatal forebrain amoeboid microglial cell proliferation and development by the transcription factor Runx1. *J. Neurosci.* 32, 11285–98.

Acknowledgements

I would like to express my deepest gratitude to Prof. Dr. Harald Neumann for providing me the opportunity to work in his group. I am thankful for his ideas and guidance that helped me all these years. I am also grateful for his support in exchanging my ideas with other scientists at local, national or international meetings. He was also the initiator of the collaborations that helped me building up the thesis. I would like to thank Prof. Dr. Waldemar Kolanus that kindly agreed to participate as the second referee to the thesis dissertation. His contribution to my work was enhanced by providing a great working environment within the Collaborative Research Centre (SFB) 704 and the associated Integrated Research Training Group. This granted me the opportunity to integrate and interact better with Bonn's scientific community. I am also grateful to Prof. Dr. Walter Witke for agreeing to participate as referee. I thank Prof. Dr. Jochen Walter for his collaboration and for agreeing to act as referee for my thesis.

I thank my overseas collaborators, the groups of Dr. Chris Gaiteri, Prof. Dr. Valur Emilsson, Prof. Dr. Eric Schadt, Dr. Bin Zhang and Prof. Dr. Jun Zhu for their great team work and spirit. Sincere thanks goes also to Luxemburg, to Dr. Lasse Sinkkonen and his team for their analysis and discussions. Without them important aspects of this work would not have been revealed.

Many thanks to all my colleagues, both former and current members of the Neumann's lab: Anahita, Bettina, Christine, Clara, Holger, Isabella, Janine, Jens, Jessica, Johannes, Jo, Kristin, Marcus, Mona, Moritz, Ozkan, Rita, Vanessa, Vera, Viola and Yiner. Also I thank Dr. Sandra Blaess and her great working team. I sincerely thank all for the help, discussions, advice and comments in and outside the lab. I am grateful to the entire Reconstructive Neurobiology Institute that contributed in the creation of a great working environment. It was great to work and have fun altogether.

I thank Mona Marthews, Dr. Bettina Linnartz-Gerlach and my wife for taking the time to proofread this thesis. Thank you for your useful comments and suggestions - you've done a great job!

Last and for sure not least, I am grateful to my wife for all her support. I would not have reached here without her.

Curriculum Vitae

Liviu-Gabriel Bodea

Address Neural Regeneration Group, Institute of Reconstructive Neurobiology
Life & Brain Center, University of Bonn,
Sigmund-Freud-Str. 25, 53127 Bonn, Germany
Tel. +49-228-6885-543; e-mail: LBodea@uni-bonn.de

Education and Professional Experience

2009 – present **PhD student**

Thesis title: *"The Implication of TREM2/DAP12 Complex in Microglia-mediated Tissue Homeostasis under Healthy and Pathological Conditions"*

Coordinator: Prof. Dr. Harald Neumann, Neural Regeneration Group, Institute of Reconstructive Neurobiology, LIFE & BRAIN Center, University of Bonn, Germany

Member of the Integrated Research Training Group (IRTG)

Life & Medical Sciences Institute, University of Bonn, Germany

Member of the Department Medical Neuroscience, the International Graduate School of Theoretical and Experimental Medicine (THEME), University of Bonn, Germany

2013 LabStatistics Course

Institute of Medical Biometry, Informatics and Epidemiology (IMBIE), Bonn, Germany

2013 INCF Short Course on Neuroinformatics, Neurogenomics and Brain Disease

Fraueninsel, Germany

2012 Flow Cytometry Workshop

Institute of Molecular Medicine and Experimental Immunology (IMMEI), Bonn, Germany

2007 – 2009 **MSc in Biochemistry and Molecular Biology**

Thesis title *"Influence of Inflammation on Dap12 Associated Receptors"*

Coordinators: Prof. Dr. Anca Dinischiotu, Department of Biochemistry and Molecular Biology, University of Bucharest, Romania and Prof. Dr. Harald Neumann, Institute of Reconstructive Neurobiology, LIFE & BRAIN Center, University of Bonn, Germany

2006 – 2008 Undergraduate and Graduate Research Assistant, Multi Users Research Centre in Molecular Biology, University of Bucharest, Romania

2003 – 2007 **BSc in Biochemistry**

Thesis title: *"The Oxidative Stress Effect Induced by Manganese (II) on Hsp70 and Hsp30 genes expression in Carassius auratus auratus"*

Coordinators: Dr. Cristina M. Munteanu and Prof. Dr. Anca Dinischiotu, Department of Biochemistry and Molecular Biology, University of Bucharest, Romania

Fellowships and Academic Honors

2008 ERASMUS Fellowship, Center of Molecular Biotechnology (CEMBIO),
University of Bonn, Germany

2007 – 2008 Scholarship for Scientific Performance, University of Bucharest, Romania

2003 – 2007 Merit Scholarship, University of Bucharest

Publications

- Zhang B.*, Gaiteri C.*, **Bodea L.G.***, Wang Z., McElwee, Podtelezchnikov A.A., Zhang C., Xie T., Tran L., Dobroin R., Fluder E., Clurman B., Melquist S., Narayanan M., Suver C., Shah H., Mahajan M., Gillis T., Mysore J., MacDonald M.E., Lamb J.R., Bennett D.A., Molony C., Stone D.J., Gudnason V., Myers A.J., Schadt E.E., Neumann H., Zhu J., Emilsson V. *“Integrated systems approach identifies genetic nodes and networks in late-onset Alzheimer’s disease”* **Cell** (153):707-720 ***equal contribution**
- Kopatz J., Beutner C., Welle K., **Bodea L.G.**, Reinhardt J., Claude J., Linnartz-Gerlach B., Neumann H. *“Siglec-h on activated microglia for recognition and engulfment of glioma cells”* **Glia**, 61(7), 1122–33.
- Linnartz B., **Bodea L.G.**, Neumann H. *“Microglial carbohydrate-binding receptors for neural repair”* **Cell Tissue Res.** 329(1):215-27

Manuscripts submitted

- **Bodea L.G.**, Wang Y., Linnartz-Gerlach B., Kopatz J., Sinkkonen L., Musgrove R., Kaoma T., Muller A., Vallar L., Di Monte D.A., Balling R., Neumann H. *“Repeated systemic challenge with lipopolysaccharides induces dopaminergic neurodegeneration by activation of the complement-phagosome pathway”*

Oral presentations

- *“TREM2/DAP12 pathway involvement in neurodegeneration”* – ImmunoSensation Cluster Science Day, October 22, 2013
- *“Investigating the role of microglial TREM2 receptor under normal and pathological conditions”* – 15th EURON PhD Student Meeting, Bonn, Germany, September 22-23, 2012
- *“The role of microglial TREM2 receptor”* – IntegratedResearchTrainingGroup-SFB704 Retreat, Knechtsteden, Germany, July 4-7, 2011

International conferences proceedings

- **Bodea L.G.**, Colonna M., Neumann H. *“Lack of microglial TREM2 receptor increases susceptibility to dopaminergic degeneration via neuroinflammation”* – XI Meeting on Glial Cells in Health and Disease, Berlin Germany, July 3-6, 2013, *Glia* 61:S1 (2013) T03-06A
- **Bodea L.G.**, Wang Y., Kopatz J., Sinkkonen L., Nicot N., Vallar L., Balling R., Neumann H. *“Fast occurring microglia-mediated dopaminergic degeneration after chronic systemic challenge with lipopolysaccharides”* - 8th International Conference on Innate Immunity, Barcelona, Spain, July 14-18, 2012 Abstract p.489 no.103.26
- **Bodea L.G.**, Linnartz B., Colonna M., Neumann H. *“Microglial TREM2 receptor has a protective role for the nigrostriatal system”* – 10th Meeting on Glial Cells in Health and Disease, Prague, Czech Republic, October 13-17, 2011 *Glia* 59:S1 (2011) p.S71 no.P2-06
- **Bodea L.G.**, Linnartz B., Colonna M., Neumann H. *“Accelerated microglial activation and neurodegeneration in triggering receptor expressed on myeloid cells-2 (TREM2) deficient mice after systemic inflammatory challenge”* - 10th International Congress of Neuroimmunology, Barcelona, Spain, October 26-30, 2010 *JNeuroimmunol* vol. 228(1-2), p. 172 no. 359
- **Bodea L.G.**, Linnartz B., Colonna M., Neumann H. *“Triggering Receptor Expressed on Myeloid cells-2 (TREM2) influences brain immune homeostasis”* –7th FENS Forum of European Neuroscience, Amsterdam, Netherlands, July 3-7, 2010 Abstract book p. 111, poster no. 050.18
- **Bodea L.G.**, Dannenberg H., Colonna M., Neumann H. *“Regulation of DAP12 associated receptors in microglia by systemic inflammatory stimuli”* - 9th European Meeting on Glial Cells, Paris, October 8-12, 2009 *Glia* 2009, Vol. 57: S13

Declaration

I, hereby confirm that this work submitted is my own. This thesis has been written independently and with no other sources and aids than stated. The presented thesis has not been submitted to another university and I have not applied for a doctorate procedure so far.

Hiermit versichere ich, dass die vorgelegte Arbeit – abgesehen von den ausdrücklich bezeichneten Hilfsmitteln – persönlich, selbständig und ohne Benutzung anderer als der angegebenen Hilfsmittel angefertigt wurde. Aus anderen Quellen direkt oder indirekt übernommenen Daten und Konzepte sind unter Angabe der Quelle kenntlich gemacht worden.

Die vorliegende Arbeit wurde an keiner anderen Hochschule als Dissertation eingereicht. Ich habe früher noch keinen Promotionsversuch unternommen.

Liviu-Gabriel Bodea, Author

October 31st, 2013